

**Functional analysis of plastid-encoded genes.
Application of reverse genetics on *Nicotiana tabacum*.**

Dissertation der Fakultät für Biologie
der Ludwig-Maximilian-Universität München

vorgelegt von
Magdalena Świątek
aus Wrocław, Polen

2002

1. Gutachter: **Prof. Dr. R. G. Herrmann**
2. Gutachter: **Prof. Dr. H. U. Koop**

Tag der mündlichen Prüfung: 19.06.2002

CONTENT

ABBREVIATIONS	VI
INTRODUCTION	1
2. MATERIALS AND METHODS	16
2.1 Materials	16
2.1.1 Plant material.....	16
2.1.2 Bacterial strains.....	16
2.1.3 Vectors.....	16
2.1.4 Recombinant plasmids.....	16
2.1.5 Primer list	16
2.1.6 Antibodies.....	18
2.1.7 Chemicals, enzymes, molecular weight markers.....	19
2.1.8 Media for growth of plants and bacteria.....	19
2.1.9 Buffers and solutions.....	21
2.1.10 Transfer membranes.....	22
2.2 Methods	22
2.2.1 Construction of plant transformation vectors.....	22
2.2.1.1 Construction of the recombinant plasmid for <i>ycf9</i> inactivation.....	22
2.2.1.2 Construction of the recombinant plasmid for <i>ycf10</i> inactivation.....	22
2.2.2 Plant transformation.....	23
2.2.2.1 Seed sterilization.....	23
2.2.2.2 Plastid transformation.....	23
2.2.2.3 Selection and regeneration of mutants.....	24
2.2.3 Isolation and fractionation of chloroplasts.....	24
2.2.3.1 Isolation of intact chloroplasts.....	24
2.2.3.2 Fractionation of chloroplasts into stroma and thylakoid membranes.....	25
2.2.3.3 Isolation of the major thylakoid protein complexes.....	25
2.2.3.4 Washing of thylakoid membranes with Na ₂ CO ₃	26
2.2.3.5 Purification and fractionation of chloroplast envelope membranes.....	26
2.2.4 Overexpression of proteins <i>in vitro</i>	27
2.2.4.1 Cloning of <i>ycf9</i> for overexpression.....	27
2.2.4.2 Overexpression of proteins in <i>E. coli</i>	28
2.2.5 Protein analysis.....	28
2.2.5.1 Determination of the protein concentration.....	28
2.2.5.2 Phosphorylation of proteins <i>in vitro</i>	29

2.2.5.3	Protein gel electrophoresis.....	30
2.2.5.3.1	SDS-denaturing polyacrylamide (PAA) gels.....	30
2.2.5.3.1.1	Laemmli gel system	30
2.2.5.3.1.2	Schägger/von Jagow gel system.....	30
2.2.5.3.2	Non-denaturing PAGE.....	32
2.2.5.3.2.1	Non-denaturing Deriphath-PAGE.....	32
2.2.5.3.2.2	Non-denaturing Blue-Native PAGE.....	33
2.2.5.4	Staining of PAA gels.....	34
2.2.5.4.1	Coomassie Brilliant Blue staining.....	34
2.2.5.4.2	Silver staining.....	35
2.2.6	Immunological detection of proteins on membranes.....	36
2.2.6.1	Transfer of proteins onto nitrocellulose and PVDF membranes.....	36
2.2.6.2	Staining of blots with Ponceau S.....	36
2.2.6.3	Immunological detection of proteins.....	37
2.2.6.3.1	Western analysis using horseradish peroxidase-conjugated antibodies.....	37
2.2.7	Antibody generation.....	38
2.2.7.1	Preparation of probes for the rabbit immunization.....	38
2.2.7.2	Subcutaneous injection of rabbits and antibody preparation.....	38
2.2.8	Nucleic acids analysis.....	39
2.2.8.1	Standard methods.....	39
2.2.8.2	DNA analysis.....	39
2.2.8.2.1	Sequence searches and alignments.....	39
2.2.8.2.2	Isolation of total DNA and plastid DNA.....	40
2.2.8.2.3	Southern analysis of DNA.....	40
2.2.8.2.4	Radioactive probe labeling.....	41
2.2.8.2.4.1	Radioactive labeling of PCR products.....	41
2.2.8.2.4.2	Radioactive labeling of oligodesoxynucleotides.....	41
2.2.8.2.5	Hybridization procedure.....	41
2.2.8.2.6	Isolation of DNA from agarose gels.....	42
2.2.8.3	RNA analysis.....	42
2.2.8.3.1	Isolation of total RNA from plants.....	42
2.2.8.3.2	Construction of radiolabeled RNA probes.....	42
2.2.8.4	Pulsed-field gel electrophoresis of DNA.....	43
2.2.8.4.1	Sample preparation.....	43
2.2.8.4.2	Pulsed-field gel electrophoresis.....	44
2.2.8.4.3	Isolation of DNA from pulsed-field gels.....	44
2.2.9	Electron microscopy.....	45
2.2.10	Pigment analysis.....	45
2.2.11	Non-photochemical quenching.....	45
2.2.12	Measurement of photosynthetic O ₂ evolution with the Clark Electrode.....	46
2.2.13	Chlorophyll fluorescence analysis.....	46

2.2.13.1	77K fluorescence analysis.....	46
2.2.13.2	Chlorophyll fluorescence measurements using the PAM fluorometer.....	47
2.2.13.3	Fluorescence detection using the FluorCam-Video Imaging System.....	47
3.	RESULTS.....	48
3.1	Functional analysis of the <i>ycf9</i> gene product.....	48
3.1.1	Comparison of the Ycf9 sequences.....	48
3.1.2	Construction of a recombinant plasmid for <i>ycf9</i> inactivation.....	49
3.1.3	Plant transformation, selection and regeneration of mutants.....	50
3.1.4	Growth phenotypes of the $\Delta ycf9$ plants.....	51
3.1.5	Ultrastructure of $\Delta ycf9$ chloroplasts.....	53
3.1.6	Investigation of the homoplastomic state of mutant plastome.....	54
3.1.6.1	Sequence analysis.....	54
3.1.6.2	Southern analysis.....	55
3.1.6.3	PCR analysis.....	56
3.1.6.4	PCR analysis of DNA purified by pulsed-field gel electrophoresis.....	57
3.1.6.4.1	Southern analysis of $\Delta ycf9$ PFGE purified plastid DNA.....	58
3.1.7	Northern analysis.....	58
3.1.8	Overexpression of the Ycf9 protein in <i>E. coli</i>	60
3.1.9	Generation of antisera against the Ycf9 protein.....	61
3.1.10	Immunological detection of the Ycf9 protein.....	62
3.1.11	Changes in the polypeptide content in thylakoid membranes from $\Delta ycf9$ mutants.....	64
3.1.11.1	SDS-PAGE analysis of the polypeptide content of $\Delta ycf9$ plants.....	64
3.1.11.2	Serological analysis of the $\Delta ycf9$ thylakoid proteins.....	65
3.1.11.2.1	The effect of Ycf9 deletion on minor antenna protein complexes.....	66
3.1.11.3	Isolation of the major protein complexes from the thylakoid membranes.....	68
3.1.11.3.1	Isolation of the thylakoid protein complexes by sucrose density gradient centrifugation.....	68
3.1.11.3.1.1	Serological analysis of sucrose gradient fractions.....	70
3.1.11.3.2	Isolation of the major protein complexes from the thylakoid membranes by two-dimensional gel electrophoresis.....	71
3.1.11.3.2.1	Deriphat-PAGE gel analysis.....	71
3.1.11.3.2.2	Blue-native PAGE analysis.....	73
3.1.12	Alteration of protein phosphorylation in the $\Delta ycf9$ mutant.....	74
3.1.12.1	Alteration of protein phosphorylation in the $\Delta ycf9$ mutant.....	74
3.1.12.2	Influence of light intensities on protein phosphorylation patterns of wild-type and $\Delta ycf9$ thylakoids.....	75
3.1.12.3	Phosphorylation pattern of fractionated thylakoids from the wild-type and $\Delta ycf9$ mutants.....	77

3.1.12.4	<i>In vitro</i> phosphorylation of thylakoid proteins.....	79
3.1.13	Non-photochemical quenching in the $\Delta ycf9$ plants.....	80
3.1.14	Pigment composition and xanthophyll cycle in the $\Delta ycf9$ plants.....	83
3.1.15	Chlorophyll fluorescence analysis.....	84
3.1.15.1	77K chlorophyll fluorescence analysis.....	84
3.1.15.1.1	Analysis of PSI and PSII supercomplexes assembly; excitation spectra by emission at 735 and 690 nm.....	84
3.1.15.1.2	Chlorophyll <i>b</i> emission spectra.....	85
3.1.15.2	Chlorophyll fluorescence measurements at room temperature.....	87
3.2	Functional analysis of the <i>ycf10</i> (<i>cemA</i>) gene product.....	88
3.2.1	Comparison of the Ycf10 sequences.....	88
3.2.2	Construction of a recombinant plasmid for <i>ycf10</i> inactivation.....	90
3.2.3	Plant transformation, selection and regeneration of mutants.....	91
3.2.4	Growth phenotypes of the $\Delta ycf10$ plants.....	91
3.2.5	Ultrastructure of the $\Delta ycf10$ chloroplasts.....	93
3.2.6	Investigation of the homoplastomic state in the $\Delta ycf10$ mutants.....	94
3.2.6.1	Nucleotide sequence analysis.....	94
3.2.6.2	Southern analysis.....	96
3.2.6.3	PCR analysis.....	96
3.2.6.3.1	Hybridization analysis of $\Delta ycf10$ PCR products.....	97
3.2.7	Northern analysis.....	98
3.2.8	Localization of the <i>ycf10</i> product.....	100
3.2.9	Isolation of thylakoid protein complexes from $\Delta ycf10$ mutants by sucrose density gradient centrifugation.....	101
3.2.10	Serological analysis of the $\Delta ycf10$ mutants.....	101
3.2.11	Chlorophyll fluorescence analysis.....	103
3.2.12	C ₁ -dependent O ₂ evolution.....	104
3.3	Pulsed-field electrophoresis as a new method for the determination of the homoplastomic status of transformed plants.....	106
3.3.1	DNA separation in pulsed-field agarose gel electrophoresis.....	106
3.3.2	Isolation of monomeric plastid DNA from the agarose gel.....	107
3.3.3	Investigation of the purity of plastid DNA isolated by pulsed-field gel electrophoresis.....	107
3.3.3.1	Presence of contaminating nuclear DNA in different plant DNA preparations.....	107
3.3.3.2	Presence of contaminating mitochondrial DNA in different plant DNA preparations.....	108

3.3.4 Analysis of the $\Delta ycf10$ homoplasmic state by pulsed-field gel electrophoresis.....	109
3.3.5 Quantitative estimation of wild-type chromosome copies detected by PCR analysis.....	111
3.3.6 Sensitivity level of the PCR.....	111
4. DISCUSSION.....	113
4.1 Functional analysis of the <i>ycf9</i> gene product.....	114
4.2 Functional analysis of the <i>ycf10</i> gene product.....	125
5. SUMMARY.....	130
6. REFERENCES.....	132
ACKNOWLEDGMENTS.....	149
PUBLICATIONS.....	150
CURRICULUM VITAE.....	151

ABBREVIATIONS

A	absorbance
amp	ampicillin
APS	ammonium persulfat
ATP	adenosine 5'-triphosphate
BAP	6-benzylaminopurin
bp	base pairs
BSA	bovine serum albumin
cDNA	complementary DNA
chl	chlorophyll
DMSO	dimethyl sulfoxide
DNase	deoxyribonuclease I
DNA	deoxyribonucleic acid
DTT	dithiotreitol
EDTA	ethylenediamine tetraacetic acid
ELIP	early light-inducible proteins
EtBr	ethidium bromide
EtOH	ethanol
g	gram
h	hour
HEPES	N-(2-hydroxyethyl)piperazine N'-(2-ethane sulfonic acid)
IAA	iodoacetamide
IgG	immunoglobulin G
IPTG	isopropyl β -D-thiogalactoside
IR	inverted repeat
kb	kilobases
kDa	kilo Dalton
LB	Luria broth
LHC	light harvesting complex
LSC	large single-copy region
MES	2-N-morpholinoethanesulfonacid
min	minute
MOPS	4-morpholinopropansulfonacid

NAA	α -naphthalene acetic acid
nm	nanometer
NPQ	nonphotochemical quenching
NTP	nucleoside triphosphate
OD	optical density
OEC	oxygen-evolving complex
ORF	open reading frame
PAA	polyacrylamide
PAGE	polyacrylamide gel electrophoresis
PBS	phosphate-buffered saline
PCR	polymerase chain reaction
PEG	polyethylene glycol
PNK	polynucleotid kinase
PSI	photosystem I
PSII	photosystem II
Pt	plastid
RC	reaction center
rpm	rotations per minute
RNase	ribonuclease
RT	room temperature
PFGE	pulsed-field gel electrophoresis
PFD	photon flux densities
RuBisCo	ribulosebiphosphat carboxylase/oxygenase
SDS	sodium dodecylsulfate
SDS-PAGE	sodium dodecylsulfate polyacrylamide gel electrophoresis
sec	second
SSC	standard saline citrate
SSC	small single-copy region
TBE	Tris-borate-EDTA buffer
TCA	trichloroacetic acid
TE	Tris-EDTA
TEMED	N,N,N',N'-tetramethylethylene diamine
Tris	Tris(hydroxymethyl)aminomethane
Tween 20	polyoxyethylensorbitanmonolaurat

Vol	volume
v/v	volume pro volume
w/v	weight pro volume

Amino acids

A, Ala	Alanine	M, Met	Methionine
C, Cys	Cysteine	N, Asn	Asparagine
D, Asp	Aspartic acid	P, Pro	Proline
E, Glu	Glutamic acid	Q, Gln	Glutamine
F, Phe	Phenylalanine	R, Arg	Arginine
G, Gly	Glycine	S, Ser	Serine
H, His	Histidine	T, Thr	Threonine
I, Ile	Isoleucine	V, Val	Valine
K, Lys	Lysine	W, Trp	Tryptophan
L, Leu	Leucine	Y, Tyr	Tyrosine

Bases

A:	Adenine
C:	Cytosine
G:	Guanine
T:	Thymine
U:	Uracil

1. INTRODUCTION

Plastids are essential organelles for the plant function and comprise one of the primary features that distinguish plants from other eukaryotes. In multicellular plants, all forms of plastids are derived from undifferentiated proplastids, which during cell differentiation form a variety of cell-specific organelles, including amyloplasts, chromoplasts, leucoplasts, elaioplasts and chloroplasts. Chlorophyll-containing plastids, chloroplasts, are considered to be the most complex type of plastids, containing six different compartments (outer and inner membranes with the periplasmatic space, thylakoid membranes, lumen and stroma), and performing processes vital for plant cell function. The biochemical key process of chloroplasts is photosynthesis, which supplies the cell with fixed carbon and energy in the forms of ATP and NADPH. Chloroplasts contain the entire enzymatic machinery for the process of photosynthesis, including both thylakoid membrane system and stroma. The organelle possesses further biogenetic potential, such as fatty acid or amino acid biosynthesis (Galili 1995, Ohlrogge and Browse 1995).

Thylakoid membranes consist of approximately 50% each lipid and proteins. Most of the polypeptides complement is comprised of five major protein complexes which span the lipid bilayer and are associated with both peripheral and soluble polypeptides in stroma and lumen, respectively. The protein complexes are designated photosystem II with the water oxydation system, photosystem I, antenna complexes LHCI and LHCII associated with both photosystems, cytochrome *b₆f* complex, ATP synthase and NAD(P)H dehydrogenase (reviewed in Herrmann et al. 1991, Wollman et al. 1999). These assemblies catalyze the photosynthetic light reaction, i.e. they utilize light energy to drive electron transport from water to NADP^+ with coupled proton translocation across the thylakoid membrane that generates a proton motive force for synthesis of ATP.

Photosystem II (PSII) mediates electron transfer from water to plastoquinone as a result of the light-induced charge separation between the primary chlorophyll donor P680 and a pheophytin acceptor molecule. In higher plants and green algae, the PSII core is associated with several light harvesting antenna units. The core complex of PSII comprises six polypeptide subunits: D1 and D2 proteins, which bear two tyrosine donors Y_Z and Y_D , cytochrome b_{559} (PsbE and PsbF), two low molecular weight subunits PsbI and PsbW and two inner-antenna CP43 and CP47. The reaction center also contains six chlorophyll *a* molecules,

two pheophytin *a* molecules, plastoquinone, non-heme iron and two β -carotenes. At its luminal face PSII harbors the oxygen-evolving complex (OEC, also designated oxygen evolving enhancer, OEE) which contributes to catalyze water oxidation. In plants, OEC contains three peripheral subunits, O, P, and Q, also called OE33, OE23 and OE16. The OEC bears the Mn-cluster which is essential for catalytic activity. Studies of the structure of dimeric supercomplexes of photosystem II, that in the dimeric form associate light-harvesting antenna, by electron microscopy and single-particle image analysis presented arrangement of peripheral antenna proteins and the destabilization of the dimeric structure upon removal of 33 kDa protein. Removal of the extrinsic 23 and 16 kDa proteins induced changes in the position of the peripheral antenna proteins, in particular, movement of CP29 was recorded (Boekema et al. 2000). The mechanism of the PSII dimer-stabilizing effect of OEC33 proteins remains unclear, although the possibility that the 33 kDa protein partially shields the central region of the PSII core dimer was proposed (Boekema et al. 2000). Advanced x-ray structure studies of photosystem II crystals obtained from cyanobacteria (Vasil'ev et al. 2001, Zouni et al. 2001) provided insight into the protein composition and dynamics of the complex. The membrane-integral part of PSII monomer was shown to contain 36 transmembrane α -helices, of which twenty-two were assigned to D1, D2, CP43 and CP47, two further to the α and β subunits of cytochrome b_{559} , and another five α -helices were assigned to PsbH, PsbI, PsbL, PsbK and PsbX proteins. Seven additional transmembrane α -helices, one in proximity of CP47, six located close to CP43 and one close to cytochrome b_{559} , have been found in the electron density map but could not be assigned (Zouni et al. 2001). Analysis of excited-state dynamics in photosystem II from the x-ray crystal structure revealed a crucial role of CP43- and CP47-associated chlorophyll molecules in energy transfer from antenna to the reaction center (RC) complex (Vasil'ev et al. 2001). Altogether the PSII consists of more than 25 polypeptide subunit species, 200 - 250 chlorophyll molecules per P680 and a chlorophyll *a/b* ratio of 2 - 3 (Green and Durnford 1996, Barber et al. 1997, Hankamer et al. 1999, Wollman et al. 1999, Barber and Kühlbrandt 1999, Messinger 2000).

Photosystem I (PSI) is formed by a core complex with an attached light harvesting complex (LHCI). It drives the electron transfer from plastocyanin at the luminal side to ferredoxin located in the chloroplast stroma. The electron transfer within PSI occurs via the primary electron donor P700, which is a chlorophyll *a* dimer, and five electron acceptors, a chlorophyll *a* monomer (A0), vitamin K (A1) and the three 4Fe-4S clusters, F_X , F_A , F_B (A2-A4). The integral core of PSI is formed by PsaA and PsaB and several small transmembrane

subunits. PsaG, PsaH, and PsaK proteins have been shown to be involved in the interaction between LHCI and PSI core (Jensen et al. 2000), PsaI and PsaJ subunits appear to be responsible for the organization of peripheral proteins, PsaL stabilizes the PSI trimer (Jordan et al. 2001), and the PsaM subunit may be involved in cyclic electron flow around photosystem I (reviewed by Chitnis 1996). The peripheral subunit PsaE, localized at the stromal face of photosystem I, forms a ferredoxin-docking pocket (Rousseau et al. 1993, Jordan et al. 2001) and, as discussed below, plays a role in cyclic electron flow around photosystem I (Yu et al. 1993). The docking pocket for plastocyanin is formed by luminal-face exposed PsaF (Chitnis 1996, Jordan et al. 2001). Crystal structure of cyanobacterial photosystem I and PSI-LHCI complexes established that the complex is made of up to 17 subunits and 127 cofactors comprising 96 chlorophylls, 2 phylloquinones, 3 Fe₄S₄ clusters, 22 carotenoids, 4 lipids, a putative Ca²⁺ ion and 201 water molecules. The chlorophyll *a/b* ratio is more than 5 (Mullet et al. 1980ab, Xu et al. 1994, Wollman et al. 1999, Jordan et al. 2001).

Antenna proteins (LHC). The common ancestor of the LHC proteins is believed to be a cyanobacterial high-light inducible protein with one membrane-spanning helix (Dolganov et al. 1995). After endosymbiotic chloroplast formation, the *Lhc* gene progenitor was transferred to the nuclear genome, where subsequent duplication and deletion events took place, eventually leading to the large *Lhc* gene family that exists today (Green and Kühlbrandt 1995, Herrmann 1997, Jansson 1999). The LHC-encoding genes are all of nuclear origin. The protein precursors contain an N-terminal transit peptide that is cleaved off during import into the chloroplast, after which the mature proteins are inserted into the thylakoid membrane with one to four membrane-spanning helices (Cline and Henry 1996). The CP29, CP26, CP24 apoproteins are encoded by the nuclear genes *Lhcb4*, *Lhcb5* and *Lhcb6* and after integration into thylakoid membranes form a minor antenna complex associated with the core of PSII. The LHCI antenna (genes: *Lhca1-4*) associate exclusively with PSI, and LHCII (*Lhcb1-3*) antenna mainly associate with PSII. The latter may also migrate to PSI as a mobile antenna pool capable of light-energy distribution between the two photosystems upon a mechanism regulated by phosphorylation/dephosphorylation of LHCII proteins (Allen et al. 1981, Allen 1992). Two additional groups of proteins with homology to the LHC family, PsbS (Funk et al. 1995) and early light-inducible proteins (ELIPs; Adamska 1997), have been identified in higher plants. All LHC-related proteins have been shown to bind chlorophylls and carotenoids (Peter and Thornber 1991, Kühlbrandt et al. 1994, Funk et al. 1995, Green and Kühlbrandt 1995, Jansson 1999, Xiao-Ping et al. 2000).

The **cytochrome b_6f** complex, as the mitochondrial cytochrome bc_1 complex, belongs to the bc -type cytochromes, which couple electron transfer and proton translocation across the membrane. The cytochrome b_6f complex transfers electrons from plastoquinol to a soluble electron carrier located in the thylakoid lumen, plastocyanin. The electron transfer is accompanied by forming a proton gradient across the thylakoid membrane, which is used by the ATP synthase to generate ATP. The cytochrome b_6f complex is formed by the Rieske protein (containing [2Fe-2S] cluster, PetC), the cytochromes f (PetA) and b_6 (PetB), subunit IV (PetD), and several small subunit species: PetG, PetL, PetM, PetN including the newly described subunit V encoded by the nuclear gene *petO* (Staehelin and Arntzen 1983, Vener et al. 1997, Wollman et al. 1999, Hamel et al. 2000). The PetL subunit has been shown to play a role in stability of the cytochrome b_6f dimer (Breyton et al. 1997). The existence of cytochrome b_6f dimers was also proven by electron crystallography of *Chlamydomonas* complexes (Bron et al. 1999). The mechanism for the bc -type complexes is a “Q-cycle” proposed by Mitchell (1975) and modified by Crofts et al. (1983). According to this model, two electron paths exist within the complex, a high potential pathway composed of the [2Fe-2S] cluster of Rieske protein and the c -type heme of cytochrome f , and a low potential chain, composed of the two hemes of the b -type cytochrome, designated b_L and b_H . Two quinol/quinone binding sites are located on opposite sites of the membrane: the Q_o on the luminal face of the membrane, and the Q_i site on the stromal side of the membrane. Binding of the plastoquinol to the Q_o site comprises a two-electron transfer, one electron reducing the Rieske protein, which in turn reduces the c -type cytochrome, and the other electron reducing two b -type cytochrome hemes. These events are associated with the release of two protons into the luminal space. A second cytochrome b_6f turnover reduces another plastocyanine molecule and places both b_L and b_H hemes of cytochrome b_6 in a reduced state. Oxidation of the b -type cytochrome hemes occurs through a two-step reduction of a plastoquinone at the Q_i site coupled with an uptake of two protons from the stromal space. This mechanism contributes to generating the proton gradient that drives ATP synthesis. An unique feature of cytochrome f is the existence of an internal chain of five water molecules, which may serve as a “proton wire” for protons to be translocated across the membrane (Martinez et al. 1996). Beside its role in photosynthetic electron transfer, the cytochrome complex is also recruited for redox sensing and signal transduction in chloroplasts (summarized in Wollman 2001).

Binding of the plastoquinol at the Q_o site and subsequent reduction of cytochrome b_6f complex triggers kinase activation, which results in LHCII complex phosphorylation and its movement from PSII to PSI in the so-called state 1/state 2 transition mechanism (Gal et al. 1987, Bennett et al. 1988, Vener et al. 1997, Zito et al. 1999). The contribution of Rieske protein in this process was proposed. Oscillation of the Rieske protein between the proximal (close to Q_o) and distal (close to cytochrome f) site were observed in the Q-cycle process (Zhang et al. 1998). The switch of the Rieske protein into the proximal position was proposed to trigger kinase activity (Vener et al. 1997, Zito et al. 1999). Cytochrome b_6f complex through its interaction with the plastoquinone pool acts as a redox-sensor, thus playing a major role in acclimatization processes of plants.

The chloroplast **ATP synthase** belongs to the family of F_1 -type ATPases that is also present in bacteria and mitochondria (Nelson 1992). It generates ATP from ADP and inorganic phosphate using energy derived from a *trans*-thylakoid electrochemical proton gradient. The ATP synthase contains a membrane-embedded proton channel, CF_0 , and a catalytic sector with ATP synthase activity, CF_1 , located at the stromal face of thylakoids. The entire ATP synthase complex comprises four transmembrane I - IV subunits of the CF_0 sector (encoded by the genes *atpF*, *atpG*, *AtpH* and *atpI*), and five stromal subunits of CF_1 with the stoichiometry α_3 , β_3 , γ_1 , δ_1 , ϵ_1 (encoded by the genes *atpA*, *atpB*, *AtpC*, *AtpD* and *atpE*). The supramolecular organization of the ATP synthase has recently been resolved by x-ray crystallography (Engelbrecht and Junge 1997, Stock et al. 1999, Menz et al. 2001). The catalytic sites are in the β subunits at the α/β subunit interface (Abrahams et al. 1994). The ATP formation is known as the “binding change mechanism” (Boyer 1993), in which rotation of the central stalk (composed of subunits γ , δ , and ϵ) is accompanied by conformational changes in the three β subunits, which cycle sequentially through structural states corresponding to low, medium, and high nucleotide affinities. These three states are probably associated with the release of the product (ATP), binding of substrates (ADP and inorganic phosphate), and ATP formation, respectively. The membrane-embedded ring formed by subunits III of CF_0 sector has been proposed to be a part of a rotary motor, converting electrochemical energy into chemical energy stored in ATP. X-ray structure analysis revealed

a varied number of subunits III in yeast and *E. coli* depending on the carbon source, which could reflect a regulatory mechanism of ATP synthesis (Stock et al. 1999).

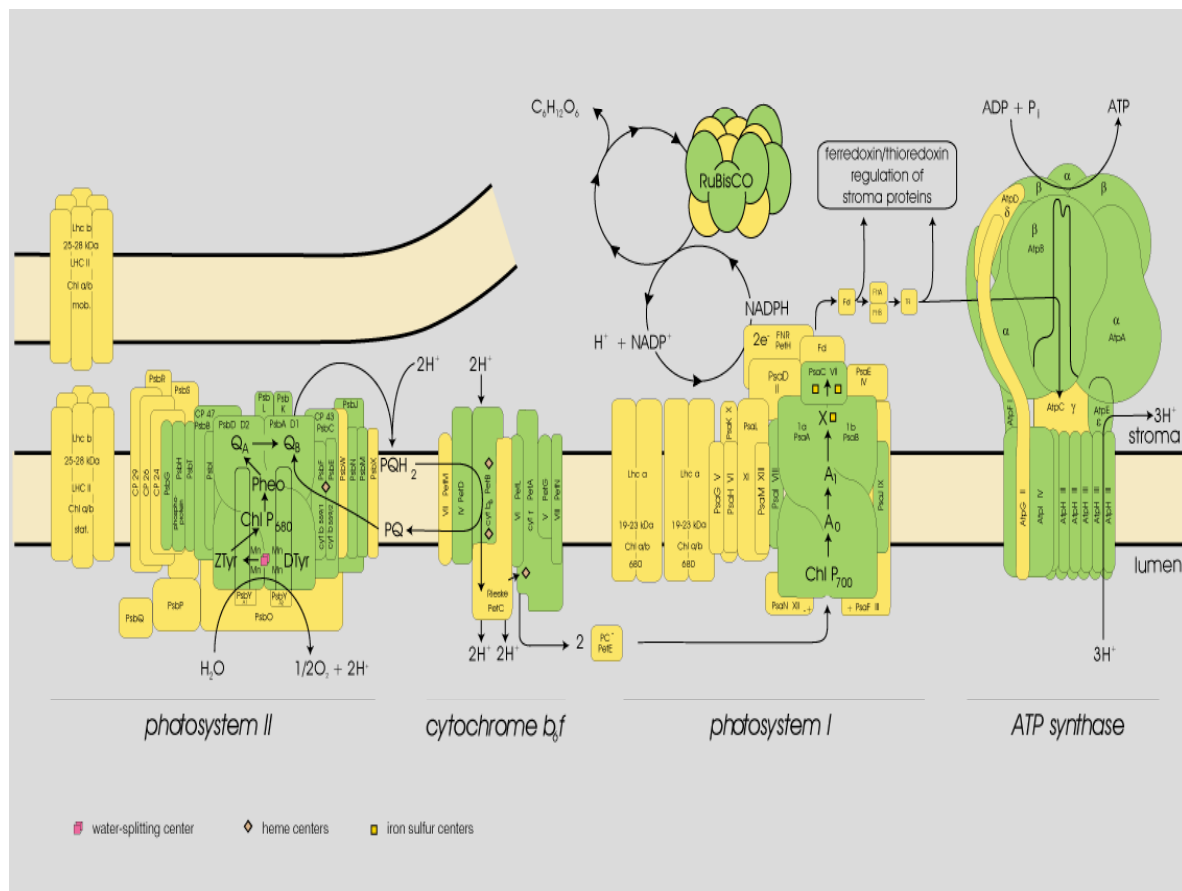


Fig. 1. Model scheme of the thylakoid membrane. The main protein complexes are indicated. Subunits marked in green are plastid-encoded, those in yellow are nuclear-encoded (adapted from Race et al. 1999).

The **NAD(P)H-dehydrogenase** complex (Ndh complex), homologous to the complex I of the mitochondrial respiratory chain, is formed by eleven plastid-encoded gene products (*ndhA-K*). Mutation studies of NAD(P)H dehydrogenase complex indicated its role in the cyclic electron flow around photosystem I in the light and chlororespiration in the dark (Yu et al. 1993, Burrows et al. 1998, Kofer et al. 1998, Shikanai et al. 1998, Casano et al. 2000, Joët et al. 2001). Except from its function in linear photosynthetic electron transfer, PSI also functions in a cyclic process, transferring electrons through the cytochrome *b₆f* complex so that additional protons can be translocated across the membrane for the purpose of supplying additional ATP (Bendall and Manasse 1995). The cyclic electron flow has been shown to be an important mechanism by which plants can produce extra ATP when exposed to stress

conditions, such as high light, high temperature or drought (Bendall and Manasse 1995). In the light, the Ndh complex may mediate an electron flow from the stromal reductant NAD(P)H produced indirectly by PSI to the plastoquinone. In the dark, Ndh complex may function as a component of a respiratory chain, whose purpose will be to generate ATP in plastids using the stromal reductant NAD(P)H (Burrows et al. 1998). In the chlororespiration process, reduction of the plastoquinone pool by NAD(P)H is followed by an oxygen-dependent oxidation, resulting in the formation of a pH gradient across the thylakoid membranes (Bennoun 1982). Interestingly, it has been shown that *ndh* mutants displayed a reduced ability of nonphotochemical quenching. The major component of non-photochemical quenching, qE, arises from the trans-thylakoid pH gradient. In the wild-type, oxidation of stromal reductant by the NAD(P)H dehydrogenase complex, accompanied by pumping protons, generates a proton gradient necessary to form qE. Thus, the Ndh complex-mediated electron transport may also be important for the down-regulation of PSII (Burrows et al. 1998).

One of the striking features of thylakoid membranes and the photosynthetic apparatus is their flexibility to acclimate to changing environmental conditions. **The adaptation processes** can differ in time ranges from seconds or minutes (*short-term*), to days and even longer periods (*long-term*). One of the key processes of *short-term* adaptation is the redox-controlled kinase/phosphatase system operating in the energy spill-over between the two photosystems, a process also known as state 1/state 2 transitions (Allen 1992, Allen and Nillson 1997, Gal et al. 1997). During the operation of the state transition mechanism, reduction of plastoquinone (an electron carrier ultimately connecting both photosystems) and the cytochrome *b₆f* complex activates a thylakoid-bound kinase which then phosphorylates the LHCII antenna, causing a change in protein recognition that results in redistribution of energy from photosystem II (state 1) to photosystem I (state 2). As discussed above, the cytochrome *b₆f* complex plays a role of a redox sensor, which upon binding of a reduced plastoquinone molecule at the Q_o site changes the position of the Rieske protein from distal to proximal (Zito et al. 1999, Vener et al. 1997, Wollman 2001). The reverse transition is initiated by a turnover of plastoquinol at the cytochrome *b₆f* binding site, followed by a switch of the Rieske protein conformation from proximal to distal, subsequent inactivation of the protein kinase, and return of dephosphorylated LHCII to PSII (Figure 2). Activation of an LHCII kinase therefore decreases the absorption of light by photosystem II and increases that by photosystem I. This adaptation typically occurs in the range of a few seconds. Thylakoid

membrane proteins which can be phosphorylated in a redox-regulated and light-dependent way are PSII proteins, namely D1 and D2, CP43, PsbH, antenna apoprotein and the PSI protein PsaH which is required for the docking of phospho-LHCII when it acts as a light-harvesting antenna of photosystem I (Gal et al. 1997, Lunde et al. 2000, Vener et al. 2001). The existence of two independent kinase systems, one for PSII core proteins and another for LHCII proteins has been proposed (Gal et al. 1997, Rintamäki et al. 1997, Carlberg et al. 1999, Rintamäki et al. 2000, Lunde et al. 2000), although none of them has been verified until now. Recently, Rintamäki et al. (2000) have shown that regulation of the activity of LHCII kinase is likely to be mediated by the chloroplast ferredoxin-thioredoxin system in which the LHCII kinase activity is modulated not only by the redox state of plastoquinon and the cytochrome *b₆f* complex, but also by redox reactions of its disulfide bonds through thioredoxin. In spite of various attempts, no distinct LHCII kinase has been identified with certainty, however, recent analyses of Snyder and Kohorn (1999) identified three related kinases in *Arabidopsis*, designated TAK 1 - 3, which originate in nuclear genes and could be imported into chloroplasts. They reside in thylakoids, and were able to phosphorylate LHCII *in vitro*.

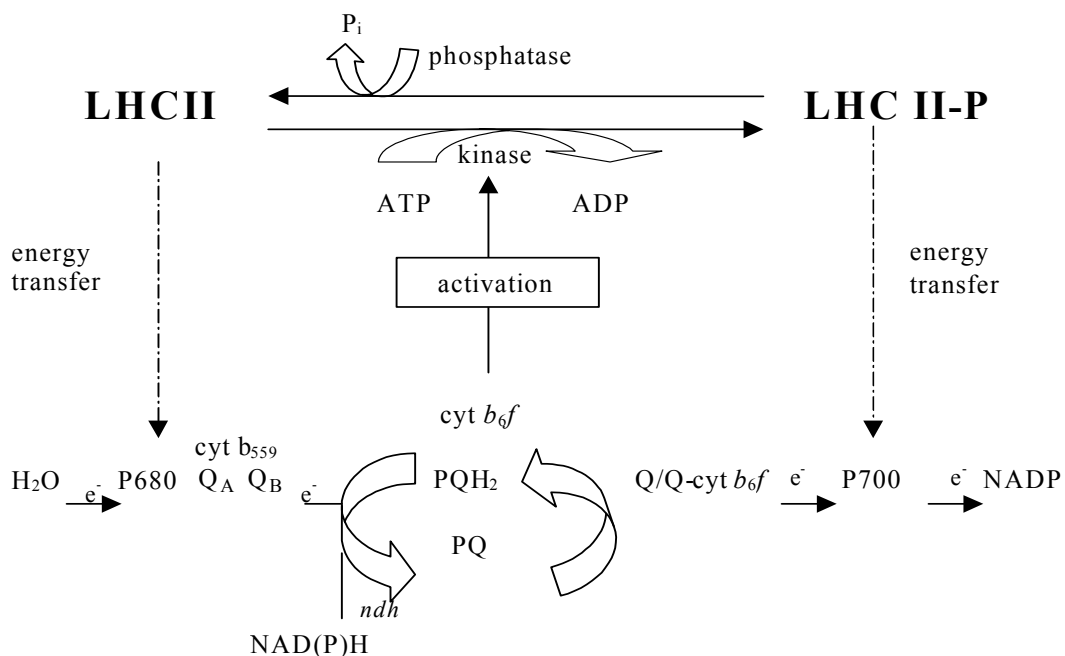


Fig. 2. Control of distribution of excitation energy between PSII (P680) and PSI (P700). The redox status of the plastoquinone pool activates or inactivates an LHCII protein kinase resulting in phosphorylation or dephosphorylation of LHCII, respectively. The LHCII phosphatase is redox-independent. The plastoquinol pool is oxidized by PSI and reduced by PSII as well as by NAD(P)H dehydrogenase (*ndh*). Adapted from Allen 1992.

Protection against photooxidative damages of the photosynthetic apparatus. When light energy absorbed by plants becomes excessive relative to the capacity of photosynthesis, the xanthophyll cycle represents one means to protect plants from photooxidative damage. During illumination of chloroplasts at high photon flux densities the accumulation of excitation energy in the light-harvesting antenna of the photosystems favors the production of triplet excited chlorophyll molecules (^3Chl) that can interact with O_2 to generate reactive singlet oxygen ($^1\text{O}_2$), and subsequently a production of damaging reactive oxygen species, such as superoxide, hydrogen peroxide, or hydroxyl radicals. In the xanthophyll cycle, the xanthophyll violaxanthin is reversibly deepoxidized to zeaxanthin via the intermediate antheraxanthin under the action of the enzyme violaxanthin deepoxidase (Figure 3). Deepoxidation of violaxanthin is involved in the conversion of PSII to a state of high thermal energy dissipation and low chlorophyll fluorescence emission. The violaxanthin cycle takes place in PSII and PSI from a free pool of violaxanthin at the interface between the LHCs and a lipid environment. It is correlated with the process of nonphotochemical thermal dissipation of the absorbed photons excess (non-photochemical quenching, NPQ). The minor PSII antenna proteins, CP24, CP26, and CP29, contain protonatable amino acid residues which might sense a low lumenal pH, and trigger NPQ as an answer to the acidification of the thylakoid lumen (Walters et al. 1994, Walters et al. 1996, Pesaresi et al. 1997, Ruban et al. 1998). However, recently reported antisense inhibition of the CP26 and CP29 proteins in *Arabidopsis* excluded their direct role in the formation of NPQ (Andersson et al. 2001). The involvement of minor antenna proteins in the NPQ mechanism is probably due to carotenoid binding. Carotenoids are able to function in photoprotection by both quenching $^1\text{O}_2^*$ and/or by preventing its formation from $^3\text{Chl}^*$. Transition to the S_1 excited state of carotenoids makes an energy transfer from the $^1\text{O}_2^*$ to the xanthophyll molecule possible. In principle, any xanthophyll molecule with more than 9 conjugated double bonds should exhibit an S_1 state level lower than singlet oxygen. The process of $^3\text{Chl}^*$ quenching has been proposed to act in a similar way (Demmig-Adams 1990, Horton 1996, Ramelli et al. 1999, Croce et al. 1999, Bassi et al. 1999, Verhoeven et al. 1999, Havaux and Niyogi 1999, Ruban et al. 1999, Ruban et al. 2000). As yet, the molecular mechanism of NPQ is not fully understood. However, an increasing number of mutants with impaired violaxanthin cycle and NPQ, such as the *Arabidopsis* violaxanthin de-epoxidation mutant (Niyogi et al. 1998) or the barley *chlorina f2* mutant lacking chlorophyll *b* and LHCII apoproteins (Tardy and Havaux 1997), show a clear interaction between the processes of NPQ and the xanthophyll cycle. The recently isolated *Arabidopsis* mutant *npq4-1*, defective in the qE component of NPQ, was lacking PsbS, a

nuclear-encoded, intrinsic chlorophyll-binding protein of PSII. The structure of the four-helical PsbS protein was proposed to resemble that of the LHC protein ancestor. However, its primary function would be energy dissipation rather than light harvesting (Xiao-Ping et al. 2000).

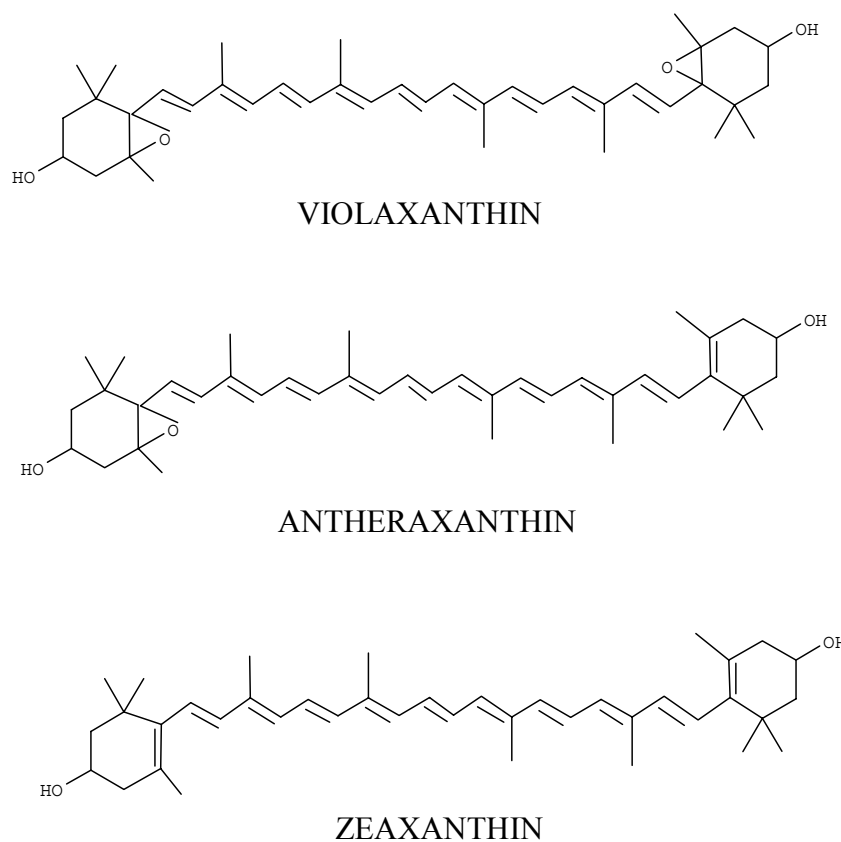


Fig. 3. Molecular structure of xanthophyll – cycle pigments.

The genetic system of plastids. At the beginning of this century the observation of non-Mendelian mutants (Baur 1909, Correns 1909) suggested the existence of a genetic system in plastids. More than thirty years ago the existence of a unique DNA species in plastids was verified (Sager and Ishida 1963). Since then, the structure of the plastid genome and expression of its genes is a field of intensive studies. It is now undisputable that chloroplasts, as well as mitochondria, are of prokaryotic origin and arose from free-living, oxygen-producing cyanobacteria (chloroplast) and oxygen-consuming proteobacteria (mitochondria), respectively, being incorporated into a proto-eukaryotic and eukaryotic cell by an endosymbiotic process (Margulis 1970, Gray 1992, Bhattacharya and Medlin 1998, Herrmann 1997, Martin and Müller 1998). During evolution, the incorporated genomes exported their genes to the nucleus through endosymbiotic gene transfer, which resulted in the compartmented, integrated eukaryotic genetic system under the regulatory dominance of the nucleus (Brennicke et al. 1993, Herrmann 1997, Martin and Herrmann 1998, Martin et al. 1998, Race et al. 1999).

Chloroplast DNAs of higher plants are double-stranded, circular molecules with sizes between 120 - 160 kbp. They consist of two copies of inverted repeats (IR_A and IR_B), separated by a large and a small single-copy region (LSC and SSC, respectively). The genes found in plastid chromosomes have been divided into several categories:

1. Genes for the photosynthetic apparatus:
 - a. Photosystem I, II and cytochrome *b₆f* genes;
 - b. ATP synthase genes;
 - c. NAD(P)H dehydrogenase genes;
 - d. RuBisCo;
2. RNA genes and genes for the genetic apparatus;
3. Other genes:
 - a. conserved ORFs;
 - b. potential protein genes.

During the last decade, the plastid chromosomes from several photosynthetic organisms, including *Nicotiana tabacum* (Shinozaki et al. 1986), *Pisum sativum* (Bookjans et al. 1986), *Marchantia polymorpha* (Ohya et al. 1986), *Oryza sativa* (Hiratsuka et al. 1989), *Pinus thunbergii* (Wakasugi et al. 1994), *Zea mays* (Maier et al. 1995), *Arabidopsis thaliana* (Sato

In addition to approximately 100 identified genes, plastid genomes encode several reading frames of unknown function (named *ycf*, hypothetical chloroplast reading frame) which most probably represent functional genes, since they are often genetically conserved. The principal aim of this thesis was the identification and functional characterization of the proteins encoded by two such reading frames of the tobacco plastid genome, namely *ycf9* (ORF62) and *ycf10* (ORF229).

The function of plastid-encoded genes can be effectively analyzed using reverse genetics methods (Boynton et al. 1988, Svab et al. 1990). Plastid DNA transformation techniques have been developed during the past 20 years and were optimized for transformation of algae as well as for three higher plant species: tobacco (Svab et al. 1990), potato (Sidorov et al. 1999) and tomato (Ruf et al. 2001). Until now, two methods for introduction of foreign DNA into chloroplast DNA have been established: particle bombardment, first established for *Chlamydomonas* (Boynton et al. 1988), and subsequently for *Nicotiana tabacum* (Svab et al. 1990), and a polyethylene glycol (PEG)-based approach with protoplasts (Golds et al. 1993, O'Neil et al. 1993, Koop and Kofer 1995, Koop et al. 1996). With both methods, once the foreign DNA is delivered into the chloroplasts, it is becoming incorporated into plastid genome by homologous recombination. The transformation of plastid chromosomes requires a plastid-specific selectable marker gene to promote segregation of transformed and wild-type genome copies. The most popular marker is the prokaryotic *aadA* (aminoglycoside adenylyl transferase) gene conferring resistance to spectinomycin and streptomycin (Goldschmidt-Clermont 1991).

Because the chloroplast genome is present in multiple copies, the primary plastid transformant is usually heteroplastomic, containing a mixture of transformed and wild-type genome copies. The regeneration of transformants under selective pressure allows plastome segregation and leads to cell lines that may carry only the mutated plastome copies. This state is designated as “homoplastomic” (Allison et al. 1996, Koop et al. 1998). However, only disruption of chloroplast genes whose functions are not necessary for cell viability leads to the homoplastomic state after a few regeneration cycles. Inactivation of an essential gene leads to a heteroplastomic state which remains as long as the selective pressure for the disrupted gene is maintained (Drescher et al. 2000).

Estimation of the homoplastomic status of chloroplast transformants is crucial and one of the more controversial points of molecular analysis. In contrast to unicellular algae like *Chlamydomonas reinhardtii* (Rochaix 1995 and 1997) that contain only a single plastid with approximately 80 chromosome copies per cell, the higher plant plastome with its 5.000 - 10.000 chromosomes per cell (Herrmann and Possingham 1980) is an especially difficult material for homoplastomy state analyses. Analysis is even more complicated by the finding that higher plants may contain copies of promiscuous plastid DNA fragments in both, nucleus and mitochondria (Ellis 1982, Stern and Lonsdale 1982, Ayliffe and Timmis 1992) that analytically may be interpreted as residual wild-type plastid DNA copies even if all non-transformed plastid chromosome copies have been segregated and eliminated. Thus, a method for isolation of pure, uncontaminated plastid DNA is lacking. In this thesis a protocol of pulsed-field gel electrophoresis (Schwartz and Cantor 1984) was established that can fulfil this task.

The gene *ycf9* is ubiquitous among organisms performing oxygenic photosynthesis, both in prokaryotes (cyanobacteria) and eukaryotes (Cryptophyta, Euglenoids, Glaucocystophyceae, Rhodophyta, Stramenopiles and Viridiplantae). It is a small open reading frame of 62 codons present in all chloroplast genomes of photosynthetically active organisms analyzed so far, and has not been phylogenetically transferred into the nucleus, as various other chloroplast open reading frames. In tobacco, *ycf9* is located in a small gene cluster, flanked upstream by the PSII genes *psbD* and *psbC* and downstream by the *trnG* gene. To understand the function of the *ycf9* the site-directed inactivation approach was applied to tobacco plants. *Ycf9*, which is predicted to encode a 6.5 kDa protein with two putative membrane spanning segments, was an interesting case for reverse genetic analyses, because no reliable analyses of its function in plant cells had been presented at the beginning of my work. It was previously observed that *Chlamydomonas* strains with inactivated *ycf9* displayed a wild-type phenotype when grown under heterotrophic conditions (i.e. on medium containing acetate as a carbon source) (Higgs et al. 1998). Presently, several other research groups attempted to clarify the role of *ycf9* in higher plants. However, this yielded widely different conclusions not only of localization of its protein product, but also of its function for cell viability, ranging from potential lethality to neutrality. Mäenpää et al. (2000) presented results of experiments based on the *ycf9* gene inactivation in tobacco and concluded that it was an essential gene, since no homoplastomic transformants could be recovered. These authors had suggested that the product was localized in the chloroplast stromal membranes and likely to be associated with PSI. In yet another

study, also based on chloroplast gene inactivation in tobacco (Ruf et al. 2000), homoplastomic transformants were recovered, but the *ycf9* product was now presented as the first member of a new family of antenna proteins.

The gene *ycf10* is conserved in algae and in higher and lower plants. It consists of 229 - 231 amino acid residues forming four membrane spanning domains. The gene was shown to be cotranscribed with the *petA* gene in pea (Willey and Gray 1990), and to be located upstream of the *petA* gene in tobacco (Shinozaki et al. 1986), rice (Hiratsuka et al. 1989), and *Marchantia* (Ohyama et al. 1986). The putative *ycf10* gene product was first designed HBP (for heme-binding protein) because of a short region of homology to the heme-binding domain of two cytochrome *b* polypeptides (Willey and Gray 1990). After immunolocalization in the inner envelope membrane of the pea chloroplasts (Sasaki et al. 1993), the gene was renamed *cemA* (chloroplast envelope membrane protein A). The cyanobacterial *cotA* gene, which displays high sequence identity to *ycf10* from higher plants (Katoh et al. 1996a) has been shown to play a role in the light-induced proton extrusion (Katoh et al. 1996b). In *Chlamydomonas reinhardtii* *ycf10* was disrupted using biolistic chloroplast transformation, and its role in the inorganic carbon (Ci) uptake into chloroplasts has been proposed (Rolland et al. 1997). Results presented below are based on the application of the site-directed mutagenesis approach in *Nicotiana tabacum* to clarify the role of the *ycf10* gene product in higher plants.

2. MATERIALS AND METHODS

2.1 Materials

2.1.1 Plant material

For plant transformation experiments as well as for biochemical and biophysical analyses tobacco plants (*Nicotiana tabacum* L. cv. Petit Havana) were grown axenically under standard light conditions ($100 \mu\text{E m}^{-2} \text{ s}^{-1}$) or under low (ca. $10 \mu\text{E m}^{-2} \text{ s}^{-1}$) light regimes generally at 20°C or 25°C, and 16/8 h light/dark cycles (Osram L85W/25 Universal White fluorescent lamps). For a phenotypic comparison, plants were also grown in soil under greenhouse conditions. For the NPQ analysis plants were additionally grown at 17°C under light regimes indicated in the experimental procedures.

2.1.2 Bacterial strains

<i>E. coli</i> DH5 α	Hanahan (1983), Gibco/BRL (Eggenstein)
<i>E. coli</i> XL1-Blue	Stratagene (Heidelberg)
<i>E. coli</i> Top 10	Invitrogen (San Diego, USA)

2.1.3 Vectors

pGEM-Zf(-)	Promega (Madison, USA)
pThioHis	Invitrogen (San Diego, USA)

2.1.4 Recombinant plasmids (cDNA insert)

pTB20	Shinozaki et al. (1986)
pTB22	Shinozaki et al. (1986)
pUC16S <i>aadA</i>	Koop et al. (1996)

2.1.5 Primer list (5' to 3' end)

Oligonucleotides were obtained from MWG-Biotech GmbH (Ebersberg).

ycf9 cloning and sequencing

ycf9 for	CATATAGAATCAATGGATTCAT
ycf9 rev	CATATTCTCTTCGGAACGAT
M13 for	GTAAAACGACGGCCAGT
M13 rev	CAGGAAACAGCTATGAC

ycf9 overexpression

ycf9EcoRI1	CGGAATTCATGACTCTTGCTTTCCA
ycf9EcoRI2	CGGAATTCCTCGTTGTATTTGCTTCT
ycf9XbaI1	GCTCTAGATCAAGAGATGAGAGAATTAA
ycf9XbaI2	GCTCTAGAACCAGAAAATACAACATT

ycf10 cloning and sequencing

ycf10 for	AATAGATTCATTAGTCCGATA
ycf10 rev	TCCCCGATGGTTAGAAAT
ycf10 rev2	AGATGATATTTGTCGAGAAG

aadA primers

aadALI 59	TGCTGGCCGTACATTTGTACG
aadARE 60	CACTACATTTGCTCATCGCC

Primers for pulsed-field gel electrophoresis isolated DNAplastid DNA:

ycf9 for PF	CATATAGAATCAATGGATTCAT
ycf9 rev PF	ACAACGGGTACGCTAATCAA
ycf10 for PF	CTCAGTTAATAAATGTCTGGAA
ycf10 rev PF	TGTATCTTGATTAATTGGAT

mitochondrial DNA:

cox for	CAATGGACGAGGTAGTCGTA
cox rev	CTATTATAGTCCGAATACTCAT

nuclear DNA:

Hex3P CCCTCCTATTTGATGCGCACAC
Hex9M GGATGCATAGGGTATGCACGTCC

Primers for construction of RNA radiolabeled probes

ycf9 for2 TTTGCATTAATTGCAACTTC
ycf9 revT7 CGCGCGTAATACGACTCACTATAGGGCATATTCTC
 TTCGGAACGAT
ycf9 rev2T7 CGCGCGTAATACGACTCACTATAGGGTCTAAATCG
 TCCACACTAAC
psbC for GGAGCAATGAACCTATTTGA
psbC revT7 CGCGCGTAATACGACTCACTATAGGGTCTAAATCG
 TCCACACTAAC
trnG for TCCCGGCACTGCACAA
trnG revT7 CGCGCGTAATACGACTCACTATAGGGATATATTTA
 ATGCTATTTATG
aadA60 revT7 CGCGCGTAATACGACTCACTATAGGGCACTACATT
 TCGCTCATCGCC
ycf10 revT7 CGCGCGTAATACGACTCACTATAGGGATGATAT T
 TGTCGAGAAG
ycf4 for TGGCGATCAGAACATATATG
ycf4 revT7 CGCGCGTAATACGACTCACTATAGGGAGGAATATG
 CGACGATT
petA for CTGTTCTTATTTTACCGGAGG
petA revT7 CGCGCGTAATACGACTCACTATAGGGTACTCGTT
 AATGGTTGATCA

2.1.6 Antibodies

Polyclonal goat anti-rabbit IgG peroxidase-conjugate antibodies were obtained from Sigma Chemical Company (Munich). Rabbit polyclonal anti-phosphothreonine antibodies were obtained from Zymed Laboratories (San Francisco, USA).

2.1.7 Chemicals, enzymes, molecular weight markers

Chemicals

The chemicals used in this work were obtained from Biomol (Hamburg), Difco Laboratories (Detroit, USA), Merck AG (Darmstadt), Roche (Basel, Switzerland), Roth GmbH & Co. (Karlsruhe), Serva Feinbiochemica (Heidelberg), Sigma Chemical Company (Munich), and Qiagen (Hilden).

Restriction enzymes

Restriction enzymes and nucleoside triphosphates were obtained from New England Biolabs (Bad Schwalbach), MBI Fermentas (Vilnius, Lithuania), and Roche (Basel, Switzerland).

Radiolabeled nucleotides

Radiolabeled nucleotides were obtained from Amersham Pharmacia biotech (Freiburg i. Br.).

Molecular weight standards

DNA marker	GIBCO/BRL (Karlsruhe)
RNA marker	GIBCO/BRL (Karlsruhe)
λ DNA-PFGE marker	Amersham Pharmacia biotech (Freiburg i. Br.)

Protein molecular weight standards for SDS page

SDS 17S	Sigma Chemical Comp. (Munich)
SDS 7	Sigma Chemical Comp. (Munich)
<i>See Blue</i> prestained marker	Invitrogen (San Diego, USA)

2.1.8 Media for growth of plants and bacteria

Plant growth media

The B5 medium was prepared according to Gamborg et al. (1968), protoplast culture media (PCN and PIN) according to Koop and Kofer (1995). RMOP medium for shoot regeneration was prepared according to Svab and Maliga (1993).

Table 1. Composition of plant growth media (adapted from Brunner 1997).

	mg/l	B5	F-PCN	F-PIN	RMOP
Macro salts	NH ₄ NO ₃				1650
	KNO ₃	2500	1012	1012	1900
	CaCl ₂ *2H ₂ O	150	440	440	440
	MgSO ₄ *7H ₂ O	250	370	370	370
	KH ₂ PO ₄		170	170	170
	NaH ₂ PO ₄ *H ₂ O	150			
	(NH ₄) ₂ SO ₄	134			
	NH ₄ -Succinat			0.2 mM	0.2 mM
Micro salts	EDTA-Fe(III)Na	40	40	40	40
	KJ	0.75	0.75	0.75	0.83
	H ₃ BO ₃	3	3	3	6.2
	MnSO ₄ *H ₂ O	10	10	10	22.3
	ZnSO ₄ *7H ₂ O	2	2	2	8.6
	Na ₂ MoO ₄ *2H ₂ O	0.25	0.25	0.25	0.25
	CuSO ₄ *5H ₂ O	0.025	0.025	0.025	0.025
	CoCl ₂ *6H ₂ O	0.025	0.025	0.025	0.025
Vitamins	Inositol	100	200	200	100
	Pyridoxin-HCl	1	2	2	
	Thiamin-HCl	10	1	1	1
	Biotine		0.02	0.02	
	Nicotinic acid	1	2	2	
Others	BAP		1	1	1
	NAA		0.1	0.1	0.1
	Polybuffer 74		10 ml	10 ml	
	Sucrose	20 000		130 000	30 000
	Glucose		85 000		
	pH	5.7 (KOH)	5.8 (KOH)	5.8 (KOH)	5.8 (KOH)
	Osmolarity		550 (mosm/l)	550 (mosm/l)	
	Agar	7000			8000

Protoplast isolation (Dovzhenko et al. 1998)

Enzymes	100 mg/ml	Macerozym R10 and Cellulase R10 (Serva, Heidelberg)
---------	-----------	--

Bacteria growth medium

LB medium (1 l)	10.0 g	peptone
	5.0 g	yeast extract
	10.0 g	NaCl

2.1.9 Buffers and solutions

TE buffer	10.0 mM	Tris-HCl, pH 8.0
	1.0 mM	EDTA
10xTBE	1.0 M	Tris-HCl, pH 8.0
	20.0 mM	EDTA
	0.5 M	boric acid
10xMOPS	0.05 M	Na-acetate, pH 7.0
	0.1 M	MOPS
	0.1 M	EDTA
20xSSC	3.0 M	NaCl
	0.2 M	trisodium citrate x 2H ₂ O
	pH 7.4	
20xSSPE	0.2 M	NaH ₂ PO ₄
	0.3 M	NaCl
	20.0 mM	EDTA
	pH 7.4	
10xPBS	0.75 M	NaCl
	30.0 mM	KCl
	45.0 mM	Na ₂ HPO ₄
	15.0 mM	KH ₂ PO ₄

50 x Denhardt solution	10% (w/v)	bovine serum albumine (BSA)
	10% (w/v)	polyvinylpyrrolidone 10 000
	10% (w/v)	Ficoll 400

2.1.10 Transfer membranes

Hybond nitrocellulose membranes for nucleic acid transfer were purchased from Amersham (Braunschweig). PVDF and nitrocellulose PROTRAN membranes for protein transfer were obtained from Schleicher & Schuell (Dassel) or PALL (Portsmouth, England).

2.2 Methods

2.2.1 Construction of plant transformation vectors

2.2.1.1 Construction of the recombinant plasmid for *ycf9* inactivation

A 2425 bp BamHI-EcoRI fragment of tobacco plastid DNA containing *ycf9* was excised from the plasmid pTB20 with BamHI (nucleotide position 36463) and EcoRI (position 38889), ligated into the vector pGEM-Zf(-), and cloned into *E. coli* DH5 α . The *ycf9* gene was inactivated by digestion with MunI at nucleotide position 37609, followed by filling in the recessed ends with the Klenow fragment of DNA polymerase I, and subsequent ligation with the blunt-ended, terminator-less *aadA* cassette. An individual clone carrying the *aadA* cassette in the same polarity as *ycf9* was used for transformation.

2.2.1.2 Construction of the recombinant plasmid for *ycf10* inactivation

A 3235 bp fragment of tobacco plastid DNA containing *ycf10* was excised from the plasmid pTB22 with KpnI (nucleotide position 62075) and SalI (nucleotide position 65310), ligated into the vector pGEM-Zf(-), and cloned into *E. coli* DH5 α . The *ycf10* gene was inactivated by digestion with BbsI at nucleotide position 63571, and ligation with the blunt-ended, terminator-less *aadA* cassette. An individual clone carrying the *aadA* cassette in the same polarity as *ycf10* was used for transformation.

2.2.2 Plant transformation

2.2.2.1 Seed sterilization

Tobacco seeds were sterilized by 1 min incubation in 70% (v/v) ethanol followed by 5 min incubation in 5% (w/v) Dimanine C (Bayer, Leverkusen) solution. The sterilized seeds were washed 3 x in sterile water.

2.2.2.2 Plastid transformation

The biolistic transformation technique (Boynton et al. 1988, Svab et al. 1990, Svab and Maliga 1993) was applied. 60 mg of gold particles (0.6 μm ; BioRad, USA) were suspended in 220 μl sterile water and mixed with 25 μl of purified plasmid DNA (1 $\mu\text{g}/\mu\text{l}$), 250 μl of 2.5 M CaCl_2 , 50 μl spermidin (0.1 M), followed by 2x washing of DNA-gold particles in 100% ethanol (p.a.), and final suspension of DNA-gold particles in 72 μl of 100% ethanol. The gold particles were delivered into plant cells using the Particle Gun - PDS 1000/He, Bio-Rad (USA).

Parameters used with the Particle Gun

Helium pressure:	1100 psi
Rupture discs:	900 psi
Distance rupture disc/macrocarrier:	8 - 10 mm
Distance macrocarrier/stopping screen:	10 mm
Distance stopping plate/table:	7 cm
Vacuum:	0.85 bar (26 – 27 inches Hg)

For each construct 20 leaves were shot and dissected 48 h after particle bombardment into 3 x 3 mm segments that were kept under non-selective conditions for 3 days, and then under selective conditions.

2.2.2.3 Selection and regeneration of mutants

Selection with 500 mg/liter of spectinomycin started three days after transformation. Green colonies began to appear and grow vigorously after approximately 3 weeks, while untransformed cell lines were bleaching and showed impaired growth. Resistant calluses were transferred to RMOP medium and cultivated in Petri dishes until shoot formation. For further segregation transplastomic lines were transferred into Petri dishes containing fresh medium at 3 - 4 week intervals. After several rounds of segregation, small green shoots of homoplastomic lines were transferred to 750 ml glass jars containing B5 agar with antibiotic, and grown for 4 - 6 weeks until use.

2.2.3 Isolation and fractionation of chloroplasts

2.2.3.1 Isolation of intact chloroplasts

Isolation of intact plastids was performed according to Müller and Eichacker (1999).

Homogenization Medium

0.4 M	sorbitol
50 mM	HEPES-KOH, pH 8.0
2 mM	EDTA, pH 7.5

Percoll Gradient Solution

45% / 85%	Percoll (w/v)
0.4 M	sorbitol
50 mM	HEPES-KOH, pH 8.0
2 mM	EDTA, pH 7.5

Washing Buffer

0.4 M	sorbitol
50 mM	HEPES-KOH, pH 8.0

10 - 20 g of freshly harvested leaf material was homogenized in approximately 100 ml of homogenization medium. The homogenate was filtrated through two layers of Miracloth (100 μm , Calbiochem, La Jolla, USA), and centrifuged at 4000 x g for 1 min. The sediment was carefully suspended in 1 ml of homogenization medium and loaded onto 45 - 85% Percoll gradients. The gradients were prepared by loading 10 ml of 45% and 5 ml of 85% Percoll in Corex tubes. After centrifugation of 8 min at 4000 x g in a “swing out” rotor the lower band containing intact plastids was collected using a Pasteur pipette and washed once in washing buffer (centrifugation 3 min, 1000 x g). All preparation steps were performed at 4°C, and isolated plastids were stored in darkness on ice.

2.2.3.2 Fractionation of chloroplasts into stroma and thylakoid membranes

TMK Buffer

10 mM	Tris-HCl, pH 6.8
10 mM	MgCl ₂
20 mM	KCl

Freshly prepared chloroplasts were osmotically ruptured with TMK buffer in a ratio of 100 μg chlorophyll to 0.5 ml buffer. The chloroplasts were lysed for 10 min in darkness on ice and centrifuged for 3 - 5 min at 2000 x g. The supernatant (stroma fraction) was collected, the pellet (thylakoids) was washed twice by centrifugation in TMK buffer. The final pellet was resuspended in TMK buffer. Aliquots of the thylakoids were stored at -70°C .

2.2.3.3 Isolation of the major thylakoid protein complexes

The major thylakoid protein complexes, equivalent to 3×10^8 chloroplasts were solubilized 10 min on ice by 1.5% (w/v) β -dodecylmaltoside (final concentration) as described by Müller and Eichacker (1999). The thylakoid lysate was loaded onto linear 0.1-1.0 M sucrose gradients and centrifuged for 16.5 h at 36 000 x g at 4°C (Beckman “swing out” rotor SP 40 Ti). The sucrose gradients were top-to-bottom fractionated into 35 fractions of 300 μl each using an ISCO 640 gradient fractionator (Instrumentation Specialties Company, USA). For further analyses individual gradient fractions were precipitated with 10% (w/v) trichloroacetic acid and washed with 100% acetone.

2.2.3.4 Washing of thylakoid membranes with Na₂CO₃

HS Buffer

0.1 M	sucrose
10 mM	HEPES-KOH, pH 8.0

Carbonate Buffer

0.1 M	Na ₂ CO ₃
0.1 M	sucrose
10 mM	HEPES-KOH, pH 8.0

To dissociate peripherally associated proteins from thylakoid membranes a Na₂CO₃ washing step was applied. Thylakoid samples at a concentration of 0.5 mg chlorophyll/ml were washed with HS buffer and incubated with 100 µl Na₂CO₃ for 10 min on ice. Washed thylakoids were pelleted by centrifugation for 30 min at 18 000 x g and suspended in an appropriate volume of HS buffer.

2.2.3.5 Purification and fractionation of chloroplast envelope membranes

Tricine Solution (1l)

20 ml	0.5 M Tricine, pH 7.9
2 ml	0.5 M EDTA, pH 8.0
72 µl	β-mercaptoethanol
1 ml	PMSF

0.65 M sucrose (200 ml)

44.48 g	sucrose
4.0 ml	0.5 M Tricine, pH 7.9
14.4 µl	β-mercaptoethanol
0.2 ml	PMSF

Sucrose Gradients (each 200 ml)

	0.996 M	0.800 M	0.465 M
sucrose	68.57 g	54.76 g	31.82 g
0.5 M Na _i PO ₄ , pH 7.9	4 ml	4 ml	4 ml
0.5 M EDTA, pH 8.0	0.4 ml	0.4 ml	0.4 ml

Na_iPO₄ Buffer Stock

93.2 ml 0.5 M Na₂HPO₄
6.5 ml 0.5 M NaH₂PO₄
pH 7.9

Na_iPO₄ Buffer (1l)

20 ml 0.5 M Na_iPO₄ Buffer Stock, pH 7.9
72 µl β-mercaptoethanol
1 ml PMSF

Purified intact plastids (see Section 2.2.3.1) were suspended in 10 ml of 0.65 M sucrose and ruptured by homogenization in a Dounce homogenizer on ice. The suspension of broken chloroplasts was filled up to 40 ml with Tricine solution and centrifuged for 1 h at 186 000 x g (Beckman TT45 rotor) at 4°C. The thylakoid pellet containing the envelope fraction was then suspended in Tricine solution and loaded onto sucrose gradients consisting of 7 ml 0.996 M / 10 ml 0.800 M / 8 ml 0.465 M sucrose solutions. Envelope membranes were isolated by centrifugation at 113 000 x g (Beckman SW27 rotor) for 3 h at 4°C. During this centrifugation step envelope membranes separate into three bands: outer envelope + RuBisCo (in 0.465 M sucrose), outer envelope (0.465 M/0.800 M sucrose), inner envelope (0.800 M/0.966 M sucrose), and thylakoid membrane pellet. Inner and outer envelope membranes were collected and washed 1:3 in Na_iPO₄ buffer by 1 h centrifugation at 113 000 x g at 4°C.

2.2.4 Overexpression of proteins *in vitro***2.2.4.1 Cloning of *ycf9* for overexpression**

A DNA fragment containing the *ycf9* gene was amplified using the relevant primer pair with introduced EcoRI and XbaI restriction sites on their 5' ends (listed in Section 2.1.5). For

overexpression of truncated proteins three additional PCR products were amplified using the primer pairs ycf9EcoRI1 and ycf9XbaI2, ycf9EcoRI2 and ycf9XbaI1, ycf9EcoRI1 and ycf9XbaI2. Amplified *ycf9* fragments were digested with EcoRI and XbaI enzymes and cloned into the pThioHis expression vector (His-Path ThioFusion Expression system, Invitrogen, USA).

2.2.4.2 Overexpression of proteins in *E. coli*

An overnight culture of *E. coli* Top 10 cells was transformed with the overexpression plasmid and induced by 100 mM IPTG. The samples from 0, 1, 2, 3 and 4 hrs of induction were fractionated to soluble and insoluble fraction. Bacterial cells were suspended in buffer containing 20 mM Tris-HCl (pH 8.0), 2.5 mM EDTA and 5 mM imidazol and disrupted by three sonication-freeze-thaw cycles (Branson Sonifier W-250). Soluble and insoluble protein fractions were separated by a 10 min centrifugation at 10 000 x g. Additionally, remaining homogenat samples were precipitated with 10% (v/v) TCA followed by washing of proteins with 100% acetone. The samples were analyzed by SDS-PAGE and Western analyses.

2.2.5 Protein analysis

2.2.5.1 Determination of the protein concentration

The Bradford assay (Bradford, 1976) was used for the determination of protein concentrations.

Bradford Stock Solution

100 ml	100% ethanol
200 ml	80% phosphoric acid
359 mg	Serva Blue G

Bradford Working Buffer

425 ml	H ₂ O
15 ml	100% ethanol
30 ml	80% phosphoric acid
30 ml	Bradford Stock Solution

A protein solution (maximal 100 μ l) was mixed with 1 ml of Bradford Working buffer. After 10 min the absorbance of the sample was measured at 595 nm. The protein concentration in the sample was determined using a standard curve with samples of known protein concentrations (BSA from 1 to 20 μ g)

2.2.5.2 Phosphorylation of proteins *in vitro*

Phosphorylation Mixture

50 mM	Tricine-NaOH, pH 7.8
100 mM	sorbitol
5.0 mM	MgCl ₂
10 mM	NaF
0.5 μ l/100 μ l reaction volume	[γ ³² P]-ATP

4x LSB (Laemmli Sample Buffer)

0.25 M	Tris-HCl, pH 6.8
8% (w/v)	SDS
40% (w/v)	glycerol
20% (v/v)	β -mercaptoethanol
0.016% (v/v)	Bromophenol Blue

Thylakoid membranes with a concentration of 1.0 - 1.5 mg chlorophyll/ml were pelleted and resuspended in 100 μ l of phosphorylation mix. The phosphorylation reaction was carried out for 30 min in light at room temperature and stopped directly by addition of 30 μ l of 4 x LBS. Autoradiographs for the phosphorylation analyses were evaluated using Fuji Bio Imaging plates type BASIII, a Fuji Bio Imaging analyzer, the BAS200025 software package (Fuji, Japan) and the TINA software package v2.08 beta (Raytest, Spröckhovel).

2.2.5.3 Protein gel electrophoresis

2.2.5.3.1 SDS-denaturing polyacrylamide (PAA) gels

2.2.5.3.1.1 Laemmli gel system (Laemmli 1970)

10 x Laemmli Buffer

0.25 M	Tris-HCl, pH 8.5
1.92 M	glycine
1% (w/v)	SDS

Pipetting scheme of Laemmli gels

	15% separating gel	12% separating gel	stacking gel
30% acrylamide / 0.8% bisacrylamide	30 ml	24 ml	2.7 ml
3M Tris-HCl, pH 8.8	7.5 ml	7.5 ml	-
1M Tris-HCl, pH 6.8	-	-	1.25 ml
10% (w/v) SDS	0.6 ml	0.6 ml	0.1 ml
10% (w/v) APS	180 μ l	180 μ l	50 μ l
TEMED	60 μ l	60 μ l	17 μ l
H ₂ O	ad 60 ml	ad 60 ml	ad 10 ml

2.2.5.3.1.2 Schagger/von Jagow gel system (Schagger and von Jagow 1987)

Gel Buffer

3 M	Tris-HCl, pH 8.45
0.3% (w/v)	SDS

5 x Cathode Buffer

0.5 M	Tris
0.5 M	Tricine
0.5% (w/v)	SDS
	pH 8.25

5 x Anode Buffer

1 M	Tris-HCl, pH 8.9
-----	------------------

Sample Buffer (carbonate buffer)

100 mM	Na ₂ CO ₃
10% (w/v)	sucrose
50 mM	DTT

Pipetting scheme of gels

	10% separating gel	13% separating gel	20% separating gel	stacking gel
49.5% acrylamide / 3% bisacrylamide	12.2 ml	15.75 ml	20 ml	2 ml
Gel Buffer	20 ml	20 ml	20 ml	6.2 ml
glycerol	8 g	8 g	8 g	-
10% (w/v) APS	200 µl	200 µl	200 µl	200 µl
TEMED	20 µl	20 µl	20 µl	20 µl
H ₂ O	ad 60 ml	ad 60 ml	ad 60 ml	ad 25 ml

2.2.5.3.2 Non-denaturing PAGE

2.2.5.3.2.1 Non-denaturing Deriphat-PAGE

Pipetting scheme of Deriphat-PAGE gels

	4% separating gel	8% separating gel	4% stacking gel
48% acrylamide/ 1.5% bisacrylamide	1.3 ml	2.6 ml	0.6 ml
120 mM Tris, 480 mM glycine	1.6 ml	1.6 ml	1 ml
glycerol (50% w/v)	3.2 ml	3.2 ml	2 ml
APS 10% (w/v)	32 μ l	32 μ l	40 μ l
TEMED	12 μ l	12 μ l	10 μ l
H ₂ O	ad 16 ml	ad 16 ml	ad 10 ml

Cathode Buffer

12 mM Tris
96 mM glycine
0.1% (w/v) Deriphat-160
pH 8.3

Anode Buffer

12 mM Tris
96 mM glycine
pH 8.3

Solubilization Mixture

1.6% (w/v)	α -dodecylmaltoside
12 mM	Tris-HCl, pH 8.6
96 mM	glycine
10% (w/v)	glycerol

From a preparation of thylakoid membranes with a chlorophyll concentration of 2 mg/ml, a sample corresponding to 12.5 μ g chlorophyll was taken and solubilized by vortexing for 1 min with an equal volume of solubilization buffer. The sample was then centrifuged for 10 min at 10 000 x g and the supernatant was applied to the gel. The Deriphat-PAGE experiments were performed by Dr. A. Sokolenko.

2.2.5.3.2.2 Non-denaturing Blue-Native PAGE (Schägger and von Jagow 1991)

Stacking Gel (4%)

4% PAA	[acrylamid/bisacrylamid = 30/0.8]
500 mM	ϵ -aminocapronic acid
50 mM	bis-Tris/HCl pH 7,0

Separating Gel

6-12% PAA	[acrylamid/bisacrylamid = 30/0,8]
500 mM	ϵ -aminocapronic acid
50 mM	bis-Tris/HCl, pH 7.0

Cathode Buffer

50 mM	Tricine
15 mM	bis-Tris/HCl, pH 7.0
0,02% (w/v)	Serva Blue G

Anode Buffer

50 mM	bis-Tris/HCl, pH 7.0
-------	----------------------

ACA Buffer

750 mM	ϵ -aminocaproic acid
50 mM	bis-Tris/HCl, pH 7.0
0.5 mM	EDTA

Solubilization Buffer

2% (w/v)	SDS
66 mM	DTT
66 mM	Na ₂ CO ₃

The method is based on the Schagger and von Jagow (1991) system for separation of “native” protein complexes. Thylakoid membranes corresponding to 1×10^8 plastids were suspended in 60 μ l of ACA buffer and solubilized in 5 μ l DM (10% (w/v) in H₂O). Solubilized thylakoids were mixed with a buffer containing 5 μ l of 5% (w/v) Serva Blue G, 750 mM ϵ -aminocaproic acid. The samples were then loaded onto the gel and electrophoresed at 150 V. After entering the separation gel, electrophoresis was continued at 500 - 1000 V. When the gel front reached half the distance, cathode buffer containing Serva Blue G was replaced by the same buffer without staining reagent. All solutions were pre-cooled to 4°C; electrophoresis was performed at 10°C. The specifications refer to 20 \times 20 \times 0,075 cm gels. For the 2nd dimension electrophoresis, gel slices were cut out and incubated at room temperature in solubilization buffer for 20 min. The incubated gel slices were loaded onto denaturing PAA gels.

2.2.5.4 Staining of PAA gels

2.2.5.4.1 Coomassie Brilliant Blue staining

Staining Solution

40%	ethanol
5%	acetic acid
0.3% (w/v)	Coomassie Brilliant Blue R 250 (Serva, Heidelberg)

Destaining Solution

20%	ethanol
7%	acetic acid

The gels were incubated in staining solution for 30 min under constant shaking, and destained until protein bands appeared well.

2.2.5.4.2 Silver staining

Fixation Solution

50%	methanol
12 %	acetic acid
0.05%	37% formaldehyde

Thiosulfate Solution

0.02% (w/v)	Na ₂ S ₂ O ₃
-------------	---

Silver Solution

0.2% (w/v)	AgNO ₃
5%	37% formaldehyde

Developing Solution

6% (w/v)	Na ₂ CO ₃
0.05%	37% formaldehyde
4 mg/ml	Na ₂ S ₂ O ₃

Stopping Solution

50%	methanol
12%	acetic acid

The 1.5 mm gel was incubated for at least 1 h in fixation solution, washed three times for 30 min in 50% ethanol and soaked for 1.5 min in thiosulfate solution. Then, the gel was washed three times for 30 sec with water and incubated in silver solution for 30 min in darkness with constant agitation. The gel was then washed again with water and incubated in developing

solution until the bands reached the desired intensity. The reaction was ended in stopping solution.

2.2.6 Immunological detection of proteins on membranes

2.2.6.1 Transfer of proteins onto nitrocellulose and PVDF membranes

Anode Buffer I

0.025 M Tris

Anode Buffer II

0.3 M Tris

Cathode Buffer

40 mM ε-aminocaproic acid

0.01% (w/v) SDS

Transfer membranes and PAA gels were incubated for 10 min in anode buffer II prior to transfer. PVDF membranes were prewetted in 100% methanol. The proteins were transferred onto membranes using a semi-dry blotting system. Three sheets of Whatman paper were soaked in cathode buffer and placed onto the cathode. The gel was placed on the cathode buffer-soaked Whatman paper and covered with the transfer membrane. Gel and transfer membrane assembly was covered by two layers of Whatman paper soaked in anode buffer II and three layers of Whatman paper soaked in anode buffer I. The transfer was performed for 1.5 - 2.5 h with constant current according to the formula: mA = gel size in cm² x 0.8

2.2.6.2 Staining of blots with Ponceau S

Ponceau S Solution

0.2% (w/v) Ponceau S

1.0% acetic acid

After blotting the membrane was incubated in Ponceau S (3-hydroxy-4-[2-sulfo-4-(sulfo-phenylazo)phenylazo]-2,7-naphthalene disulfonic acid) solution for 10 min at room temperature with agitation. The membrane was rinsed with water and the positions of the molecular marker bands were marked. The membrane was finally destained in water.

2.2.6.3 Immunological detection of proteins

2.2.6.3.1 Western analysis using horseradish peroxidase-conjugated antibodies

Blocking Buffer

1x PBS	
5% (w/v)	dry milk powder
1% (v/v)	Tween 20

Washing Buffer

1x PBS	
1% (v/v)	Tween 20

Solution I Stock

0.25 M	luminol (in DMSO)
0.09 M	p-coumaric acid (in DMSO)

Solution I

2.5 mM	luminol
0.4 mM	p-coumaric acid
0.1 M	Tris-HCl pH 8.5

Solution 2

5.4 mM	H ₂ O ₂
0.1 M	Tris-HCl, pH 8.5

After electrophoretic transfer of the proteins from a PAA gel the membrane was incubated in blocking buffer for 1 h at room temperature. The antisera diluted to the desired concentration in blocking buffer were incubated with the membrane for 2 h at room temperature or

overnight at 4°C. The first antibodies were removed by washing the membrane four times for 10 min in blocking buffer. Anti-rabbit antibodies were diluted in blocking buffer and incubated with the membrane for 1 h at room temperature. The membranes were then washed four times for 10 min in washing buffer and developed in a mixture of solution 1 and 2 (1:1) by incubation for 1.5 min. They were exposed to X-ray films (Hyperfilm; Amersham Life Science, England) for 1 - 20 min.

2.2.7 Antibody generation

2.2.7.1 Preparation of probes for the rabbit immunization

Overexpressed fusion proteins pThioHis-*ycf9* were prepared as described in Sections 2.2.4.1 and 2.2.4.2 and loaded onto 12% PAA gels. After separation, proteins were transferred onto nitrocellulose membrane and, after Ponceau S staining, a band corresponding to overexpressed fusion protein pThioHis-*ycf9* was excised from the membrane. This membrane sector was then dissolved in DMSO and mixed with adjuvant TiterMax™ (CytRX Corporation, Atlanta, USA) at a ratio 1:1. Alternatively, a synthesized Ycf9 oligopeptide, PVVFASPDGWSSNKNVVS, coupled with BSA was used for immunization of rabbits by mixing 350 µg of BSA-Ycf9 protein with 200 µl TiterMax™.

2.2.7.2 Subcutaneous injection of rabbits and antibody preparation (Harlow and Lane 1988)

The injections were started near the back of the neck. The antigen-TiterMax™ suspension was injected generally at three sites. After four weeks, the injection was repeated. Serum samples were taken in two-week intervals after the second boost. Bleeds were done from the ear vein of the rabbits and about 15 ml of blood was taken from each animal. After collection, the blood was allowed to clot for 30 - 60 min at 37°C. The clot was placed at 4°C overnight. The serum was then separated from the clot by centrifugation at 10 000 x g for 10 min at 4°C. Na-azide (0.01%) was added to the supernatant, which was aliquoted and stored at -20°C.

2.2.8 Nucleic acid analysis

2.2.8.1 Standard methods

The presented methods were described (if not indicated otherwise) by Sambrook et al. (1989):

- isolation of plasmid DNA (Birnboim and Doley 1979);
- determination of DNA and RNA concentrations;
- electrophoresis of DNA in agarose gels;
- electrophoresis of RNA in agarose/MOPS/formaldehyd gels;
- restriction of DNA;
- sequencing by the chain termination method (Sanger et al. 1977);
- dephosphorylation with alkaline phosphatase;
- “fill in”-reaction with Klenow DNA polymerase;
- ligation with T4 DNA ligase;
- preparation of competent *E. coli* cells using the CaCl₂ method;
- transformation of *E. coli*;
- polymerase chain reaction (“PCR”, White et al. 1989);
- Southern analysis of DNA;
- Northern analysis of RNA (Ausubel et al. 1987).

2.2.8.2 DNA analysis

2.2.8.2.1 Sequence searches and alignments

Amino acid sequences for predicted *ycf9* and *ycf10* ORFs were retrieved from the fourth iteration of a ψ -blast search (Altschul et al. 1997) run on the server of the National Centre for Biotechnology Information (<http://www.ncbi.nlm.nih.gov/blast/psiblast.cgi>) with the default parameters. Sequence alignments were performed using the CLUSTAL X multiple sequence alignment program (Jeanmougin et al. 1998). Amino acid sequence and protein bank accession numbers are obtained from the following references: *Arabidopsis thaliana* (GI:7525030) (Sato et al. 1999), *Chlamydomonas reinhardtii* (GI:3123110) (Higgs et al. 1998), *Marchantia polymorpha* (GI:140316) (Ohyama et al. 1986), *Nicotiana tabacum* (GI:140318) (Shinozaki et al. 1986), *Oenothera elata* (GI:6723731) (Hupfer et al. 2000),

Oryza sativa (GI:140317) (Hiratsuka et al. 1989), *Pinus thunbergii* (GI:7524713) (Wakasugi et al. 1994), *Pisum sativum* (GI:3123098) (Bookjans et al. 1986), *Spinacia oleracea* (GI:7636103) (Schmitz-Linneweber et al. 2001), and *Zea mays* (GI: 3123113) (Maier et al. 1995).

2.2.8.2.2 Isolation of total DNA and plastid DNA

Isolation of DNA from plants was performed according to Doyle and Doyle (1990).

Extraction Buffer

2% (w/v)	CTAB
1.4 M	NaCl
20 mM	EDTA, pH 8.0
100 mM	Tris-HCl, pH 8.0
100 mM	β -mercaptoethanol

For total cell DNA preparations fresh leaf tissue was used. Plastid DNA preparations started from intact plastids (see Section 2.2.3.1). Small amounts of plant material were homogenized with extraction buffer (100 μ l for a leaf piece, up to 500 μ l for plastid suspensions) and heated for 30 min at 60°C. Proteins were removed from samples by two chloroform/isoamylalcohol (24:1) washing steps, and DNA was precipitated with 2/3 assay volume of 2-propanol. The DNA was pelleted by centrifugation for 20 min at 10 000 x g, washed with 70% ethanol, and dissolved in TE buffer or sterile H₂O.

2.2.8.2.3 Southern analysis of DNA

For a Southern analysis 5 μ g of plastid DNA was restricted with the desired enzyme and electrophoretically separated in an agarose gel. DNA transfer from the gel to nitrocellulose membranes was performed by capillary blotting as described in Sambrook et al. (1989). DNA was fixed to membranes by UV crosslinking (2 x Autocrosslink on “UV-Stratalinker™ 2400”, Stratagene).

2.2.8.2.4 Radioactive probe labeling

2.2.8.2.4.1 Radioactive labeling of PCR products

PCR products (100 ng DNA) were radio-labeled by the random priming method with Klenow enzyme and ^{32}P -dATP or ^{32}P -dCTP (according to Sambrook et al. 1989). For this assay, the Random Primed DNA Labeling Kit from Roche (Basel, Switzerland) was used according to the manufacturer's protocol.

2.2.8.2.4.2 Radioactive labeling of oligodesoxynucleotides

Reaction Mixture (25 μl)

0.5 μg	oligodesoxynucleotides
2.5 μl	10 x PNK buffer
7 μl	$[\gamma\text{-}^{32}\text{P}]\text{-ATP}$
1 μl	T4 polynucleotidkinase

The 5' hydroxy group of synthetic oligonucleotides (primers) was radioactively labeled by 30 minutes incubation at 37°C with T4 polynucleotidkinase (New England Biolabs, Bad Schwalbach). Residual radioactive mononucleotides were removed with 100% ethanol.

2.2.8.2.5 Hybridization procedure

Hybridization Buffer (0.2 l)

10 ml	100 x Denhardt solution
50 ml	20 x SSPE
2 ml	20% (w/v) SDS
4 ml	herring sperm DNA (10 mg/ml)

The membrane was prehybridized for at least 2 h at 65°C in the hybridization buffer. Hybridization was performed by incubation of the membrane with the denatured radiolabeled probe in 10 ml of hybridization buffer overnight at 65°C.

2.2.8.2.6 Isolation of DNA from agarose gels

The GenElute™ Agarose Spin Columns (Supelco, Bellefonte, USA) were used to isolate DNA from agarose gels. The agarose gel slice containing the DNA was placed in the TE buffer washed GenElute Agarose spin column and centrifuged for 10 min at 10 000 x g at room temperature. DNA was precipitated by 3 M sodium acetate : 100% ethanol (0.1 : 2, v/v), and washed with 70% ethanol.

2.2.8.3 RNA analysis

2.2.8.3.1 Isolation of total RNA from plants

Total RNA from plants was isolated using TRIzol Reagent (GIBCO BRL, Karlsruhe) according to the manufacturer's protocol. A small amount of fresh tissue (100 - 200 mg) was frozen in liquid nitrogen and homogenized with TRIzol (1 ml reagent per 100 mg material). The homogenized sample was incubated for 5 min at room temperature, mixed with chloroform (0.2 ml chloroform per 1 ml of TRIzol reagent) and centrifuged for 15 min at 12000 x g at 4°C. RNA was precipitated from the aqueous phase with 100% 2-propanol. The RNA pellet was washed once with 70% ethanol, dried and dissolved in RNase-free water. For Northern analyses 5 µg of total plant RNA was used.

2.2.8.3.2 Construction of radiolabeled RNA probes

To obtain a probe for radioactive *in vitro* transcription, PCR with a single primer containing the T7 promoter sequence was performed. This resulted in an antisense transcript for the desired RNA. Approximately 100 ng of this PCR product was used for radiolabeling.

Radioactive *in vitro* Transcription Mixture (20 µl end volume)

2.0 µl	10 x transcription buffer (NEB)
2.0 µl	100 mM DTT
0.5 µl	RNasin (RNase inhibitor, Promega)
4.0 µl	rNTP mix-UTP (2.5 mM per base)
2.4 µl	100 µM UTP
x µl	PCR product

5.0 μ l	[α - ³² P]-UTP
1.0 μ l	T7 RNA polymerase (20U/ μ l)

The transcription reaction was carried for 2 h at 37°C. Subsequently, 1 μ l of DNase I was added to the mix and the sample was incubated for 15 min at 37°C. After incubation, 80 μ l of sterile water was added and two steps of chloroform purification were performed. RNA was precipitated from the aqueous phase by 2.5 volumes of 100% ethanol and 0.1 volume of 3M Na-acetate and then incubated for at least 30 min at -20°C. The RNA pellet was washed once with 70% ethanol, dried and dissolved in RNase-free water. Before hybridization the radioactive RNA sample was denatured for 5 min at 65°C. For the hybridization procedure see Section 2.2.8.2.5. Autoradiographs both for RNA and DNA analyses were evaluated using Fuji Bio Imaging plates type BASIII, a Fuji Bio Imaging analyzer, the BAS200025 software package (Fuji) and the TINA software package v2.08 beta (Raytest, Spröckhovel).

2.2.8.4 Pulsed-field gel electrophoresis of DNA

2.2.8.4.1 Sample preparation

LMP Buffer

125 mM	EDTA
330 mM	sorbitol
25 mM	Na-Citrate/HCl, pH 7.0
90 mM	β -mercaptoethanol

Buffer A

450 mM	EDTA, pH 8.0
10 mM	Tris-HCl, pH 8.0

Buffer A + detergent

450 mM	EDTA, pH 8.0
10 mM	Tris-HCl, pH 8.0
1% (w/v)	SLS

Buffer B

500 mM EDTA, pH 9.0

For a pulsed-field gel, samples of intact plastids were prepared as described in Section 2.2.3.1. The chloroplast suspension was adjusted to a chlorophyll concentration of 5 mg/ml with isolation medium and incubated for 10 min at 42°C. 0.9% Incert Agarose in LMP buffer was melted at 80°C and, after cooling down to 42°C, carefully mixed with the chloroplast suspension (3 volumes of agarose for 1 volume of chloroplasts). The chloroplasts/agarose mixture was loaded into block forms and left for solidification at 4°C in the dark. Solidified blocks were washed for 15 min at room temperature in 1.5 ml/block buffer A with SLS, and incubated overnight in 1.5 ml buffer A + SLS + 20 µg/ml RNase at 37°C with gentle agitation. Subsequently blocks were incubated for 24 h in 1.5 ml buffer A + 0.2 mg/ml Proteinase K at 50°C with gentle agitation. After 24 h the Proteinase K solution was removed and the blocks were washed 2 x for 4 h, and then overnight in 1.5 ml buffer B (50°C). The blocks were then transferred to 1.5 ml of buffer B and stored at 4°C.

2.2.8.4.2 Pulsed-field gel electrophoresis

The blocks with immobilized, treated chloroplasts were loaded onto 1% SeaKem LE agarose gels in 1 x TBE buffer, with λ-DNA PFGE as a molecular weight marker. The gel was run for 23 h at 170 mV at 12°C. Pulse periods started with 60 s and decreased to 0.1 s. After the run, gels were stained for 1 h in 150 ml TBE buffer with 7.5 µl ethidium bromide (10 mg/ml), destained in water and photographed under UV light.

2.2.8.4.3 Isolation of DNA from pulsed-field gels

The band of monomeric plastid DNA (around 150 000 bp) was excised from the gel with a scalpel blade. DNA was eluted from the agarose slice with the QIAEX®II (Qiagen, Hilden) kit for DNA extraction from agarose gels according to the manufacturer's protocol.

2.2.9 Electron microscopy

Electron microscopy was performed by Prof. G. Wanner (Botanisches Institut der LMU, München). Small leaf pieces were fixed for 2 h in 2.5% glutardialdehyde (in 75 mM sodium cacodylate, 2 mM MgCl₂, pH 7.0) at room temperature. Subsequently, the material was rinsed several times in fixative buffer and post-fixed for 1 h with 1% osmium tetroxide in fixative buffer at room temperature. After two washing steps in distilled water, the tissue pieces were stained with 1% uranyl acetate in 20% acetone for 1h. Dehydration was performed with a graded acetone series. Tissue samples were then infiltrated and embedded in Spurr's low-viscosity resin (Spurr 1969). After polymerization, ultra thin sections with thicknesses between 50 and 70 nm were cut with a diamond knife and mounted onto collodion-coated copper grids. The sections were post-stained with aqueous lead citrate (100 mM, pH 13.0). All micrographs were taken with EM 912 or EM 109 electron microscopes (LEO, Oberkochen).

2.2.10 Pigment analysis

Chlorophyll concentrations were determined according to Arnon (1949) with the formula:

$$C (\mu\text{g/ml})=20.2 \times A_{645} + 8.02 \times A_{663}.$$

Pigment analyses were performed by Dr. R. Bassi (University of Verona, Italy). HPLC analysis was done according to Gilmore and Yamamoto (1991).

2.2.11 Non-photochemical quenching

Non-photochemical quenching (NPQ) measurements were done by Dr. R. Bassi (University of Verona, Italy). Fluorescence images were harvested (25 ms exposure) by a solid state CCD video camera (mod.4710 COHU, San Diego, USA) through a red filter. For determination of NPQ, plants were dark-adapted for 15 min. Measurements were performed as follows: plants were illuminated with relatively strong actinic light (220 $\mu\text{E m}^{-2} \text{s}^{-1}$) for 10 min followed by 12 min dark recovery. Actinic light was interrupted for periods of 2 sec during which the maximum fluorescence yield (F'max) was recorded with an orange LED light of 800 $\mu\text{E m}^{-2} \text{s}^{-1}$. Images for fluorescence determination were taken 0.9 sec after the onset of the detection

light. NPQ was calculated as: $(F_{\max} - F'_{\max}) / F'_{\max}$ (Li 2000) where F_{\max} is the maximum fluorescence in the dark adapted state and F'_{\max} is the maximum fluorescence in any light-adapted state. Duration of illumination by the detecting light was 1.8 sec during the treatment with actinic light and 0.9 sec during dark recovery.

2.2.12 Measurement of photosynthetic O₂ evolution with the Clark Electrode

Oxygen evolution performed by intact tobacco chloroplasts or protoplasts was measured using a Clark-type electrode (Hansatech Instruments, Bachofer GmbH, Reutlingen). Calibration of the electrode was performed at 25°C. The zero point for O₂ synthesis was determined by calculation of the difference between measurements with oxygen-free water (1 ml H₂O + a few crystals of Na₂S₂O₄), and oxygen-saturated water (1 ml). Using the constant values of the oxygen content of air-saturated water (Seidell and Linke 1965), the μmol amount of produced O₂ was calculated for 1 ml of solution and 1 cm of recorder print. For measurements, 1 ml of suspension of intact plastids or protoplasts, equivalent to a chlorophyll concentration of approximately 0.1 mg/ml was used. Plastid (protoplast) suspensions were incubated in darkness for 5 min and then exposed to light (light source of 15 cm distance from the reaction chamber). Oxygen evolution was measured for 10 min and the desired concentration of NaHCO₃ was added into the reaction chamber. Measurements were performed until the maximum of O₂ production was reached.

2.2.13 Chlorophyll fluorescence analysis

2.2.13.1 77K fluorescence analysis

77K fluorescence analyses were performed by Dr. A. Sokolenko. 77K emission and excitation spectra were made in a JASCO FP-777 (Japan) luminescence spectrometer. For 77K measurements thylakoid membranes from tobacco plants were injected into silica tubes and frozen in liquid nitrogen. The excitation and emission spectra were measured with a slit width of 5 nm and excitation wavelengths at 475, 690 and 735 nm.

2.2.13.2 Chlorophyll fluorescence measurements using the PAM fluorometer

In vivo fluorescence of single leaves was excited and detected with a pulse amplitude modulated fluorometer (PAM 2000; Walz, Germany) as described by Meurer et al. (1996). 800 ms white light pulses of $4000 \mu\text{E m}^{-2} \text{s}^{-1}$ were used to determine the maximum fluorescence (F_M) and the ratio $(F_M - F_0)/F_M = F_V/F_M$. Actinic light of $40 \mu\text{E m}^{-2} \text{s}^{-1}$ intensity was used to drive photosynthesis. In addition, fluorescence quenching parameters qP (photochemical quenching) = $(F_M' - F_S)/(F_M' - F_0')$, and qN (non-photochemical quenching) = $1 - (F_M' - F_0')/(F_M - F_0)$ (Schreiber 1986) were recorded.

2.2.13.3 Fluorescence detection using the FluorCam-Video Imaging System

In vivo fluorescence of single leaves was excited and detected with an imaging fluorometer FluorCam-Video Imaging System (P.S.Instruments; Brno, Czech Republic) according to the manufacturer's protocol. The continuous actinic light of $100 \mu\text{E}$ (30% of maximal $350 \mu\text{mol photons m}^{-2} \text{s}^{-1}$) was given for 5 s. Images were captured with a sensitivity of 30% of its maximum and an electronic shutter intensity of 7 (2 ms).

3. RESULTS

3.1 Functional analysis of the *ycf9* gene product

3.1.1 Comparison of the *Ycf9* sequences

Ycf9 genes from a variety of photosynthetic organisms encode a well-conserved protein (Figure 6). Sequence similarity exists through all photosynthetically active organisms, with the dominant feature being two hydrophobic stretches long enough to give rise to trans-membrane (TM) α -helices (Figure 5). These putative TM helices are separated by a loop of about 15 amino acids that can be predicted to be luminal, provided the N-terminus of the protein is retained at the stromal side of the membranes. Sequence evaluation predicts a processing site for the peptidase, VFA or ALA (bold in Figure 6), located at the end of the first putative TM helix. Processing of the 6.5 kDa polypeptide at this site would yield proteins of about 3.5 and 3.0 kDa. The *Chlamydomonas* sequence shows about 60% identity with those of vascular plants, including tobacco (Figure 6).

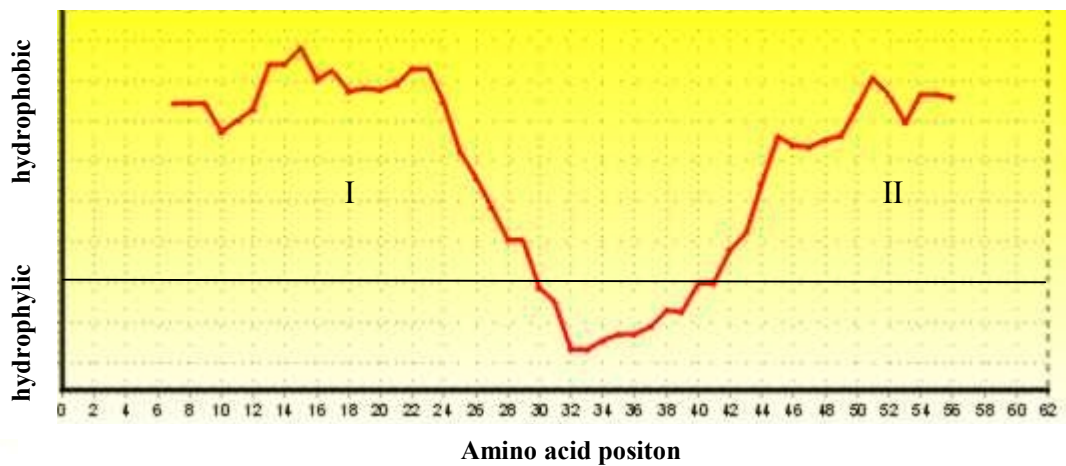


Fig. 5. Kyte and Doolittle (1982) hydrophathy profile of *Ycf9*. Amino acid positions are indicated at the bottom of the graph. The scan window size was 13. Hydrophobic amino acid residues, placed above the zero line, form two hydrophobic stretches, I and II, long enough to give rise to trans-membrane α -helices (see also Figure 6).

```

YCF9OE1   MTIAFQLAVF ALIATSSLLL ISVPVVFASP EGWSSNKNVV FSGTSLWIGL VFLVGILNSL IS
YCF9OE4   MTIAFQLAVF ALIATSSLLL ISVPVVFASP EGWSSNKNVV FSGTSLWIGL VFLVGILNSL IS
YCF9NT    MTIAFQLAVF ALIATSLILL ISVPVVFASP DGWSSNKNVV FSGTSLWIGL VFLVGILNSL IS
YCF9AT    MTIAFQLAVF ALIITSSILL ISVPVVFASP DGWSSNKNVV FSGTSLWIGL VFLVGILNSL IS
YCF9SO    MTIAFQLAVF ALIATSSILL ISVPVVFASP DGWSSNKNIV FSGTSLWLGL VFLVGILNSL IS
YCF9ZM    MNIAFQLAVF ALIATSSVLV IRGHLVFASP DGWSNNKNVV FSGTSLWIGL VFLVAILNSL IS
YCF9OS    MTIAFQLAVF ALIVTSSVLV ISVPLVFASP DGWSNNKNVV FSGTSLWIGL VFLVAILNSL IS
Ycf9PT    MTIAFQSAVF ALIAISFLLV IGVPVALASP DGWSSSKNVV FSGVSLWIGS VLFVGILNSF IS
YCF9MP    MTIAFQLAVF ALIAISFLLV IGVPVVLASP EGWSSNKNVV FSGASLWIGL VFLVGILNSF IS
YCF9ChR   MTSILQVALL ALIFVSFALV VGVPVVFATP NGWTDNKGAV FSGLSLWLLL VFVVGILNSF VV

Consensus *...*... ***...*... .....** **.....*... ***.***... .*...****. ..

```

Fig. 6. Multiple sequence alignment of predicted *ycf9* gene products with accession numbers. The consensus is indicated at the bottom: 100% of identity among all sequences is marked by asterisks, identity from 60% - 80% by dots. A potential cleavage site for the luminal peptidase is marked bold, two hydrophobic regions are underlined. Abbreviations: OE1,4: *Oenothera elata* plastome 1 and 4, NT: *Nicotiana tabacum*, AT: *Arabidopsis thaliana*, SO: *Spinacia oleracea*, ZM: *Zea mays*, OS: *Oryza sativa*, PT: *Pinus thunbergii*, MP: *Marchantia polymorpha*, ChR: *Chlamydomonas reinhardtii*.

3.1.2 Construction of a recombinant plasmid for *ycf9* inactivation

A reverse genetic approach was employed to understand the function of *ycf9*. An inactivation vector for the *ycf9* gene was constructed by introducing the promoterless *aadA* cassette into a *MunI* site in the *ycf9* gene. Correct integration of the *aadA* gene into the pGEM*ycf9* vector was monitored by PCR, restriction and sequence analyses.

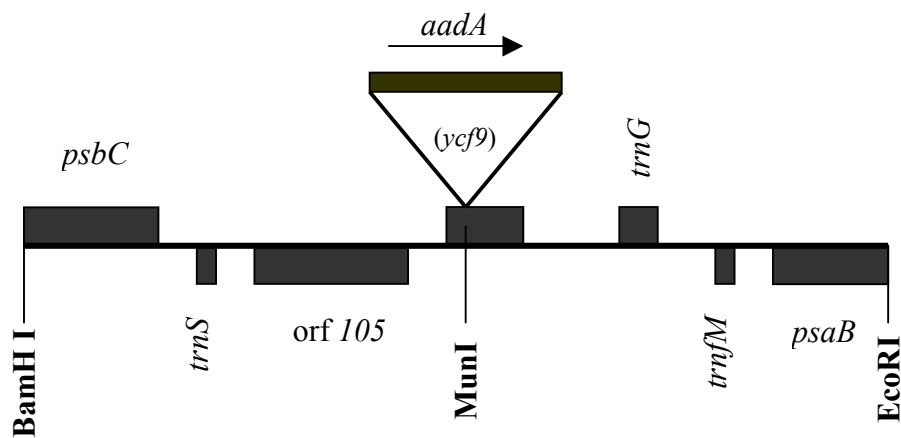


Fig. 7. Construction of the plastid transformation vector for disruption of the *ycf9* gene in the tobacco plastid chromosome. A BamHI/EcoRI fragment of the plasmid TB20 (Shinozaki et al. 1986) containing the *ycf9* gene and app. 1 kb flanking regions (necessary for homologous recombination) was cloned in the pGEM vector. Inactivation of *ycf9* was performed by insertion of the *aadA* cassette into the gene internal MunI site. The plasmid clone including the *aadA* cassette inserted in the same orientation as *ycf9* was used for further plant transformation (see Material and Methods for details). Transcription direction of the *aadA* gene is indicated by an arrowhead.

3.1.3 Plant transformation, selection and regeneration of mutants

The method of biolistic chloroplast transformation is based on the process of incorporation of foreign DNA into the plastome by homologous recombination. This method was developed for *Chlamydomonas reinhardtii* by Boynton et al. (1988), and modified for *Nicotiana tabacum* by Svab et al. (1990). Twenty leaves of *Nicotiana tabacum* were shot with gold particles carrying the recombinant plasmid pGEM $ycf9$. After three days of cultivation on non-selective RMOP medium leaves were cut and transferred to selective RMOP medium (for details see Section 2.2.2.2). Resistant green colonies (calli) began to grow vigorously after approximately three weeks, while non-transformed material displayed retarded growth and turned brownish. The transformation with *ycf9* yielded 4 independent mutant lines. Segregation of the mutant plastomes was performed by transferring early appearing shoot tops or green calluses onto fresh selection medium in three week intervals. For molecular analyses, the mutant lines had undergone at least five cycles of shoot regeneration from leaf explants.

3.1.4 Growth phenotypes of the $\Delta ycf9$ plants

$\Delta ycf9$ plants were regenerated from the green calluses or plant shoot (described in Section 2.2.2.3) using antibiotic-supplied medium, and further cultivated parallel *in vitro* and in the greenhouse. In the latter case, the mutant tobacco lines were able to survive in soil, and produced fertile seeds. This confirmed that their phenotype was photoautotrophic. However, the lines showed two clear non-wild-type phenotypes, depending on the growth conditions used. Under standard heterotrophic conditions ($100 \mu\text{E m}^{-2} \text{s}^{-1}$, 25°C , growth medium supplemented with sucrose), $\Delta ycf9$ plants developed pale green leaves of the reticulate type when compared to wild-type material (Figure 8A). This corresponded to a 2.5-fold decrease in the chlorophyll content compared with the wild-type plant. This effect was less apparent when plants were grown in soil in the greenhouse. No differences in growth rates between wild-type and mutant plants grown under heterotrophic and photoautotrophic conditions were observed at 25°C (at both standard and low light intensities). When transferred to the lower temperatures (e. g. 17°C or 20°C), $\Delta ycf9$ plants displayed a drastic decrease in growth rate at low light intensities ($10 \mu\text{E m}^{-2} \text{s}^{-1}$). The dwarf phenotype was progressively lost with increasing light intensities ($100 \mu\text{E m}^{-2} \text{s}^{-1}$; Figure 8A). The same effect was observed when plants were grown in soil under the same conditions ($10 \mu\text{E m}^{-2} \text{s}^{-1}$, 20°C ; Figure 8B) which excludes that the growth medium notably influenced the phenotype.

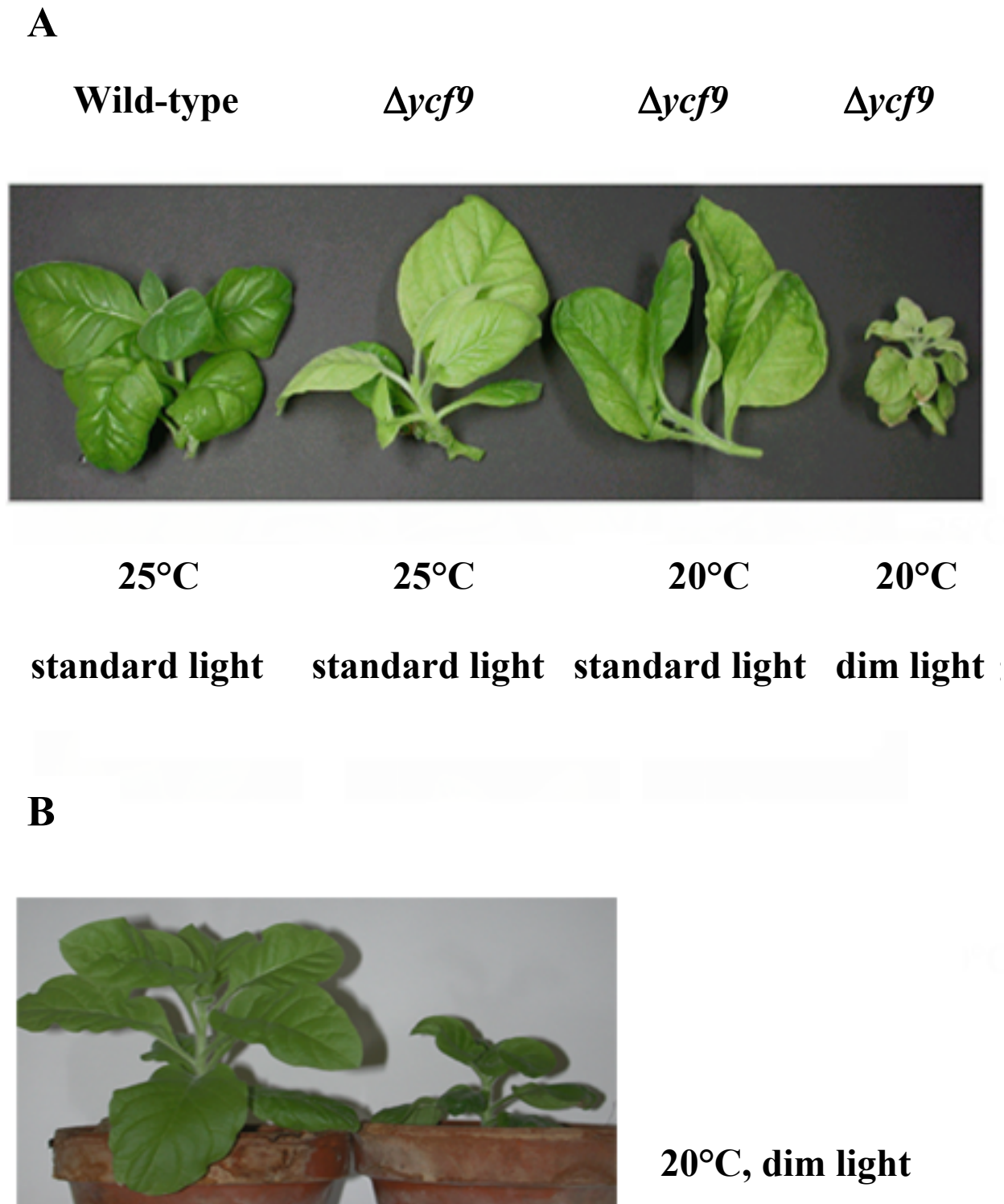


Fig. 8. Phenotypes of $\Delta ycf9$ plants. $\Delta ycf9$ plants grown under different conditions are compared with tobacco wild-type. Panel A: plants from *in vitro* cultures, Panel B: plants grown autotrophically on soil. Growth conditions used (temperature and light intensity) are indicated on the picture. Standard light intensity corresponds to $100 \mu\text{E m}^{-2} \text{s}^{-1}$, low light to $10 \mu\text{E m}^{-2} \text{s}^{-1}$.

3.1.5 Ultrastructure of $\Delta ycf9$ chloroplasts

Wild-type tobacco chloroplasts of shoot cultures grown *in vitro* are lens-shaped, relatively large, up to 12 μm in diameter and up to 4 μm thick. Their matrix is densely packed with ribosomes, and numerous stroma and grana thylakoids are prominent (Figure 9A). Starch grains are common, while only few, evenly distributed plastoglobules were present. The plastids of $\Delta ycf9$ mutants did not vary in size or shape from those of the wild-type. Nevertheless, a remarkable difference in the proportions of the stroma and grana lamellae can be observed. In wild-type plastids stroma and grana thylakoids are numerous and uniformly distributed, while in the $\Delta ycf9$ mutants no stacked grana lamellae can be observed, or only in reduced amounts. Grana and stroma thylakoids possess a distinct structure and function, the protein complexes of ATP-synthase and photosystem I are located in stroma thylakoids, while grana lamellae contain most of photosystem II. The abnormal structure of the grana thylakoids in the $\Delta ycf9$ plants suggests a defect in the PSII structure (Figure 9B).

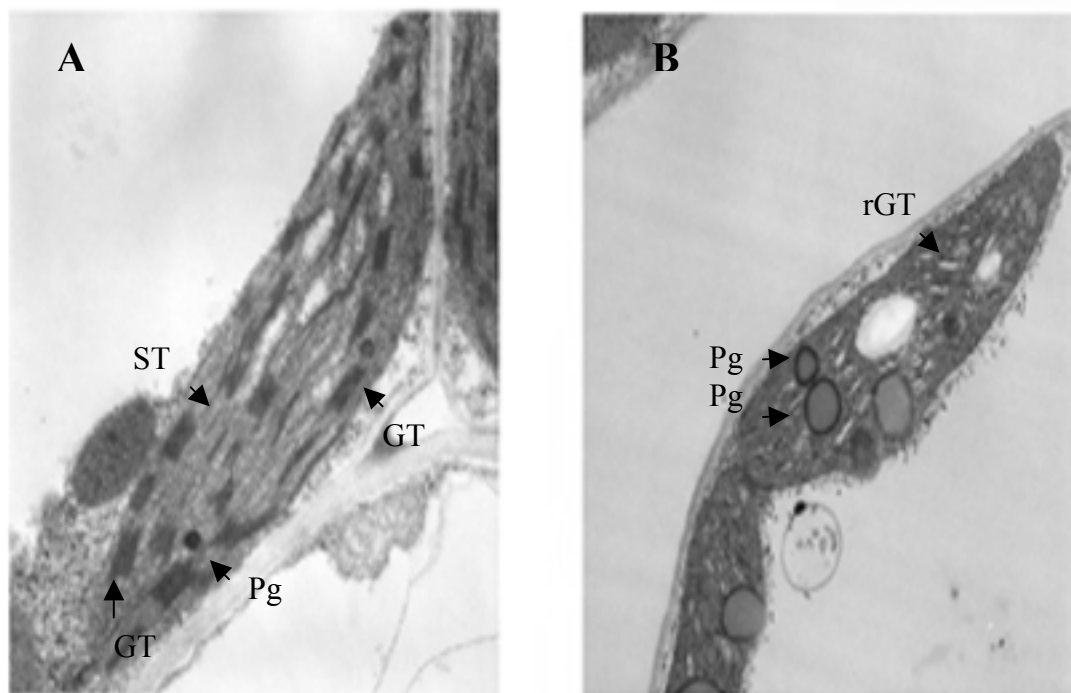


Fig. 9. Electron micrographs of wild-type and $\Delta ycf9$ mutant of *Nicotiana tabacum*. (A) Typical lens-shaped wild-type chloroplast with numerous stroma (ST) and grana thylakoids (GT in wild-type and rGT in mutant); (B) Typical $\Delta ycf9$ mutant. Grana thylakoids are strongly reduced (rGT). Mutant plastids are able to form starch grains. Large plastoglobules (marked Pg; possibly an effect of cultivation *in vitro*) show a uniform distribution.

3.1.6 Investigation of the homoplastomic state of mutant plastome

Precise approaches, including customary sequence, Southern and PCR analyses as well as pulsed-field electrophoresis with appropriate subcellular fractions were employed to assess the homoplastomic status of the mutants. Southern analysis allows to check for the correct integration of the transgene, but does not allow the demonstration of minimal numbers of wild-type DNA copies. The PCR approach is clearly superior in sensitivity of detection but it bears the risk of (co)amplifying promiscuous plastid sequences (Ellis 1982, Stern and Lonsdale 1982, Ayliffe and Timmis 1992) residing in nuclear and/or mitochondrial DNA. Pulsed-field electrophoresis including the separation of intact, virtually contamination-free circular plastid chromosomes, is an obvious approach to bypass that problem.

3.1.6.1 Sequence analysis

To confirm the correct integration of the construct carrying the *aadA* gene into the tobacco plastid chromosome, the fragment of plastid DNA coding for the *ycf9* gene was sequenced in the $\Delta ycf9$ transformants. For this purpose an amplification product of *ycf9*for and *ycf9*rev primers was purified by agarose gel electrophoresis and served as template for sequencing (Hupfer et al. 2000). The analysis of the nucleotide sequence proved the disruption of the *ycf9* gene (Figure 10). Moreover, the *aadA* insertion causes a frame-shift in the *ycf9* reading frame, preventing translational re-initiation of a transcript containing the C-terminal gene segment.

```

37525  GGATTCATGA TAAAGTAAAA TCCCTCGATG ACATATTTTA TCACAATTAA
37575  TATTTTTTGG CTGATAGAGG GATCAAATGG TATATAGTTC ATTTGTTGGT
37625  AGCTTGGAGG ATTAAAAGCA TGACTCTTGC TTTCCAATTA ATTCGCCGTC
      GTTCAATGAG AATGGATAAG AGGCTCGTGG GATTGACGTG AGGGGGCAGG
      GATGGCTATA TTTCTGGGAG CGAACTCCGG GCGATATCAC TAGTTGTAGG
      GAGGGATTCA TGGCTCGTGA AGCGGTGTTC GCCGAAGTAT CGACTCAACT
      ATCAGAGGTA GTTGGCGTCA TCGAGCGCCA TCTCGAACCG ACGTTGCTGG
      CCGTACATTT GTACGGCTCC GCAGTGGATG GCGGCCTGAA GCCACACAGT
      GATATTGATT TGCTGGTTAC GGTGACCGTA AGGCTTGATG AAACAACGCG
      GCGAGCTTTG ATCAACGACC TTTTGGAAC TTCGGCTTCC CCTGGAGAGA

```

GCGAGATTCT CCGCGCTGTA GAAGTCACCA TTGTTGTGCA CGACGACATC
ATTCCGTGGC GTTATCCAGC TAAGCGCGAA CTGCAATTTG GAGAATGGCA
GCGCAATGAC ATTCTTGCAG GTATCTTCGA GCCAGCCACG ATCGACATTG
ATCTGGCTAT CTTGCTGACA AAAGCAAGAG AACATAGCGT TGCCTTGGTA
GGTCCAGCGG CGGAGGAACT CTTTGATCCG GTTCCTGAAC AGGATCTATT
TGAGGCGCTA AATGAAACCT TAACGCTATG GAACTCGCCG CCCGACTGGG
CTGGCGATGA GCGAAATGTA GTGCTTACGT TGTCCCGCAT TTGGTACAGC
GCAGTAACCG GCAAAATCGC GCCGAAGGAT GTCGCTGCCG ACTGGGCAAT
GGAGCGCCTG CCGGCCAGT ATCAGCCCGT CATACTTGAA GCTAGACAGG
CTTATCTTGG ACAAGAAGAA GATCGCTTGG CCTCGCGCGC AGATCAGTTG
GAAGAATTTG TCCACTACGT GAAAGGCGAG ATCACTAAGG TAGTTGGCAA
37604 ATAACTGCAG GCTTGCTTTC AATTGGCTGT TTTTGCATTA ATTGCTACTT
37640 CATTAACTTT ATTGATTAGC GTACCCGTTG TATTTGCTTC TCCTGATGGC
37690 TGGTCAAGTA ACAAAAATGT TGTATTTTCT GGTACATCCT TATGGATTGG
37740 ATTAGTCTTT CTGGTGGGTA TCCTTAATTC TCTCATCTCT **TGA**ACCTATT
37790 CGTCGCAGAC CCAAAACCAA AATGACCCCC CTAATTTTTTC TCGGTTGTGA
37840 GACACATTAA ATTGGAATCT AAGTCCCCAA AGAAAACGCA AATCAAATAA
37890 AGAAAACAAA AAAATTAGAG GGGGGTCAAA CTTCTTGAAT AAAAAGAATA
37940 CAATTAATAA

Fig. 10. Nucleotide sequence of the *ycf9* gene from transformed tobacco lines. Start and stop codons of *ycf9* are indicated in bold, the inserted *aadA* sequence is underlined.

3.1.6.2 Southern analysis

The plant material obtained after 6 – 8 regeneration cycles on selective medium was used to check the ratio of transformed/wild-type plastome copies by Southern analysis. Isolated plastid DNA was restricted and used for RFLP analyses and subsequent hybridization with a radiolabeled *ycf9* probe. Different amounts of wild-type ptDNA concentrations were loaded to

estimate wild-type plastome copies in $\Delta ycf9$ plants. In all transgenic lines no wild-type hybridization signal became visible (Figure 11).

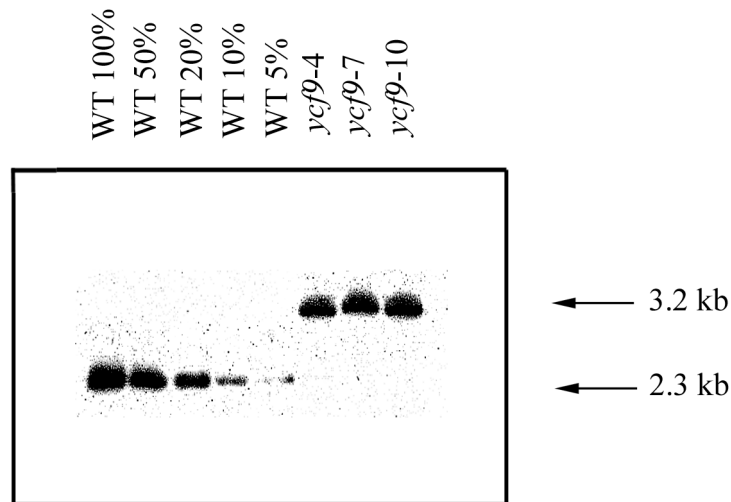


Fig. 11. Southern analysis of *ycf9* knockout plants. 5 μ g of purified tobacco plastid DNA was digested with *Ban*II and hybridized with a radiolabeled *ycf9* probe. Hybridization yields a 2.3 kb fragment for wild-type, and a 3.2 kb fragment for transformed plants. Lane 1: 100 % (5 μ g) of wild-type ptDNA, lane 2: 50%, lane 3: 20%, lane 4: 10%, lane 5: 5% of wild-type ptDNA, lane 6, 7, 8: ptDNA of three independently generated transformed lines.

3.1.6.3 PCR analysis

The PCR reaction was performed using a primer pair designed for the regions flanking the *ycf9* gene (*ycf9*for and *ycf9*rev). This primer combination allowed to distinguish signals originating from the transformed and wild-type DNA sequences. Clear signals expected from the wild-type plastome appeared when total DNA was used as a template.

To exclude the possibility of contamination of the sample by nuclear and/or mitochondrial DNA sequences DNA isolated from plastids of isopycnic Percoll gradients was subsequently used as a template for PCR. A strong reduction of the wild-type plastome product was noted, although the signal arising from the hybridization between the transformed and wild-type amplification products was still present.

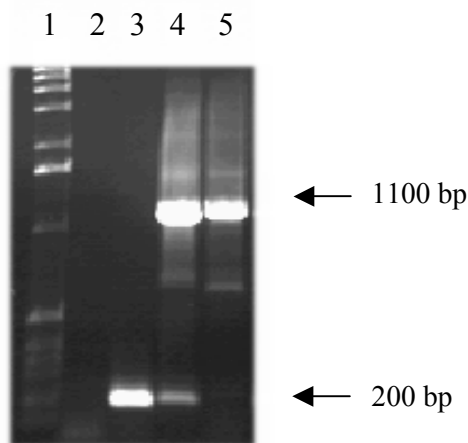


Fig. 12. PCR analysis of $\Delta ycf9$ plants. *Ycf9* was amplified from wild-type and transformed plants using *ycf9for* and *ycf9rev* primers. The wild-type signal should appear as a 200 bp band, while the transplastomic fragment should be 900 bp larger (1100 bp). Different preparations of plant DNA were used to investigate the homoplastomic status of the mutant. Lane 1: 1 kb DNA ladder, 2: primer control, 3: wild-type total DNA, 4: $\Delta ycf9$ total DNA, 5: $\Delta ycf9$ plastid DNA.

3.1.6.4 PCR analysis of DNA purified by pulsed-field gel electrophoresis

To investigate if wild-type PCR signal, detectable when even plastid $\Delta ycf9$ DNA served as a template, arises from the promiscuous DNA or residual wild-type plastid DNA molecules, the purification step including pulsed-field gel electrophoresis (PFGE) was employed. Three preparations of $\Delta ycf9$ DNA, total, Percoll gradient purified, and PFGE purified plastid DNA, were investigated for presence of wild-type DNA copies using a *ycf9forPF* and *ycf9revPF* primer pair. In contrast to total DNA and Percoll gradient-purified DNA preparation, no wild-type originating signal was detected when PFGE plastid DNA served as a template (Figure 13). The sensitivity of this approach can be further increased if the gel shown in Figure 13 is subjected to a Southern analysis with radiolabeled probe.

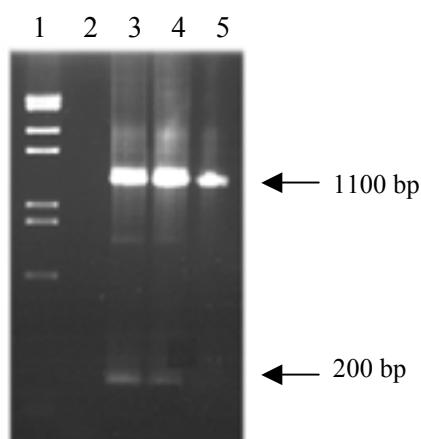


Fig. 13. PCR analysis of $\Delta ycf9$ plants. *Ycf9* was amplified from transformed plants using *ycf9forPF* and *ycf9revPF* primers. The wild-type signal appears as a 200 bp band, while the transplastomic fragment is 900 bp larger (1100 bp). Different preparations of plant DNA were used to investigate the homoplastomy state of the mutant. Lane 1: λ DNA marker, 2: primer control, 3: $\Delta ycf9$ total DNA, 4: $\Delta ycf9$ Percoll gradient-purified plastid DNA, 5: $\Delta ycf9$ PFGE-purified plastid DNA.

3.1.6.4.1 Southern analysis of $\Delta ycf9$ PFGE purified plastid DNA

Electrophoretically separated PCR products were visualized by ethidium bromide staining, subsequently blotted onto nylon membrane and hybridized with a radiolabeled, *ycf9*-specific probe (Figure 14). In contrast to the total- and Percoll gradient purified plastid DNA, no 200 bp, wild-type specific signal has been found in the PFGE purified plastid DNA sample. The detection level of this method was estimated at one wild-type gene copy to 10^4 transformed gene copies, what corresponds to one wild-type gene copy detectable in one plant cell.

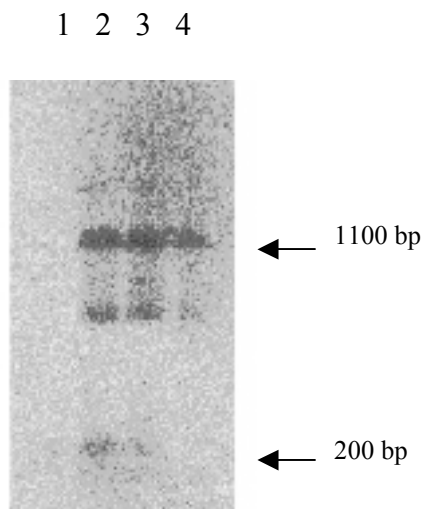


Fig. 14. PCR analysis of $\Delta ycf9$ plants. *Ycf9* was amplified from transformed plants using *ycf9*forPF and *ycf9*revPF primers. PCR products were electrophoretically separated, blotted onto nylon membrane and hybridized with a radiolabeled *ycf9*-specific oligonucleotide. The wild-type signal appears as a 200 bp band, while the transplastomic fragment is 900 bp larger (1100 bp). The intermediate band is an artefact. Different preparations of plant DNA were used to investigate the homoplasmic status of the mutant. Lane 1: primer control, 2: $\Delta ycf9$ total DNA, 3: $\Delta ycf9$ Percoll gradient purified plastid DNA, 4: $\Delta ycf9$ PFGE purified plastid DNA.

3.1.7 Northern analysis

In tobacco, *ycf9* is flanked upstream by the PSII genes *psbD* and *psbC*, and downstream by *trnG*. Insertion of the *aadA* cassette was designed to interrupt *ycf9* at the 6th codon without notably disturbing expression of the preceding genes (*psbC* and *psbD*), nor of *trnG* (Figure 15, upper panel). The RNA filter hybridization analyses performed with all relevant probes (*ycf9*, *psbC*, *trnG*, and *aadA*) was consistent with the desired genome structure. Six different transcripts were observed originating from the *psbD-psbC-ycf9* cluster, whereas *trnG* appeared to be transcribed independently, consistent with a previous report (Yao et al. 1989). Most of the transcripts identified with the *psbC*, *ycf9* and *aadA* probes in $\Delta ycf9$ plants were larger by about 0.9 kb, the size of the inserted *aadA* cassette. The expression of the downstream *trnG* gene was not detectably modified by this insertion. The complex pattern caused by post-transcriptional RNA processing was modified only in those RNA species that included the *aadA* insertion. No wild-type signals were detected, even in overloaded gels.

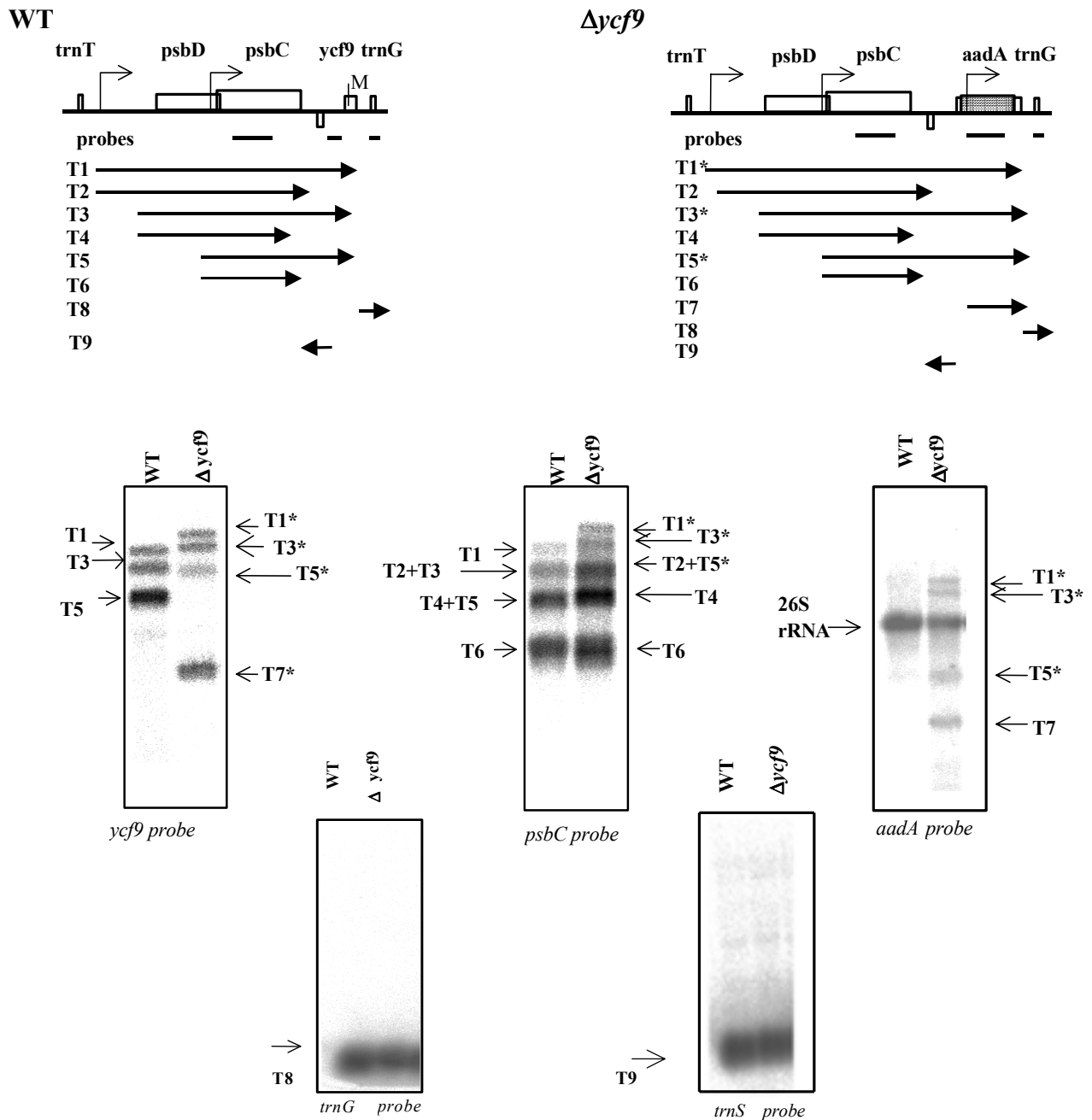


Fig. 15. Maps of the *psbD/C-ycf9* gene cluster in the wild-type and in $\Delta ycf9$ tobacco. The gene on the opposite strand, between *psbC* and *ycf9*, is *trnS*. Known promoters are indicated by bent arrows. The MunI site used for insertion of the *aadA* cassette is indicated in the wild-type restriction map (M). Below each map, horizontal lines indicate the positions of probes used for RNA filter hybridization. The deduced or known positions of transcripts are shown below the maps. The pattern in the wild-type chloroplasts is according to Yao et al. (1989), the transcripts in the $\Delta ycf9$ transformant were deduced by extrapolation from the wild-type RNAs. Transcript sizes in the wild-type are: T1: 4.4 kb, T2: 3.6 kb, T3: 3.6 kb, T4: 2.6 kb, T5: 2.6 kb, T6: 1.7 kb, T8: 0.71 kb, T9 (*trnS*): 0.7 kb. In the transformant the sizes of transcripts modified by the *aadA* insertion (indicated by asterisks) are: T1*: 5.3 kb, T3*: 4.5 kb, T5*: 3.5 kb, and 1.3 kb T7 transcript of *aadA* gene.

3.1.8 Overexpression of the Ycf9 protein in *E. coli*

To obtain an antiserum against Ycf9, the full-length *ycf9* gene was amplified by PCR using a primer pair with introduced restriction sites for EcoRI and XbaI enzymes. The *ycf9* gene was then cloned in the EcoRI/XbaI restricted pThioHis vector (carrying thioredoxin as a fusion protein; Invitrogen, USA). The construct was checked by sequencing analysis, and found to be correct, but no overexpression of the protein was detected after IPTG induction of *E. coli*. Therefore, another strategy for overexpression of a truncated form of the protein was employed. Three polypeptide parts were cloned and individually prepared for overexpression in *E. coli*:

- Polypeptide 1: MTLAFQLAVFALIATSLILLISVPVVFASPDGWSSNKNVVFSG
(N-terminal hydrophobic region + hydrophilic loop; Figure 16B),
- Polypeptide 2: PVVFASPDGWSSNKNVVFSG (hydrophilic loop; Figure 16C),
- Polypeptide 3: PVVFASPDGWSSNKNVVFSGTSLWIGLVFLVGILNSLIS
(hydrophilic loop and hydrophobic C-terminus).

Using an additional primer pair with introduced restriction sites for EcoRI and XbaI (primers *ycf9EcoRI2*, *ycf9XbaI2*) three constructs encoding the C-terminal hydrophobic region, the central hydrophilic loop and the N-terminal hydrophobic region, respectively, were cloned in the EcoRI and XbaI restriction sites of the pThioHis vector. After transformation of *E. coli* and induction with 1 mM IPTG for 3 h the overexpressed polypeptides 1 and 2 with the molecular masses of 3.5 and 2 kDa (increased by the size of the fusion protein thioredoxin to approximately 16 and 15 kDa, respectively; Figure 16A), were detected (Figure 16 B, C). After fractionation of the *E. coli* proteins into soluble and insoluble protein fractions, polypeptides 1 and 2 were found in the soluble protein fraction.

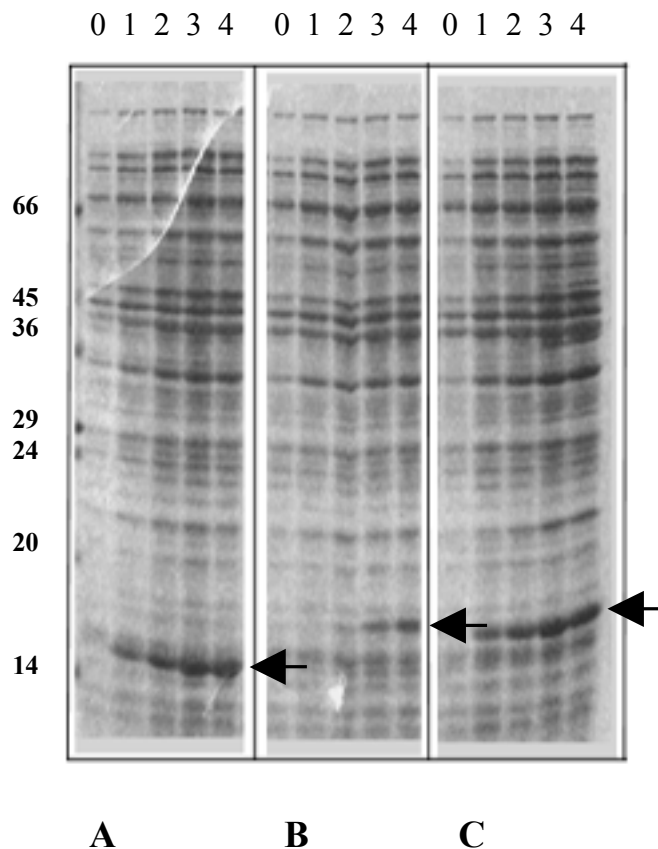


Fig. 16. Overexpression of truncated Ycf9 proteins. Three *ycf9* subclones were inserted into pThioHis vector, transformed into *E. coli*, and the proteins expressed by induction with 1 mM IPTG. Polypeptide 1, representing the N-terminal hydrophobic region with the hydrophilic loop (Panel B), and polypeptide 2, representing only the central hydrophilic loop (Panel C) were successfully overexpressed, resulting in two proteins with molecular masses of 3.5 and 2 kDa, increased by approximately 15 and 13 kDa by thioredoxin (Panel A). Only the soluble protein fractions are presented. Molecular weight markers in kDa are indicated at the left. Fractions 0, 1, 2, 3, and 4 represent cultures without (0), and after 1, 2, 3 and 4 h of IPTG induction. Arrowheads: overexpressed proteins.

3.1.9 Generation of antisera against the Ycf9 protein

To identify the localization of Ycf9 in the chloroplast antisera were raised against two fragments of truncated Ycf9 protein overexpressed in the pThioHis system (Figure 17, Panel A and B), and additionally, against a BSA-coupled, synthesized oligopeptide representing the hydrophilic loop of Ycf9 (PVVFASPDGWSSNKNVVS; Figure 17 C). Western analysis of the overexpressed proteins demonstrated a strong reaction of all three antisera with overexpressed Ycf9. A strong reaction with overexpressed fusion protein, thioredoxin, was

observed in case of two antisera directed against overexpressed Ycf9. Thus, for further analyses of plant material, antisera directed against the BSA-coupled oligopeptide were used.

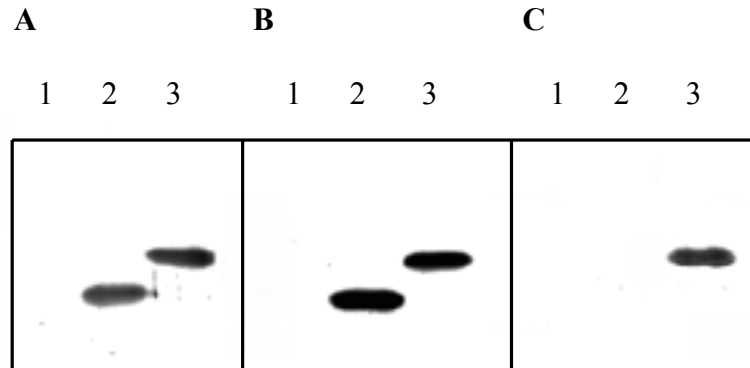


Fig. 17. Generation of antisera against Ycf9 protein. Two antisera directed against overexpressed fragments of truncated Ycf9 and one directed against the BSA-coupled, synthesized Ycf9 oligopeptide were used to detect *E. coli*-overexpressed Ycf9. Panels A, B and C represent antisera directed against overexpressed N-terminal hydrophobic and hydrophilic region of Ycf9, hydrophilic loop of Ycf9, and antiserum directed against synthesized Ycf9, respectively. Lane 1: protein extract from non-IPTG induced *E. coli* culture, 2: overexpressed thioredoxin, 3: overexpressed fusion protein thioredoxin-Ycf9 (3 h IPTG induction).

3.1.10 Immunological detection of the Ycf9 protein

To determine the localization of the Ycf9 protein, the antiserum raised against Ycf9 was employed to chloroplast subfractions (intact chloroplasts, stroma and thylakoids; Figure 18). Proteins from wild-type and $\Delta ycf9$ were separated on a 13% Schagger gel and then immunoblotted with polyclonal Ycf9 antibodies. After Western analysis, a signal of approximately 4 - 5 kDa was detected in wild-type, but not in the $\Delta ycf9$ material, demonstrating that the Ycf9 protein is an integral constituent of thylakoid membranes. For an exact localization of Ycf9 within thylakoid membrane protein complexes, several knock-out tobacco mutants were analyzed using Ycf9 antiserum. Thylakoid membranes isolated from the wild-type, $\Delta ycf9$ and PSII tobacco mutants, encompassing an insertion of the *aadA* cassette in *psbE*, *psbF*, *psbL* and *psbJ* genes, respectively (Swiatek et al. manuscript in preparation), were immunoblotted with Ycf9 antiserum (Figure 19). The Ycf9 signal was present in the wild-type sample, strongly reduced in $\Delta psbL$ and $\Delta psbJ$ plants, which possess

partially active PSII, but absent in $\Delta ycf9$, $\Delta psbE$ and $\Delta psbF$ mutants, suggesting its association with photosystem II.

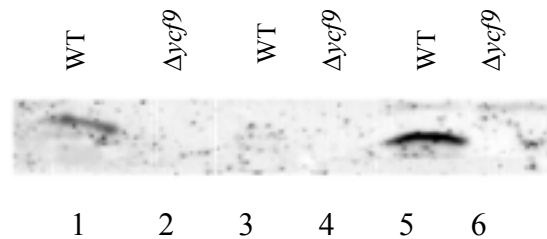


Fig. 18. Immunodetection of Ycf9 in tobacco plants grown under $100 \mu\text{E m}^{-2} \text{s}^{-1}$ at 25°C . Antiserum elicited against Ycf9 protein was reacted with the proteins of intact chloroplasts (lanes 1 and 2) and various subchloroplast fractions: stroma (lanes 3 and 4) and thylakoid membranes (lanes 5 and 6).

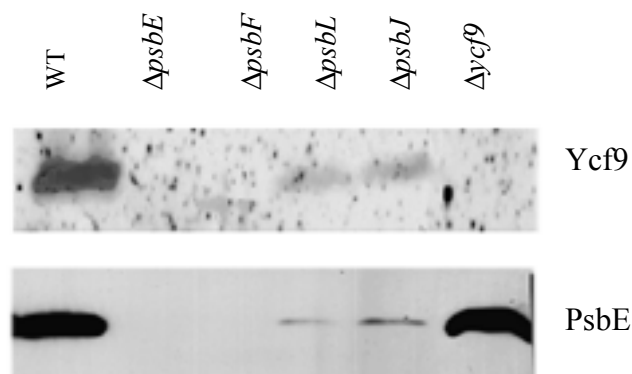


Fig. 19. Accumulation of PsbE (cytochrome b_{559}) and Ycf9 in wild-type, $\Delta psbE$, $\Delta psbF$, $\Delta psbL$, $\Delta psbJ$ and $\Delta ycf9$ plants. Thylakoid membrane proteins were separated in a 14% Schagger/von Jagow gel, electroblotted onto a PVDF membrane and incubated with antisera raised against Ycf9 or PsbE, as indicated at the right.

3.1.11 Changes in the polypeptide content in thylakoid membranes from $\Delta ycf9$ mutants

Since immunological analyses of Ycf9 demonstrated its localization in the thylakoid membrane, this chloroplast subfraction was further investigated to reveal possible differences between wild-type and $\Delta ycf9$ protein content. First analyses included SDS-PAGE gel assay, including silver staining of proteins and serological analyses. Subsequently, more refined techniques, such as two-dimensional gel electrophoresis or sucrose density gradient centrifugation, were applied.

3.1.11.1 SDS-PAGE analysis of the polypeptide content of $\Delta ycf9$ plants

Figure 20 shows a comparison of thylakoid membrane proteins from heterotrophically grown wild-type and $\Delta ycf9$ tobacco plants. After denaturing SDS-PAGE and silver staining, the $\Delta ycf9$ material revealed a polypeptide deficiency in the low molecular weight region of the gels. By analogy to the serological analyses presented in Section 3.1.10, the thylakoid protein content of photosystem II tobacco mutants, encompassing an insertion of the *aadA* cassette in the *psbE*, *psbF*, *psbL* and *psbJ* genes, respectively (produced in our group by R. Regel), was examined. All photosystem II mutants, similarly to $\Delta ycf9$ tobacco, also failed to accumulate an approximately 4 kDa protein. The deficient polypeptide corresponded to the protein immunodetected with Ycf9 antiserum and was attributed to the *ycf9* product. In comparing the wild-type and $\Delta ycf9$ tobacco protein samples, an additional quantitative difference was seen in a region of higher molecular weight, at approximately 26 kDa (arrow at the right part of Figure 20A). Immunological analysis identified this component as CP26, one of the apoproteins of the minor LHC antenna.

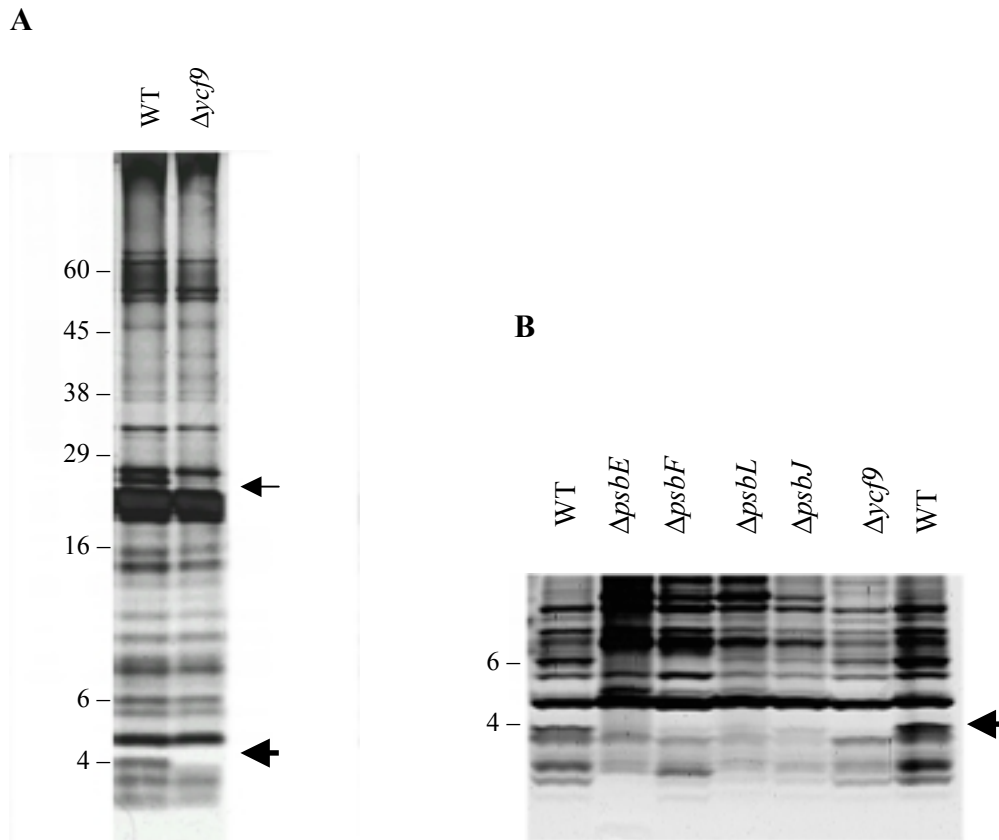


Fig. 20. Separation of thylakoid membrane polypeptides from tobacco $\Delta ycf9$, $\Delta psbE$, $\Delta psbF$, $\Delta psbL$ and $\Delta psbJ$ mutants. Proteins were revealed with silver staining. Tobacco plants were grown under $10 \mu\text{E m}^{-2} \text{s}^{-1}$ at 25°C . In Panel A arrows indicates the positions of polypeptide deficiencies in the $\Delta ycf9$ transformant. The bold arrow indicates the immunologically confirmed Ycf9 band, whereas the lighter arrow indicates CP26. Panel B shows a lower region of the gel with compared wild-type, $\Delta ycf9$, and photosystem II mutants, as indicated at the top of the figure. Arrow indicates the Ycf9 band. Molecular weights in kDa are indicated at the left of each figure.

3.1.11.2 Serological analysis of the $\Delta ycf9$ thylakoid proteins

To examine the content and the distribution of the major photosynthetic complexes in the *ycf9* mutant in comparison to wild-type tobacco, several antisera were tested with total thylakoid proteins as well as with fractions from the sucrose gradients (Table 2). Immunodetection was performed using the enhanced chemiluminescence system (ECL). The immunoblots were then scanned and the intensities of the individual signals estimated relative to these of the wild-type using the TINA software package v2.08 beta (Raytest, Spröckhovel).

Table 2. Immunological analysis of the $\Delta ycf9$ mutants and wild-type tobacco. Signals of intensity identical as in wild-type material are marked (+++), and decreasing intensities are shown as (++) or (+). OEC: oxygen evolution complex.

Gene	Product	wild-type	$\Delta ycf9$ mutants
<i>PsbP</i>	23 kDa protein of OEC	+++	+++
<i>PsbQ</i>	16 kDa protein of OEC	+++	+++
<i>psbA</i>	D1 protein of PSII core	+++	+++
<i>psbC</i>	D2 protein of PSII core	+++	+++
<i>psbD</i>	CP43	+++	+++
<i>psbE</i>	subunit 1 of cyt. <i>b₅₅₉</i>	+++	+++
<i>psbH</i>	PsbH	+++	+++
<i>PsbS</i>	PsbS	+++	+++
<i>PsbW</i>	PsbW	+++	+++
<i>psaA</i>	P700 chl-a protein 1 of PSI core	+++	+++
<i>psaB</i>	P700 chl-a protein 2 of PSI core	+++	+++
<i>PsaD</i>	ferredoxin-binding protein of PSI	+++	+++
<i>PsaE</i>	plastocyanin-binding protein of PSI	+++	+++
<i>Lhca1-4</i>	LHCI proteins	+++	+++
<i>Lhcb1-3</i>	LHCII proteins	+++	+++
<i>Lhcb4</i>	CP29	+++	++
<i>Lhcb5</i>	CP26	+++	+
<i>Lhcb6</i>	CP24	+++	+++
<i>petA</i>	cytochrome <i>f</i>	+++	+++
<i>petB</i>	cytochrome <i>b₆</i>	+++	+++
<i>petD</i>	subunit IV of cyt. <i>b₆/f</i> complex	+++	+++
<i>atpA</i>	α subunit of ATPase complex	+++	+++
<i>rbsL</i>	large subunit of RuBisCo	+++	+++

No difference in the amount of proteins from most photosynthetic complexes was observed in *ycf9* mutants compared to wild-type. Nevertheless, a clear deficiency in the amounts of CP29 and CP26 proteins was noted in the mutant.

3.1.11.2.1 The effect of Ycf9 deletion on minor antenna protein complexes

The accumulation of the minor antenna proteins CP29 and CP26 was further investigated by immunoanalyses of thylakoid membrane proteins isolated from plants grown under different light and temperature regimes. As shown in Figure 21, the content of the two minor antenna proteins strongly depends on the growth conditions. In agreement with the report from Ruf et al. (2000), it was found that under most growth conditions, less CP26 accumulated in the *ycf9*

mutant relative to the wild-type control. The deficiency in CP26 was most pronounced at 20°C in dim light, conditions under which the plants exhibited a dwarf phenotype (Figure 8). In most cases, CP29 content did not vary, with the notable exception of the dwarf $\Delta ycf9$ plants in which CP29 decreased by about 50%. In contrast, the PsbS protein, an antenna-like subunit associated with PSII, was present in unaltered quantities in both mutant and wild-type plants. Since CP43, a major PSII core antenna subunit, showed no difference between wild-type and $\Delta ycf9$ plants under each of the chosen growth conditions, it can be concluded that the absence of PsbZ had a selective effect on the accumulation of minor antenna proteins, that is independent of the overall accumulation of PSII cores.

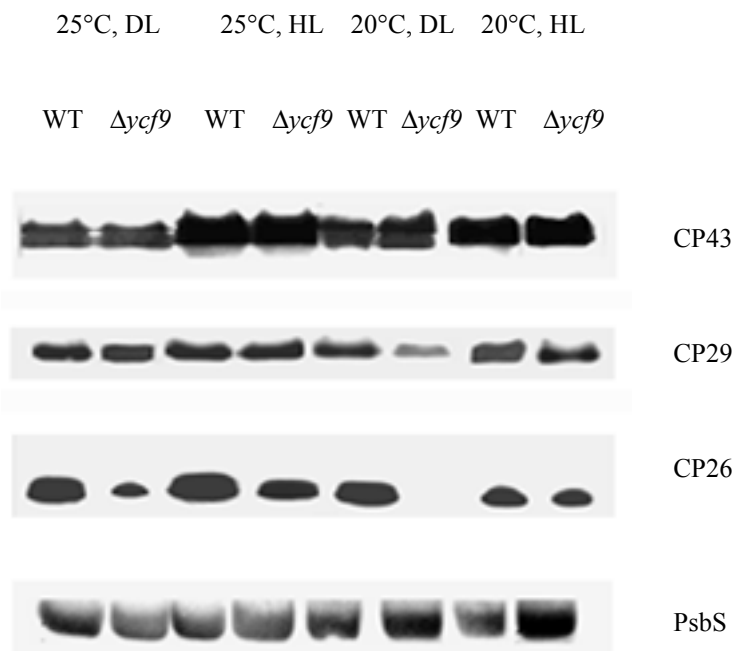


Fig. 21. Effects of the growth conditions on the minor antenna in thylakoid membranes from wild-type (WT) and $\Delta ycf9$ tobacco. Polypeptides were separated by SDS-tricine PAGE, electroblotted onto nitrocellulose and incubated with the specific antisera indicated at the right of each panel. DL, $10 \mu\text{E m}^{-2} \text{s}^{-1}$; HL, $100 \mu\text{E m}^{-2} \text{s}^{-1}$

3.1.11.3 Isolation of the major protein complexes from the thylakoid membranes

3.1.11.3.1 Isolation of the thylakoid protein complexes by sucrose density gradient centrifugation

Thylakoid protein complexes were fractionated by sedimentation through sucrose gradients, following solubilization of the membrane with β -dodecylmaltoside. Gradients from $\Delta ycf9$ and wild-type tobacco are compared in Figure 22. The heaviest green band corresponds to PSI supercomplexes, followed by slower sedimenting PSII-LHCII supercomplexes, PSII dimer, PSI+LHCI, PSII monomers, LHCII trimers, LHCII monomers with the minor antenna complex, a yellow, slowly sedimenting fraction enriched in carotenoids, and free proteins at the top of the gradient. All protein complexes were examined immunologically. A clear difference in the accumulation of PSII supercomplexes was observed in $\Delta ycf9$ material compared to wild-type, as discussed in Section 4.1.

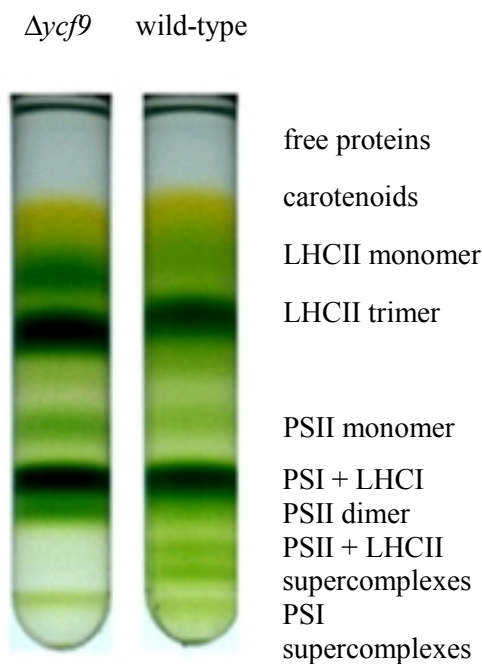


Fig. 22. Comparison of the sucrose gradients from β -dodecylmaltoside solubilized thylakoids from wild-type and $\Delta ycf9$ plants. The biochemical identification of each chlorophyll-containing band, indicated at the right, was assessed by collecting 0.3 ml fractions for silver staining and analysis using antisera against constituents of the major photosynthetic complexes.

After separation of protein complexes by sucrose density gradient centrifugation, proteins were subsequently separated in 13% Schagger/von Jagow gels (Figure 23). Silver staining of the gels uncovered two small peptides in the molecular weight range of 4 - 6 kDa which were detected in wild-type, but not in the mutant fractions. The band of 4 kDa, corresponding to the

fractions 19 - 32 containing the PSII complexes, was found in wild-type, but not in $\Delta ycf9$ material. Therefore, this protein was considered to correspond to the *ycf9* gene product. A second band of 6 kDa was also missing from $\Delta ycf9$ thylakoids. This protein was found in upper regions of the gradient, with a distribution profile that did not match that of LHCII proteins, neither that of the minor antenna complex. The 6 kDa protein may be an unprocessed form of Ycf9 not associated with PSII, or it might be an unrelated protein that is unstable in the absence of Ycf9.

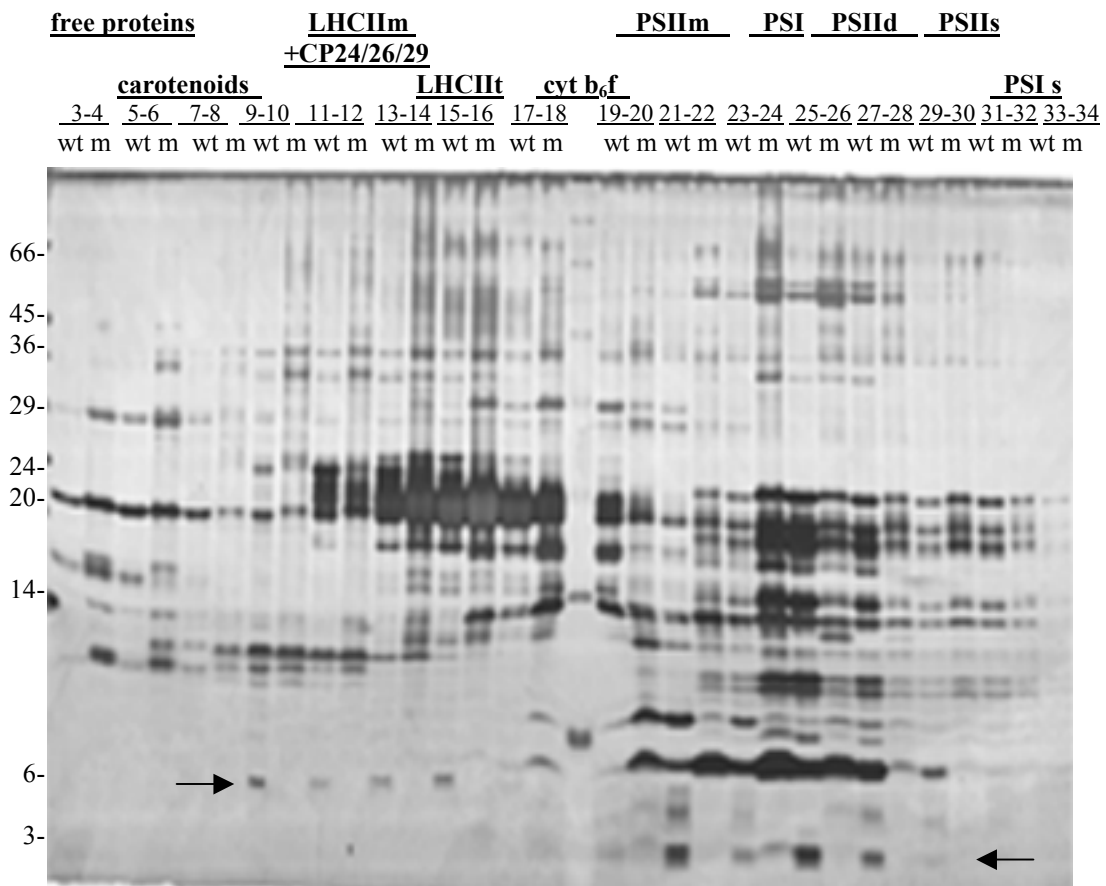


Fig. 23. Thylakoid membranes from *ycf9* mutant and wild-type plants grown at 25°C under 100 $\mu\text{E m}^{-2} \text{s}^{-1}$ were solubilized with β -dodecylmaltoside and separated in a linear 0.1 - 1.0 M sucrose gradient. Proteins from sucrose gradient fractions (600 μl each) were separated in a 13% Schagger/von Jagow gel and revealed by silver staining. Two polypeptide deficiencies, corresponding to bands at 6 kDa and 4 kDa, respectively (arrows), are observed in $\Delta ycf9$ mutant compared to wild-type. Fraction numbers and protein complexes are indicated above the figure. (wt) = wild-type, (m) = $\Delta ycf9$ tobacco. Molecular weights in kDa are indicated at the left of the figure; m: monomer, d: dimer, t: trimer, s: supercomplexes.

3.1.11.3.1.1 Serological analysis of sucrose gradient fractions

Sucrose gradients of thylakoid lysates of $\Delta ycf9$ and wild-type tobacco are compared in Figure 22. It is evident that in the $\Delta ycf9$ plants there is little or no material at the position of the PSII-LHCII supercomplexes (Figure 24). This conclusion was substantiated by immunological analyses. The sucrose gradients were fractionated and the proteins were separated by electrophoresis in denaturing 12% polyacrylamide gels, electroblotted and incubated with antisera raised against D1, LHCII and the reaction center proteins PsaA and PsaB of PSI. No changes of the PSI RC were noted between $\Delta ycf9$ and wild-type material, whereas signals of D1 and LHCII proteins were clearly absent in the fractions corresponding to the PSII supercomplexes in the wild-type tobacco (Figure 24).

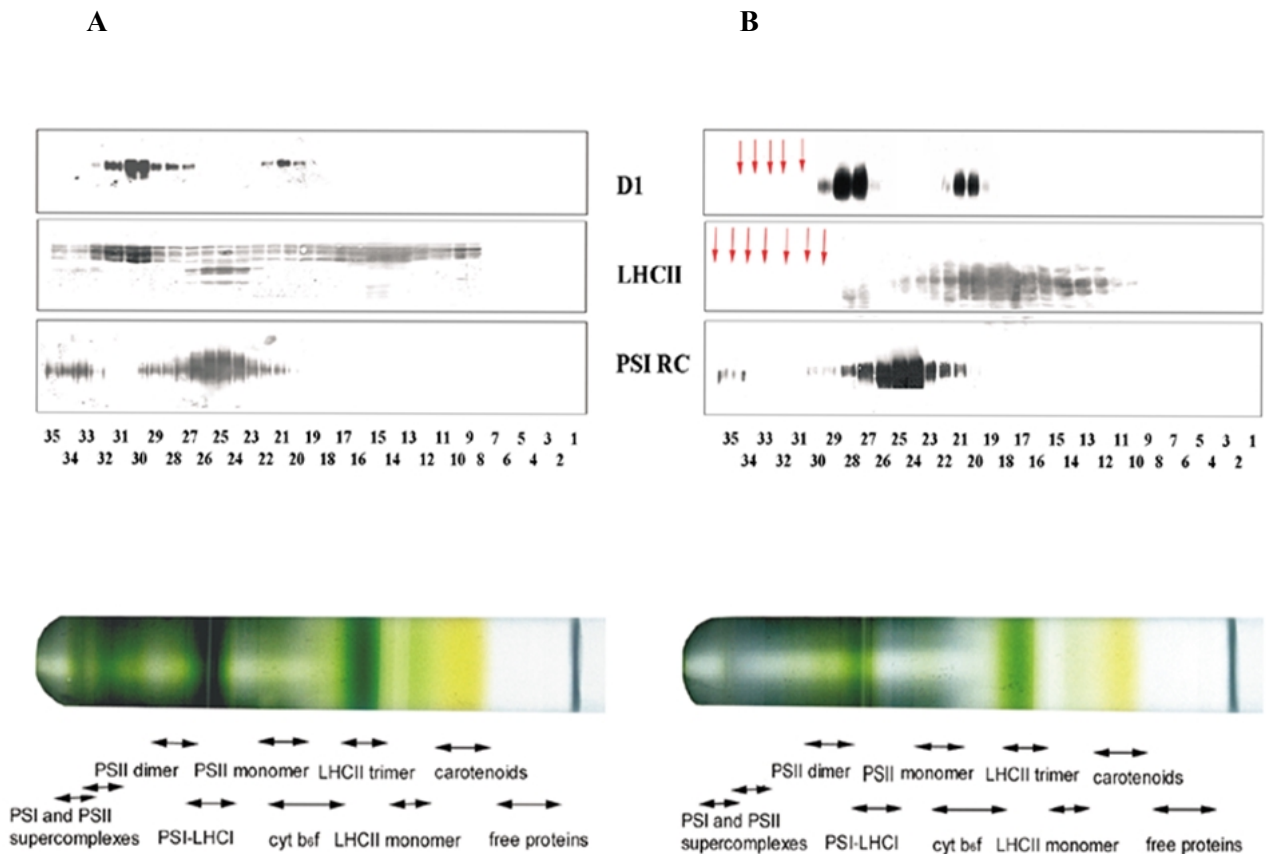


Fig. 24. Immunological analyses of all sucrose gradient fractions with antisera directed against D1, LHCII and PsaA/PsaB proteins of PSI reaction center. Identities of the complexes and the corresponding pigmented bands in the sucrose gradients are indicated at the bottom of the panels. Fraction numbers are indicated at the bottom of each blot. In the $\Delta ycf9$ panel (Panel B), vertical arrows mark fractions with a lack of immunoreactivity with D1 and LHCII antibodies different from the results with wild-type material (Panel A).

3.1.11.3.2 Isolation of the major protein complexes from the thylakoid membranes by two-dimensional gel electrophoresis

3.1.11.3.2.1 Deriphat-PAGE gel analysis

A two-dimensional gel analysis of the thylakoid membrane proteins from wild-type and $\Delta ycf9$ material grown under different light and temperature conditions ($10 \mu\text{E m}^{-2} \text{s}^{-1}$, 25°C and 20°C ; $100 \mu\text{E m}^{-2} \text{s}^{-1}$, 25°C and 20°C) proved the $\Delta ycf9$ -specific deficiency in the minor antenna protein CP26, and the impaired ability of $\Delta ycf9$ plants to form stable PSII-LHCII supercomplexes.

The Deriphat-PAGE method, in contrast to sucrose density gradient centrifugation, or Blue-Native gel system, allows to separate the entire minor antenna complex, which otherwise comigrates with LHCII monomer. Wild-type and $\Delta ycf9$ thylakoid membrane preparations were solubilized with 1% α -dodecylmaltoside, and applied to a non-denaturing Deriphat-PAGE. After separation of the protein complexes, slices of the gel, each with separated thylakoid protein complexes, were cut out and loaded onto a denaturing 12% Laemmli gel. After the electrophoretic separation protein spots were visualized using Coomassie staining. For all growth conditions reduction of the signal corresponding to CP26 protein was observed, as shown in Figure 25. No remarkable reduction of CP29 and CP24 signals was detected in the mutant material. Another deficiency observed in $ycf9$ mutants compared to the wild-type was absence, or strong reduction, of the slowly migrating protein complex representing PSII-LHCII supercomplexes, best detectable in material grown at 25°C under $100 \mu\text{E m}^{-2} \text{s}^{-1}$.

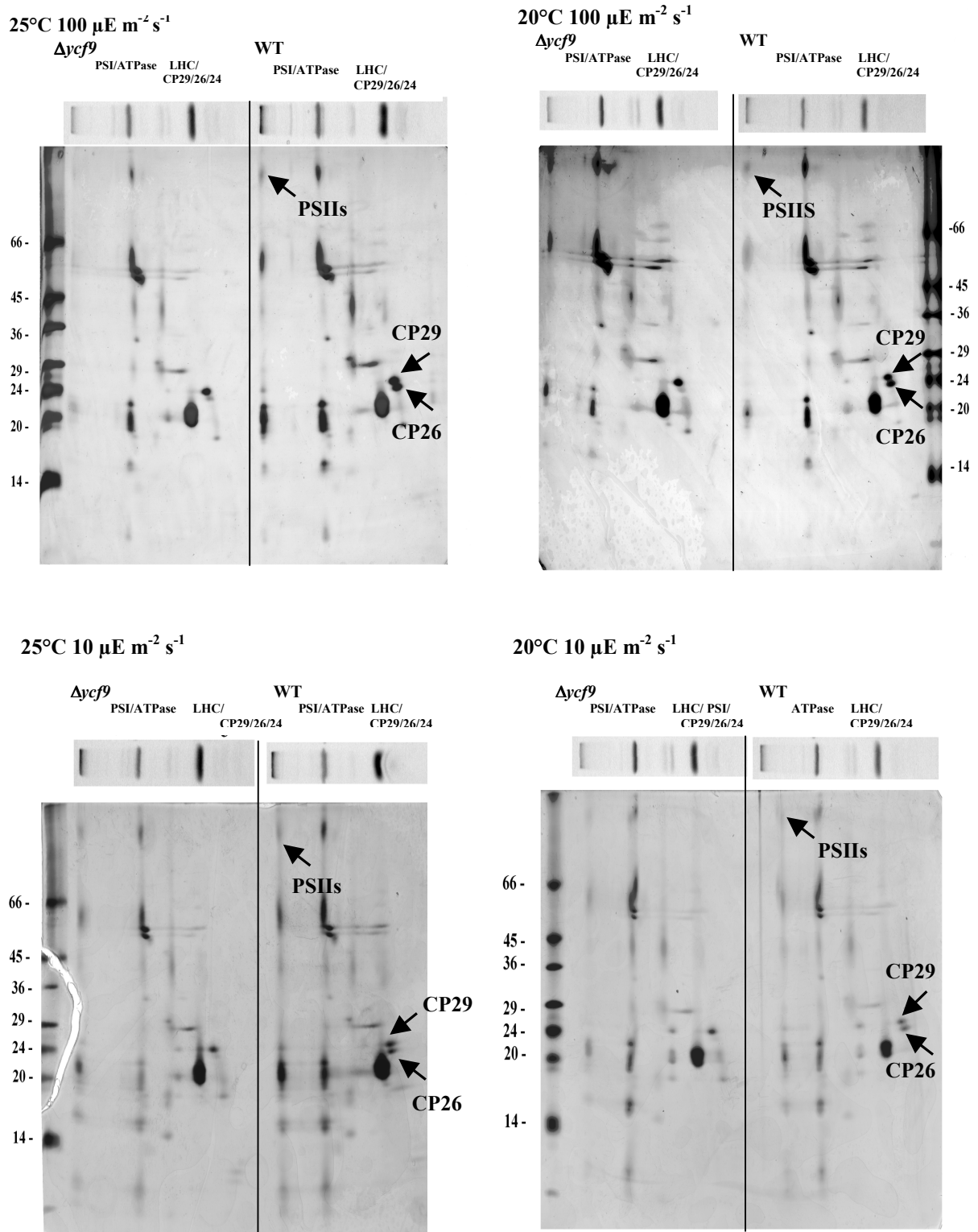


Fig. 25. 2D gel analysis of wild-type and $\Delta ycf9$ plants grown under different light and temperature regimes. 12.5 μg chlorophyll of the wild-type and the $\Delta ycf9$ thylakoid membrane preparations were solubilized with 1% α -dodecylmaltoside, applied onto a non-denaturing Deriphat-PAGE gel, and, after separation of the protein complexes, loaded onto a denaturing Laemmli gel with 2nd dimension. The molecular weight markers are indicated for the each gel, the upper part of the figure shows the 1st dimension of the non-denaturing PAGE. CP26, CP29 and PSII supercomplexes (s) proteins are indicated by arrowheads. Light and temperature regimes are indicated on the top of the left panel.

3.1.11.3.2.2 Blue-native PAGE analysis

After solubilization by β -dodecylmaltoside, the membrane complexes of wild-type and $\Delta ycf9$ material were separated by blue-native gel electrophoresis and gel stripes with separated protein complexes were subsequently loaded on denaturing 13% Schagger/von Jagow gels. Silver staining of the gels uncovered two small peptides in the molecular range of 4 - 6 kDa which were seen in wild-type, but not in mutant fractions. The band at 4 kDa, corresponding to fractions containing the PSII dimer and PSII supercomplexes, was located in wild-type but not in $\Delta ycf9$ material. A second band of 6 kDa was also missing from $\Delta ycf9$ thylakoids. This protein was found in the upper region of the gel, with a distribution profile that did not match that of LHCII proteins (Figure 26).

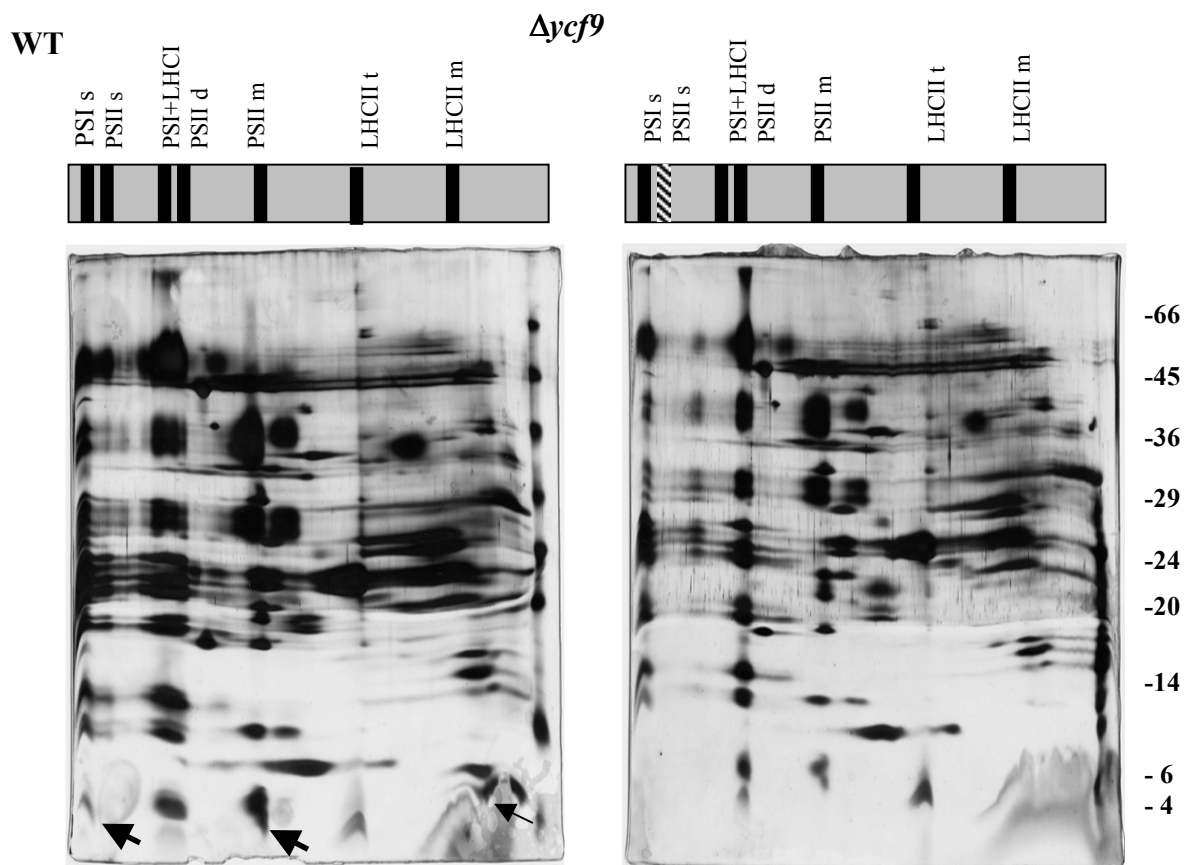


Fig. 26. Thylakoid membrane proteins from $\Delta ycf9$ (right) and wild-type (left) plants grown at 25°C under 100 $\mu\text{E m}^{-2} \text{s}^{-1}$ were separated by two-dimensional gel electrophoresis and revealed by silver staining. Two polypeptide deficiencies, corresponding to 6 kDa and 4 kDa, are observed in the $ycf9$ mutant compared to wild-type, as indicated by light and bold arrowheads, respectively. The upper part of the figure shows schematically the 1st dimension of the non-denaturing PAGE. Protein complexes are indicated: (m)- monomer, (d)- dimer, (t)- trimer, (s)- supercomplexes. The molecular weights marker in kDa is indicated at the right.

3.1.12 Alterations of protein phosphorylation in the $\Delta ycf9$ mutant

3.1.12.1 Alterations of protein phosphorylation in the $\Delta ycf9$ mutant

It is well documented that the interaction between peripheral antenna and PSII cores is controlled by phosphorylation of antenna subunits in a process known as state transitions, by which a portion of LHCII detaches from the PSII cores due to its increased phosphorylation by a redox-controlled kinase (Allen 1992). Thus, the loss of PSII-LHCII supercomplexes in the $\Delta ycf9$ mutants could result from changes in the phosphorylation patterns of PSII components as well as, or instead of, a direct steric contribution of Ycf9 to the interaction of the PSII cores with their peripheral antenna. To monitor the phosphorylation status of the thylakoid membranes, antibodies raised against phosphothreonine residues were used for immunoblot analyses.

The thylakoid membranes isolated from the tobacco mutant grown under conditions that produced a marked phenotype, displayed two notable changes (Figure 27). Phosphorylation of two PSII core subunits, CP43 and D1, was markedly decreased in $\Delta ycf9$ material compared to wild-type under the four growth conditions tested (D1 and CP43 phosphorylation patterns in Figure 27). In parallel, LHCII phosphorylation was strongly increased in $\Delta ycf9$ compared to wild-type when plants were grown at 25°C in high and dim light, whereas the opposite effect was observed at 20°C under dim light. Since the overall accumulation of PSII (as monitored by D1 amounts) and LHCII were similar in wild-type and mutant leaves grown under similar conditions, the differences observed in the phosphoprotein patterns can be attributed to changes in the steady-state phosphorylation levels between PSII and LHCII subunits. The ratio of protein phosphorylation in LHCII vs. PSII was greatly enhanced in the $\Delta ycf9$ plants under all conditions studied.

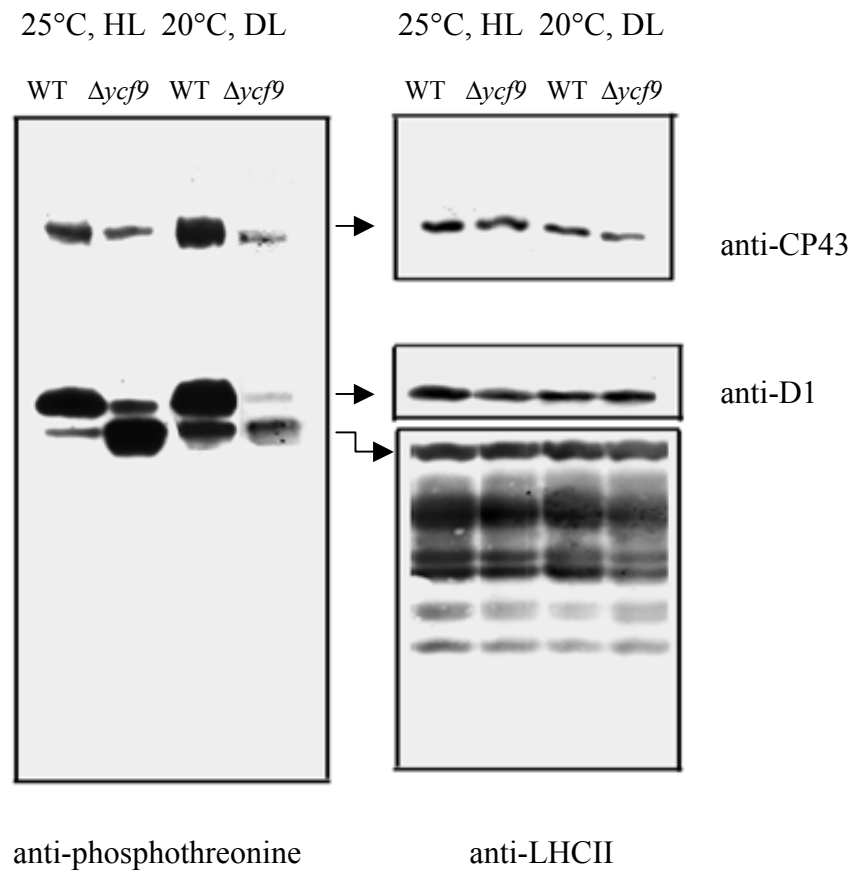


Fig. 27. Phosphorylation of thylakoid membrane proteins in wild-type and $\Delta ycf9$ mutants. Thylakoid membrane proteins from plants grown either at 25°C and 20°C under $100 \mu\text{E m}^{-2} \text{s}^{-1}$ light (HL) or under $10 \mu\text{E m}^{-2} \text{s}^{-1}$ light (DL) were separated by SDS-tricine 16.5% polyacrylamide gel electrophoresis, electroblotted onto nitrocellulose and incubated with anti-phosphothreonine, D1, CP43 and LHCII antisera (only samples grown at 25°C, $100 \mu\text{E m}^{-2} \text{s}^{-1}$ and 20°C, $10 \mu\text{E m}^{-2} \text{s}^{-1}$ light are shown). The proteins were isolated as described in Methods and the protein concentrations in the samples were normalized to the chlorophyll concentration.

3.1.12.2 Influence of light intensities on protein phosphorylation patterns of wild-type and $\Delta ycf9$ thylakoids

The influence of the light intensities on phosphorylation patterns of wild-type and $\Delta ycf9$ thylakoid proteins was examined by immunoblotting of thylakoid membrane proteins from plant material illuminated by 0 - $1000 \mu\text{E m}^{-2} \text{s}^{-1}$ using anti-phosphothreonine antibodies. The results of this Western analysis were scanned and signal intensities were estimated using the TINA software package v2.08 beta (Raytest, Spröckhovel). The phosphorylation of LHCII proteins increased with light intensity until it reached a maximum at approximately $400 \mu\text{E m}^{-2} \text{s}^{-1}$.

$^2 \text{ s}^{-1}$, then slowly decreased (Figure 28, as shown also by Rintamäki et al. 1997). In $\Delta ycf9$ material, LHCII phosphorylation increased faster and reached a higher maximum level compared to wild-type. An opposite effect was observed on the D1 phosphorylation, which increased faster in wild-type material until it reached a maximum. In $\Delta ycf9$ material the phosphorylation of D1 protein increased slower compared to the wild-type, but finally reached an identical maximal level.

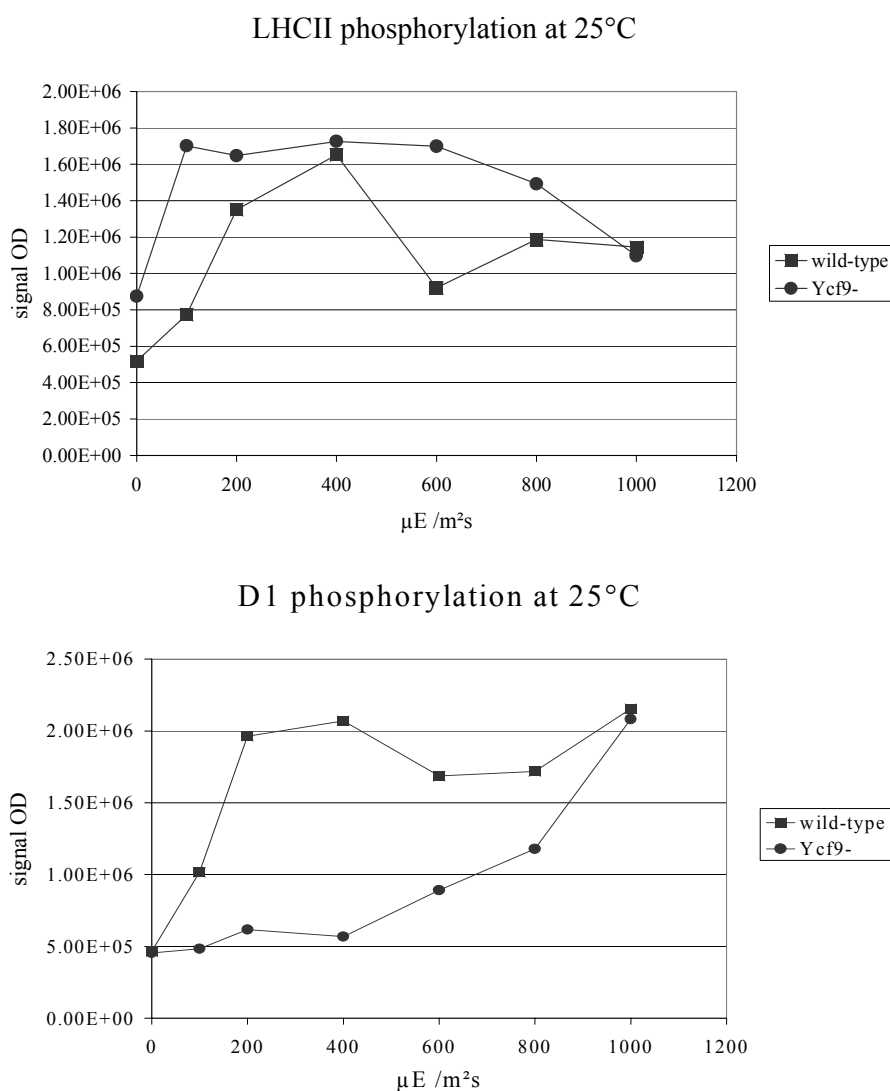


Fig. 28. Influence of light intensities on the phosphorylation patterns of wild-type and $\Delta ycf9$ thylakoid proteins. Freshly cut leaves from wild-type and $\Delta ycf9$ tobacco were illuminated for three hours with 0, 100, 200, 400, 600, 800, and 1000 $\mu\text{E m}^{-2} \text{ s}^{-1}$, and, after freezing in liquid nitrogen, membrane proteins were isolated, separated electrophoretically in a 15% PAA gel, electroblotted, and incubated with anti-phosphothreonine antibody. Additionally, the positions of the D1 and LHCII proteins were localized using specific antibodies. For the quantification of phosphoproteins, the immunoblots were scanned and the signal intensities were estimated using the TINA software package v2.08 beta. Upper panel: Phosphorylation pattern of the LHCII proteins at light intensities indicated on the X-axis, lower panel: Phosphorylation pattern of D1 protein at light intensities indicated on the X-axis.

3.1.12.3 Phosphorylation pattern of fractionated thylakoids from the wild-type and $\Delta ycf9$ mutants

For a detailed examination of the amount and localization of phosphoproteins in wild-type and $\Delta ycf9$ plants (grown at 25°C and 100 $\mu\text{E m}^{-2} \text{s}^{-1}$) proteins from the sucrose gradient fractions (see Section 3.1.11.3.1) were immunoblotted with anti-phosphothreonine antibodies. As previously observed, stronger phosphorylation of LHCII was noted in the corresponding fractions of the $\Delta ycf9$ mutant compared to wild-type (fractions 4 - 7 in Figure 29). Strong phosphorylation of D1 protein was noted in all wild-type fractions containing PSII (fractions 9 - 10 and 13 - 16 on Figure 29), which was absent in the corresponding $\Delta ycf9$ fractions. Additionally, 24 kDa phosphorylated D1 breakdown product (Kruse et al. 1997, Singh and Singhal 1999) was detected in the D1 monomeric fraction of the wild-type.

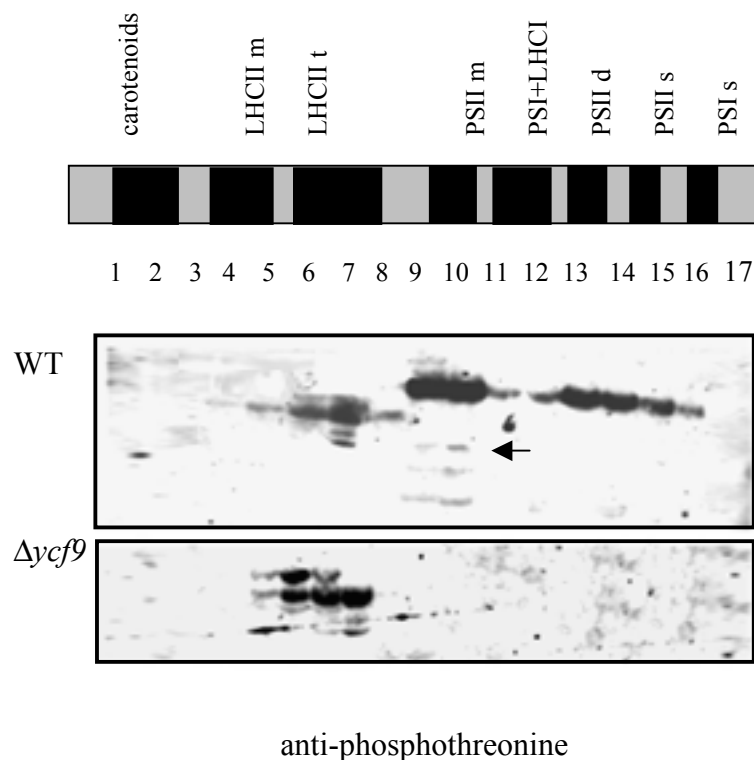


Fig. 29. Immunoblot analyses of all sucrose gradient fractions (600 μl per fraction) with antisera directed against phosphothreonine. Identities of the membrane complexes, as proved by D1 and LHCII-specific antisera and silver staining of the PAA gel, and fraction numbers are indicated at the top of the figure. Tobacco was grown on B5 medium containing 20 g/l sucrose under 100 $\mu\text{E m}^{-2} \text{s}^{-1}$ at 25°C; m: monomer, d: dimer, t: trimer, s: supercomplexes. Arrowhead: phosphorylated degradation product of D1 protein.

To examine the correlation between the phosphorylation of D1 protein and its structural organization in the various PSII complexes, the very same sucrose gradient fractions as presented above were separated by SDS-PAGE, electroblotted and probed with anti-D1 antibodies (Figure 30). For quantification the immunoblots were scanned and the intensity of signals was estimated using the TINA software package v2.08 beta.

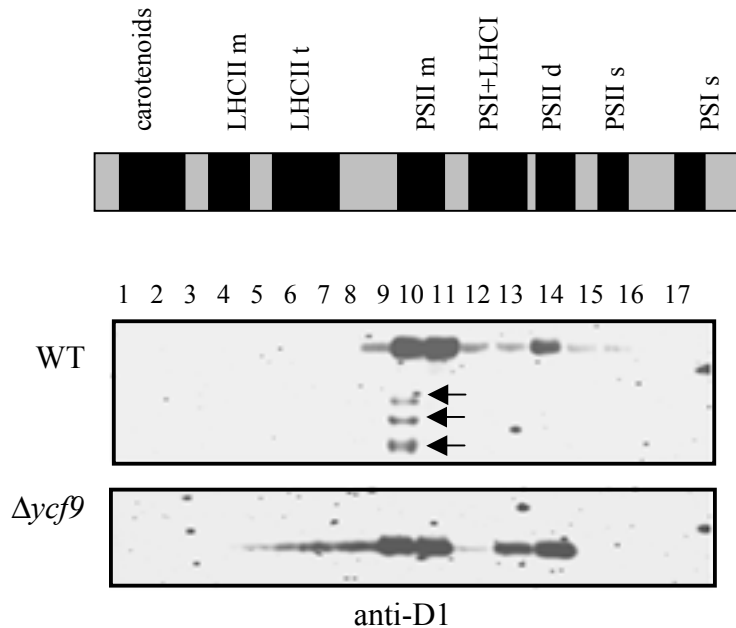


Fig. 30. Immunoblot analyses of all sucrose gradient fractions (600 μ l per fraction) with antisera directed against D1. Identities of the complexes and fraction numbers are indicated at the top of the figure. Tobacco was grown on B5 medium containing 20 g/l sucrose under $100 \mu\text{E m}^{-2} \text{s}^{-1}$ at 25°C ; m: monomer, d: dimer, t: trimer, s: supercomplexes. Arrows: degradation products of D1 protein. For comparison see Figure 29.

After comparison of Figure 29 and 30 it is evident that the phosphorylation of D1 protein in wild-type plants correlates with an increased formation of the dimeric form of D1, which is necessary to form supercomplexes (Barbato et al. 1992, Kruse et al. 1997). Lack of D1 phosphorylation in Δycf9 may be one reason for an increase of the monomeric D1 amount and an absence of the PSII-LHCII supercomplexes. Interestingly, D1 degradation products were detected by both anti-D1 and anti-phosphothreonine antibodies in the monomeric D1 fraction of wild-type tobacco, but not in the mutant material, even when an increased amount of the monomeric D1 protein was observed.

3.1.12.4 *In vitro* phosphorylation of thylakoid proteins

To examine possible qualitative or quantitative differences in the $\Delta ycf9$ and wild-type protein phosphorylation, an *in vitro* phosphorylation of thylakoid membranes was performed as described in Methods. Plants grown at all previously described light and temperature regimes were analysed in this experiment, although no phosphorylation differences were observed between the different phenotypes of $\Delta ycf9$. No qualitative notable difference was detected between wild-type and $\Delta ycf9$ phosphoproteins (Figure 31). However, a clear quantitative *in vitro* phosphorylation difference was noted between wild-type and $\Delta ycf9$ material. Under all conditions tested an approximately three times stronger phosphorylation of $\Delta ycf9$ proteins was observed as compared to wild-type.

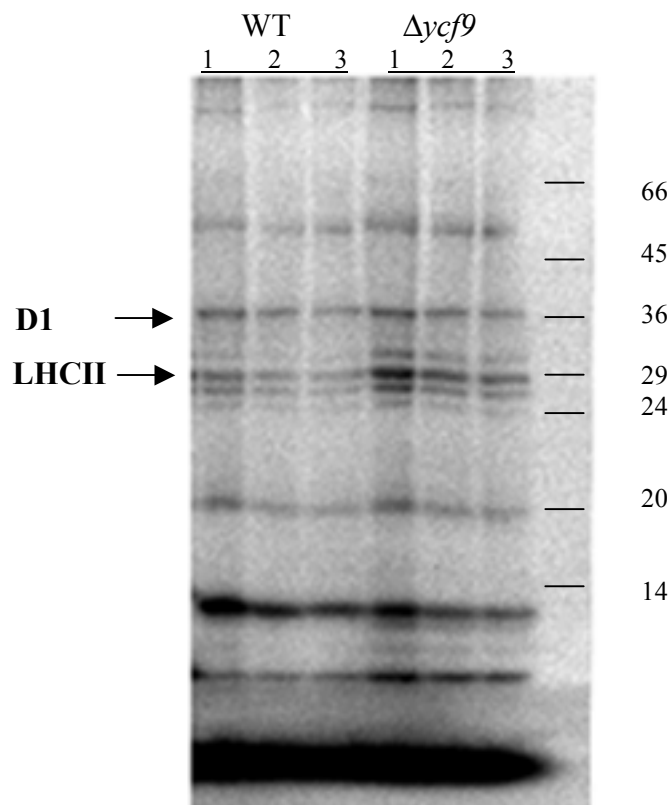


Fig. 31. *In vitro* phosphorylation of thylakoid membrane proteins from wild-type and $\Delta ycf9$ plants grown under $100 \mu\text{E m}^{-2} \text{s}^{-1}$ at 25°C . The phosphorylation assay was performed as described in Methods and the protein concentrations in the samples were normalized to the chlorophyll concentration. For each wild-type and $\Delta ycf9$ sample 20, 10 and 7 μg of chlorophyll were loaded onto the gel (as indicated at the top of the panel: lanes 1, 2 and 3, respectively). The molecular weights in kDa are indicated at the right. Arrowheads: D1 and LHCII phosphorylation.

3.1.13 Non-photochemical quenching in the $\Delta ycf9$ plants

For protection against photooxidative damage, occurring when the light energy absorbed becomes excessive relative to the capacity of photosynthesis, photosynthetic organisms developed non-radiative pathways that dissipate excess light energy absorbed by the antenna system. The xanthophyll cycle and the non-photochemical quenching of chlorophyll fluorescence (NPQ) represent processes preventing a photooxidative damage of the photosynthetic apparatus induced under high light. Non-photochemical quenching provides non-photochemical thermal dissipation of the absorbed excess photons. Thermal dissipation of the energy competes with the fluorescence emission, thus NPQ induction can be measured as a function of fluorescence quenching. Comparative measurements of the maximum level of fluorescence in dark-adapted samples (F_{max}) and after a period of high light treatment (F'_{max}), allows to calculate NPQ as $(F_{max} - F'_{max})/F'_{max}$ (Horton 1996). Figure 32 shows the induction and relaxation of NPQ in wild-type and $\Delta ycf9$ tobacco plants grown under different light and temperature conditions. Initially, 10 minutes exposure under bright light ($2200 \mu E m^{-2} s^{-1}$) caused a typical NPQ induction in both wild-type (black circle) and $\Delta ycf9$ (red circles). This process has two kinetic components, a fast phase that was completed within the first minute of illumination, and a slow phase that developed steadily over the next 9 minutes. Recovery took place in darkness with a half-life of about 6 minutes. The amplitude of the NPQ developed upon light stress was dependent on the light and temperature conditions applied for the wild type and mutant plants (Table 3 and Figure 32). In the wild type the adaptation to high light or low temperature stress induced an increase in the non-radiative energy dissipation (NPQ amplitude). In contrast, the $\Delta ycf9$ mutant displayed an opposite NPQ behaviour under the same experimental conditions, namely the decrease of the NPQ amplitude under the higher stress conditions (Table 3). At constant growth temperature, increasing the light intensity decreased the NPQ amplitude. Similarly, decreasing the temperature under constant light intensity also decreased the NPQ amplitude. For $\Delta ycf9$ plants grown under $100 \mu E m^{-2} s^{-1}$, the NPQ amplitude was 37% lower at $17^{\circ}C$ than at $25^{\circ}C$. The upper panel of Figure 32 also shows that at $17^{\circ}C$ the rate of NPQ relaxation in the dark was strongly affected in the mutant. After 10 minutes of recovery in darkness, the quenching in the wild-type leaves was reversed by 85%, whereas only 30% recovery was recorded for $\Delta ycf9$. Moreover, 50% of the recovery in the wild-type occurred within the first 2 min of dark adaptation, representing the rapidly relaxing ΔpH -dependent (qE) component of NPQ (Horton 1996). The following slow phase of recovery reflects the slowly relaxing, photoinhibition

component (qI). Only the second, slow phase of recovery was recorded in the mutant suggesting that $\Delta ycf9$ plants may have lost part of the adaptation mechanism which dissipates excess light energy under stress conditions (higher light, sub-optimal growth temperature; Huner et al. 1998). The ratios of NPQ amplitudes between $\Delta ycf9$ and wild-type plants are presented in Table 3.

Table 3. Maximal amplitude of quenching following 10 min exposure to supersaturating light. Measurements were performed at room temperature with plants grown at different light and temperature regimes. Before exposure to supersaturating light, plants were dark-adapted for 10 min. DL: $10 \mu\text{E m}^{-2} \text{s}^{-1}$, HL: $100 \mu\text{E m}^{-2} \text{s}^{-1}$.

	25°C		20°C		17°C	
	DL	HL	DL	HL	DL	HL
NPQ^{WT}	2.60	2.10	2.70	3.10	3.10	3.40
$\text{NPQ}^{\Delta ycf9}$	3.25	2.80	2.25	2.15	2.25	1.75
$\text{NPQ}^{\text{WT}} / \text{NPQ}^{\Delta ycf9}$	0.80	0.75	1.25	1.44	1.38	1.94

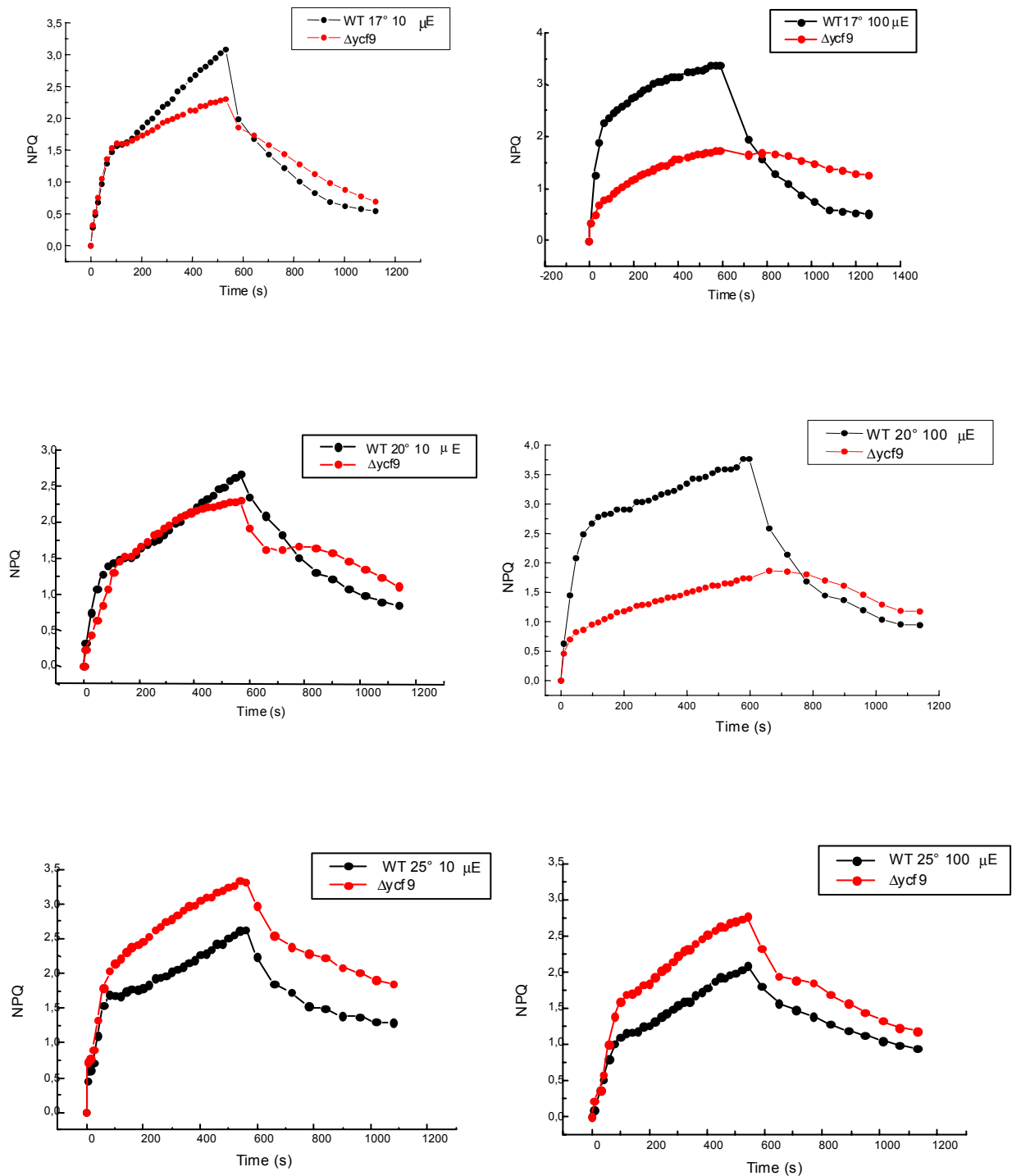


Fig. 32. Non-photochemical quenching in intact leaves of wild-type (black circles) and $\Delta ycf9$ (red circles) tobacco. Plants were grown on B5 medium containing 20 g/l sucrose under 100 $\mu E m^{-2} s^{-1}$ (right) or 10 $\mu E m^{-2} s^{-1}$ (left), and 17°C (upper panel), 20°C (middle panel) or 25°C (lowest panel). Non-photochemical quenching was induced with 2200 $\mu E m^{-2} s^{-1}$ continuous light for 10 min, and the recovery took place in darkness.

3.1.14 Pigment composition and xanthophyll cycle in the $\Delta ycf9$ plants

As mentioned above, NPQ has been correlated with the activation of the xanthophyll cycle, which promotes a reversible, ΔpH -induced deepoxidation of the xanthophyll violaxanthin to zeaxanthin via the intermediate antheraxanthin catalyzed by the enzyme violaxanthin deepoxidase. Deepoxidation of violaxanthin is involved in the conversion of PSII to a state of high thermal energy dissipation and low chlorophyll fluorescence emission (Demmig-Adams 1990). The composition of the xanthophyll cycle pigments was investigated in the wild-type and in $\Delta ycf9$ tobacco (Table 4). During the experiment plants were first exposed to dim light, and a growth regime of 20°C under $10 \mu\text{E m}^{-2} \text{s}^{-1}$, which was followed by an exposure to increased light intensity ($900 \mu\text{E m}^{-2} \text{s}^{-1}$) for 30 minutes (HL), and then by a transfer to darkness at 20°C for 10 minutes (HL+dark). The wild-type plants initially contained more than 95% violaxanthin which was subsequently converted into zeaxanthin under high light. This pigment modification corresponded to a de-epoxidation state (DS) of 0.33, with $\text{DS} = (\text{Z} + 1/2\text{A}) / (\text{Z} + \text{V} + \text{A})$ (Demmig-Adams and Adams 1992). After recovery in darkness for 10 minutes, the zeaxanthin pool decreased to about 20% of total, with a DS of 0.14. The high-light treatment of $\Delta ycf9$ plants caused a strong increase of the de-epoxidation state, with only 25% of the pigments from the xanthophyll cycle remaining as violaxanthin. Significant amounts of de-epoxidized forms, including both zeaxanthin and antheraxanthin, accumulated in parallel to the disappearance of violaxanthin (DS = 0.63). After 10 minutes recovery in the dark, the re-epoxidation was much slower than in the wild-type and the mutant leaves still contained an excess (65%) of de-epoxidized xanthophylls, corresponding to a DS of 0.56. Additionally, a higher amount of total carotenoids was detected in $\Delta ycf9$ plants as compared to the wild-type. This effect was dependent on the applied light intensities, and varied from 16% under dim light ($10 \mu\text{E m}^{-2} \text{s}^{-1}$), to 48% after 30 minutes illumination under high light. No such effect was observed for wild-type plants. Interestingly, the newly synthesized carotenoids belonged to the xanthophyll cycle pool while the content of other carotenoids, such as lutein, neoxanthin and β -carotene, remained constant. The increase in carotenoid content was not reversible during the following incubation for 10 minutes in the dark. Thus, light stress conditions specifically increased the xanthophyll pool available for deepoxidation in the mutant plants.

Table 4. HPLC analyses of changes in the pigment composition induced by high light.

Pigments ¹	DL ²		HL ²		HL+dark ²	
	wild-type	$\Delta ycf9$	wild-type	$\Delta ycf9$	wild-type	$\Delta ycf9$
neoxanthin	7.0	6.1	6.4	6.0	6.3	5.9
violaxanthin	6.5	10.3	5.1	4.4	6.3	6.1
antheraxanthin	0.0	0.1	0.0	3.9	0.8	3.8
zeaxanthin	0.3	0.5	1.7	8.9	0.7	7.6
β -carotene	3.7	3.1	4.3	3.7	3.2	4.8
lutein	13.7	16.3	14.2	20.1	14.3	17.7
VAZ	6.8	10.9	6.8	17.2	7.8	17
(Z+1/2A)/(VAZ)	0.044	0.050	0.33	0.63	0.14	0.56
Chl <i>a</i>	71.2	73.8	75.2	67.0	76.6	74.9
Chl <i>b</i>	28.8	26.2	24.8	33.0	23.4	25.1
Total Carotenoids	31.2	36.4	31.7	47.0	31.6	46.1

¹ Pigment composition was normalized to 100 moles of total (*a+b*) chlorophyll. V: violaxanthin; A: antheraxanthin; Z: zeaxanthin; Total Car: total carotenoids; VAZ: V+A+Z. The ratio (Z+1/2A)/(VAZ) refers to the de-epoxidation state as defined in Demmig-Adams and Adams (1992).

² Pigment composition was measured in leaves of tobacco plants grown at 20°C, 10 $\mu\text{E m}^{-2} \text{s}^{-1}$ (DL), exposed to high light (900 $\mu\text{E m}^{-2} \text{s}^{-1}$) for 30 min (HL), and allowed to recover in darkness for 10 min (HL+dark). Analyses were performed by HPLC of 80% acetone leaf extracts.

3.1.15 Chlorophyll fluorescence analysis

3.1.15.1 77K chlorophyll fluorescence analysis

3.1.15.1.1 Analysis of PSI and PSII supercomplexes assembly; excitation spectra by emission at 735 and 690 nm

Measurement of excitation spectra by emission at 735 or 690 nm allows to distinguish the amount of pigments, including LHC antenna, attached to PSI and PSII, respectively, reflecting the formation of PSI and PSII supercomplexes in the thylakoid membrane. Both

wild-type and $\Delta ycf9$ thylakoid membranes isolated from plants grown under different light and temperature conditions (10 and 100 $\mu\text{E m}^{-2} \text{s}^{-1}$, 20°C and 25°C) were examined. Representative results of the analysis of plant material grown at 25°C, 100 $\mu\text{E m}^{-2} \text{s}^{-1}$ are shown in Figure 33.

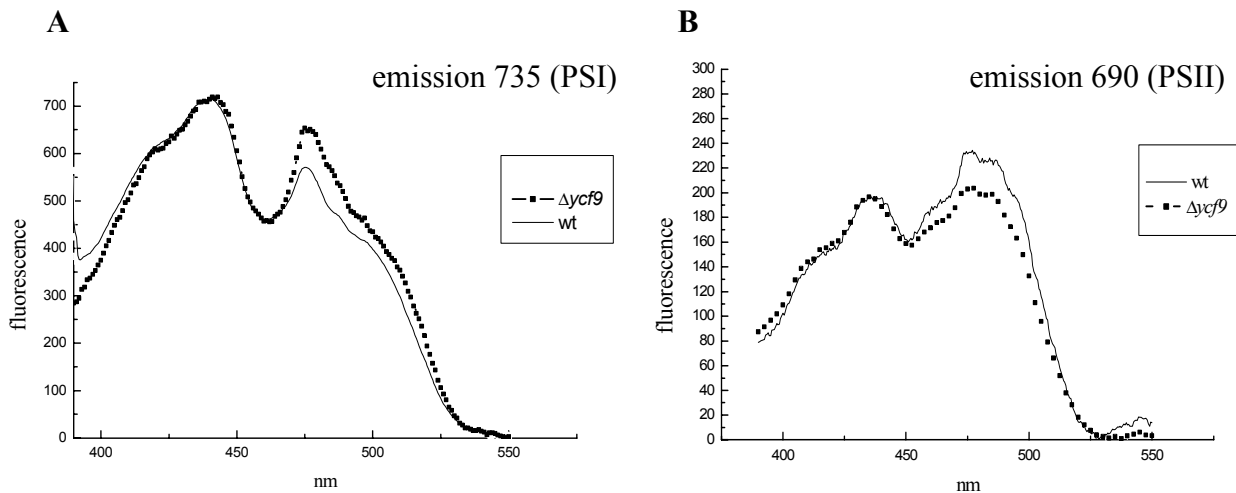


Fig. 33. 77K analyses of the wild-type and $\Delta ycf9$ plants. The excitation spectra were measured with emission wavelengths of 690 nm (PSII) and 735 nm (PSI). The peaks at 440 nm represent reaction centers (*chl a*) of PSI (Panel A) and PSII (Panel B) and the peaks at 475 nm represent PSI and PSII reaction centers with associated LHC antenna (*chl b*), corresponding to PSI and PSII supercomplexes (Panels A and B, respectively).

In agreement with results presented in Section 3.1.11, the excitation spectra of PSI and PSII of wild-type and $\Delta ycf9$ plants show differences in the assembly/stability of PSII and PSI supercomplexes. While a decreased amount of PSII reaction centers with associated antenna was observed in the $\Delta ycf9$ material compared to wild-type under all conditions tested, an opposite effect was true for the PSI.

3.1.15.1.2 Chlorophyll *b* emission spectra

Chlorophyll emission spectra after excitation at a wavelength of 475 nm enable to calculate the ratio of PSI/PSII as well as the amount of LHC antenna attached to both reaction centers. This analysis of plants grown under different light and temperature regimes offers the possibility to investigate the process of state-transitions. Wild-type and $\Delta ycf9$ thylakoid

membranes isolated from plants grown under different light and temperature conditions (20°C and 25°C, 10 and 100 $\mu\text{E m}^{-2} \text{s}^{-1}$) were investigated.

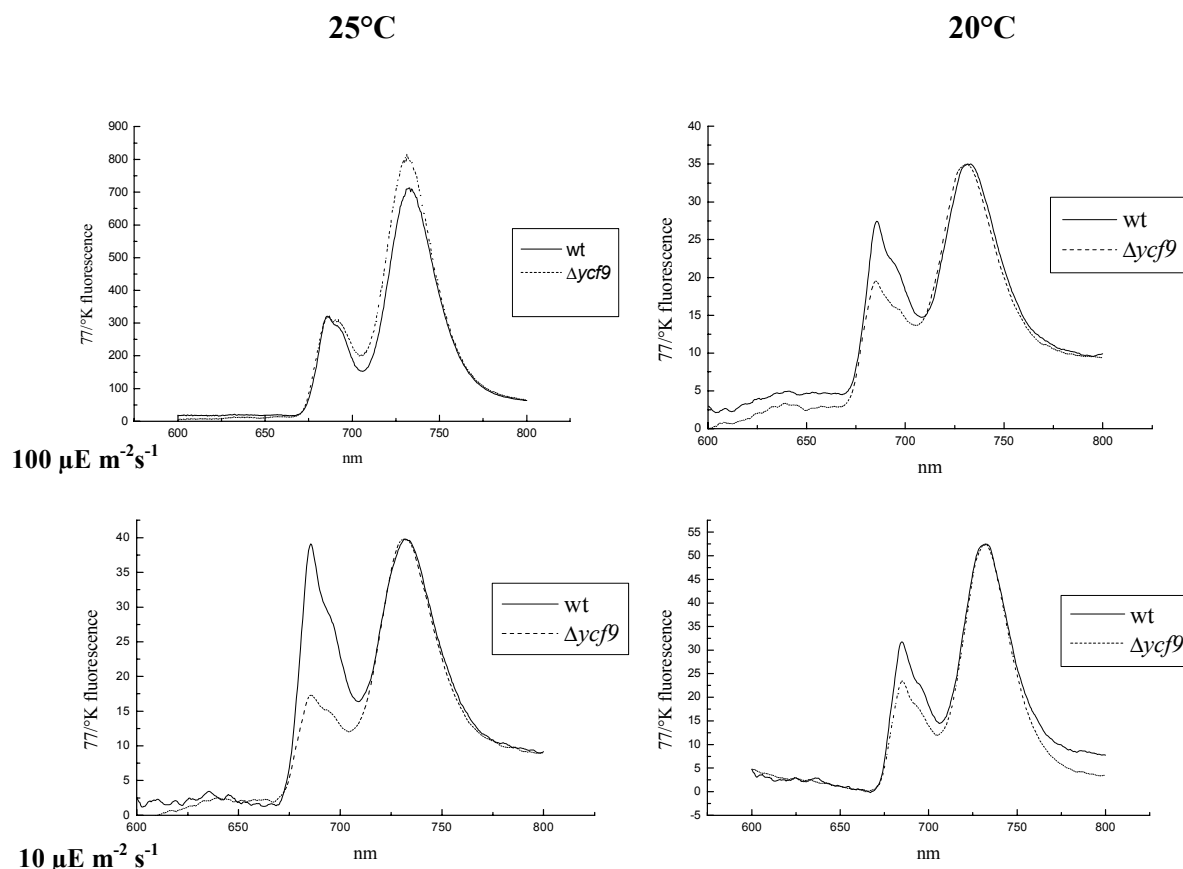


Fig. 34. Chlorophyll *b* emission spectra of the wild-type and $\Delta ycf9$ tobacco. Excitation of chlorophyll *b* at 475 nm results in two peaks representing PSII at 690 nm and PSI at 735 nm. Plants grown under light and temperature regimes as indicated above and on the left side of the graphs were analysed. The calculated PSI/PSII ratio is presented in the Table 5.

Table 5. PSI/PSII ratio of wild-type and $\Delta ycf9$ tobacco grown under different light and temperature regimes.

	25°C, 100 $\mu\text{E m}^{-2} \text{s}^{-1}$		25°C, 10 $\mu\text{E m}^{-2} \text{s}^{-1}$		20°C, 100 $\mu\text{E m}^{-2} \text{s}^{-1}$		20°C, 10 $\mu\text{E m}^{-2} \text{s}^{-1}$	
PSI/PSII ratio	WT	$\Delta ycf9$	WT	$\Delta ycf9$	WT	$\Delta ycf9$	WT	$\Delta ycf9$
	2.1	2.4	1.0	2.3	1.3	1.83	1.6	2.3

Measurements at 25°C with wild-type tobacco showed a correlation of the redistribution of LHC antenna from PSII to PSI with increasing light intensity, a process which can be

attributed to the state-transition mechanism. No such effect was observed for $\Delta ycf9$ material. Moreover, under all growth conditions tested the amount of LHC antenna attached to PSII was reduced in $\Delta ycf9$ compared to the wild-type. No clear correlation between the distribution of LHC antenna and light intensities was observed at lower temperatures. It has been previously demonstrated (Verhoeven et al. 1999) that low temperature may cause the same photoinhibitory effect as high light treatment. Thus, it can not be excluded that the conditions applied additionally affected the size or distribution of the LHC pool in both, wild-type and $\Delta ycf9$ material.

3.1.15.2 Chlorophyll fluorescence measurements at room temperature

For the spectroscopic analysis of chlorophyll fluorescence wild-type and $\Delta ycf9$ tobacco grown under different light and temperature regimes (10 and 100 $\mu\text{E m}^{-2} \text{s}^{-1}$, 20°C and 25°C) were analyzed. The maximum fluorescence (F_M) and the ratio $(F_M - F_0)/F_M = F_V/F_M$, as well as the fluorescence quenching parameters qP (photochemical quenching) = $(F_M' - F_S)/(F_M' - F_0')$, and qN (non-photochemical quenching) = $1 - (F_M' - F_0')/(F_M - F_0)$ (Schreiber 1986) were determined for all samples. The averages of at least three measurements are presented in Table 6.

Table 6. Spectroscopic analyses of wild-type and $\Delta ycf9$ mutant plants.

	WT 25°,100 μE	$\Delta ycf9$ 25°,100 μE	WT 25°,10 μE	$\Delta ycf9$ 25°,10 μE	WT 20°,100 μE	$\Delta ycf9$ 20°,100 μE	WT 20°,10 μE	$\Delta ycf9$ 20°,10 μE
F_V/F_M	0.80	0.73	0.76	0.75	0.75	0.78	0.79	0.76
qP	0.96	0.93	1.00	0.94	1.05	1.01	0.99	0.99
qN	0.26	0.24	0.28	0.18	0.34	0.36	0.29	0.29

Measurements of the maximum fluorescence (F_M) and the ratio F_V/F_M allow to estimate the electron flow through PSII and the photosynthetic activity of plants. No differences between wild-type and $\Delta ycf9$ was observed, indicating unaltered photosynthetic activity of $\Delta ycf9$ tobacco.

3.2 Functional analysis of the *ycf10* (*cemA*) gene product

3.2.1 Comparison of the Ycf10 sequences

The plastid-encoded *ycf10* gene (ORF 229, *cemA*) from photosynthetically active organisms encodes a highly conserved polypeptide of 229 - 231 amino acid residues (Figure 35). The amino acid sequence deduced for the Ycf10 protein seems to contain four membrane spanning domains (see hydrophathy plot of the Ycf10 protein in Figure 36), and a putative cleavage site for a signal peptidase between the residues Ser-24 and Phe-25 (Willey and Gray 1990, Sasaki et al. 1993)

YCF10OE1	-----	-----	-----	-----	-----	-----
YCF10OE4	-----	-----	-----	-----	-----	-----
YCF10NT	-----	-----	-----	-----	-----	-----
YCF10AT	-----	-----	-----	-----	-----	-----
YCF10SO	-----	-----	-----	-----	-----	-----
YCF10ZM	-----	-----	-----	-----	-----	-----
YCF10OS	-----	-----	-----	-----	-----	-----
YCF10PT	-----	-----	-----	-----	-----	-----
Ycf10MP	MKKNFSYWRI	FHHIFALPYC	SLEKAYKASK	RIQKIKKDYF	LYKNILFSSK	RSWQSILFYI
Consensus	-----	-----	-----	-----	-----	-----
YCF10OE1	-----	-----	-----	-----	-----	-----
YCF10OE4	-----	-----	-----	-----	-----	-----
YCF10NT	-----	-----	-----	-----	-----	-----
YCF10AT	-----	-----	-----	-----	-----	-----
YCF10SO	-----	-----	-----	-----	-----	-----
YCF10ZM	-----	-----	-----	-----	-----	-----
YCF10OS	-----	-----	-----	-----	-----	-----
YCF10PT	-----	-----	-----	-----	-----	-----
Ycf10MP	DTELNNSVFK	IYLSLLEYKL	SLWLIQLFLI	FSLFFKKNKSK	FDLILPNINE	KKKKRKRINRK
Consensus	-----	-----	-----	-----	-----	-----
YCF10OE1	-----	-----	-----	-----	-----	-----
YCF10OE4	-----	-----	-----	-----	-----	-----
YCF10NT	-----	-----	-----	-----	-----	-----
YCF10AT	-----	-----	-----	-----	-----	-----
YCF10SO	-----	-----	-----	-----	-----	-----
YCF10ZM	-----	-----	-----	-----	-----	-----
YCF10OS	-----	-----	-----	-----	-----	-----
YCF10PT	-----	-----	-----	-----	-----	-MDPIPHSIT
Ycf10MP	LAWIRATLND	LESWRRYYLF	SSFLSLDKKE	KNNFSFLQMK	SSRLTAIAYE	SIGLVPRISIT
Consensus	-----	-----	-----	-----	-----	-----
YCF10OE1	-----	-----	---MKKKKKF	LPLLYLTAIV	FFPWWISLLF	-NKGLESWVT
YCF10OE4	-----	-----	---MKKKKEF	LPLLYLTAIV	FFPWWISLLF	-NKGLESWVT
YCF10NT	-----	-----	---MAKKKAF	TPLFYLASIV	FLPWWISFSV	-NKCLESWVT
YCF10AT	-----	-----	---MAKKKAF	IPFFYFLSIV	FLPWLISLCC	-NKSLKTWIT
YCF10SO	-----	-----M	KKKMEKKKVF	IPFLYLISIV	FLPWWIYLSF	-QKSLESWVT
YCF10ZM	-----	-----	---MKKKKAL	PSFLYLVFIV	LLPWGVSFSS	-NKCLELWIK
YCF10OS	-----	-----	---MKKKKAL	PSFLYLVFIV	LLPWGVSFSS	-NKCLELWIK
YCF10PT	RTLSRFRTLEL	TSESGSLAIH	ELEVSEYKAS	ASLRYLACLV	VLPWVIPISL	-RKGLEPWVT
Ycf10MP	RTFSRFKAEL	TNQSSSLVLK	EFRLAKYQAL	ASLQYIGCLF	FIPLGVSFFF	QKCFLEPWIQ
Consensus	-----	-----	---.*.*.-	-.*.*.-.*	..*.*-.....	-.*.-*.-*.-

YCF10OE1	NWWNTTHSET	FLTDMQEKSI	LDKFIELEEL	LLLDE-MINE	YPETHLQTLG	IGIHKEMVRL
YCF10OE4	NWWNTTHSET	FLTDMQEKSI	LDKFIELEEL	LLLDE-MINE	YPETHLQTLR	IGIHKEMVRL
YCF10NT	NWWNTGQSEI	FLNNIQEKSL	LEKFIELEEL	LFLDE-MIKE	YSETHLEEFQ	IGIHKETIQF
YCF10AT	NWWNTRQCET	FLNDIQEKSF	LEKFIQLEEL	FQLDE-MIKE	YPETNLQQFR	LGIHKETIQF
YCF10SO	TWWNTKQSET	FLNDIQEKKL	LEKFIELEEL	RLLDE-MIKE	YPETQLQKLG	IGIHNETIQF
YCF10ZM	NWWNTRQSET	FLTDIQEKRI	LEGFIELEEL	FLLDE-MIKE	KPKTHVQKLP	IGIHKETIQF
YCF10OS	NWWNTRQSQT	LLTAIQEKRV	LERFMELEDL	FILDE-MIKE	KPNTHVQNP	IGIRKEIQF
YCF10PT	NWWNTVKSQK	IFDYLQEQNA	LGRFEKIEEL	FLLER-MVED	SLGTHSQSIR	IETHKETIQF
Ycf10MP	NWWNIYQSQI	FLTSFQEEKA	LKKLQEIIEEL	FWLDKVMTYS	SNKIQLQDLT	KEIHQQTIEL
Consensus	*****-....	..*-.***.*-	*.-*.....**	--*-.*-.*	-.-*-.*-.*	...*.*-...*
YCF10OE1	IKMRNEDHIH	TILHLSTNII	CFIIFRGYSI	LGKNEKLLILN	SWMQEFLYNL	SDTIKAFSIL
YCF10OE4	IKMRNEDHIH	TILHLSTNII	CFIIFRGYSI	LGKNEKLLILN	SWMQEFLYNL	SDTIKAFSIL
YCF10NT	IKIQENRIH	TILHFSTNII	CFIILSGYSI	LGNEKLVILN	SWAQEFLYNL	SDTVKAFSIL
YCF10AT	IKIHNEYNIH	TILHFSTNLI	SFVILSGYSF	WGKEKLFILN	SWVQEFLYNL	SDTIKAFSIL
YCF10SO	IKMHNEDCIH	MILHFSTNLI	CFLILGGYSI	LGKNEKLLILN	SWVQEFLYNL	SDTIKAFSIL
YCF10ZM	AKIDNEDHLH	IILHFSTNII	CLAILSGSFF	LGKEELVILN	SWVQEFFYNL	NDSIKAFFIL
YCF10OS	AKIDNEGHLH	IILHFSTNII	CLAILSGSFF	LGKEELVILN	SWVQEFFYNL	NDSVKAFFIL
YCF10PT	VEMYNEDCIQ	IISHLLTNLI	GFAFISAYII	LGKNEKLLILN	SWIQEFFYSL	SDTMKAFLLI
Ycf10MP	VQIYNNDSIK	IVLHLLTDLI	WFTLSCLFI	LGKERLVILN	SWAQELFYSL	SDTMKAFLLI
Consensus	...-***-...	-***.***.*	..-.....-	**.-**.***	**-.***.*.*	*.-***-***
YCF10OE1	LLTDFCIGFH	SPHGWELMIA	YVYKDFGFAQ	NDQIISGLVS	TFPVILDTIF	KYWIFRYLNR
YCF10OE4	LLTDFCIGFH	SPHGWELMIA	YVYKDFGFAQ	NDQIISGLVS	TFPVILDTIF	KYWIFRYLNR
YCF10NT	LLTDLICIGFH	SPHGWELMIG	SIYKDFGFVH	NDQIISGLVS	TFPVILDTIF	KYWIFRYLNR
YCF10AT	LLTDLICIGFH	SPHGWELMIG	YIYKDFGFAH	YEQIISGLVS	TFPVILDTIF	KYWIFRYLNR
YCF10SO	LVTDLICIGFH	SPQGWELLIE	SIYKDFGFAD	NDQIISGLVS	TFPVILDTIF	KYWIFRSLNR
YCF10ZM	LVTDFVGFH	STRGWELLIR	WVYNNLGWAP	NELIFTIFVC	SFPVILDTCL	KFWVFFCLNR
YCF10OS	LVTDFVGFH	STRGWELLIR	WVYNNLGWAP	NELIFTIFVC	SFPVILDTCL	KFWVFFCLNR
YCF10PT	LATDLICIGFH	SPHGWELMID	SISESYGFAH	NERIISGLVS	TFPVILDTIL	KYWIIFRRFNR
Ycf10MP	LLTDLICIGFH	SPHGWEIVIS	SCLEHFGFVH	NKHVISCFVS	TFPVILDTVF	KYLIFRHLNR
Consensus	*.*.*...***	*..***.*-	--.-..*..-	*-*.***.*	..*****..	*.*.*-***
YCF10OE1	VSPSLVVIYD	SMND-				
YCF10OE4	VSPSLVVIYD	SMND-				
YCF10NT	LSPSLVVIYH	SMND-				
YCF10AT	VSPSLVVIYH	AIND-				
YCF10SO	VSPSLVVIYH	SMND-				
YCF10ZM	LSPSLVVIYH	SISEA				
YCF10OS	LSPSLVVIYH	SISEA				
YCF10PT	ISPSLVVIYH	SMNE-				
Ycf10MP	ISPSIVATYH	TMNE-				
Consensus	-*****.	...--				

Fig. 35. Comparative analysis of Ycf10 amino acid sequences. The consensus is indicated at the bottom: 80 - 100% of identity among all sequences is marked by asterisks, identity from 60% - 80% by dots, identity below 60% by a dash. Abbreviations: OE1,4: *Oenothera elata* plastome I and IV, NT: *Nicotiana tabacum*, AT: *Arabidopsis thaliana*, SO: *Spinacia oleracea*, ZM: *Zea mays*, OS: *Oryza sativa*, PT: *Pinus thunbergii*, MP: *Marchantia polymorpha*. The predicted membrane helices are underlined, the putative cleavage site is marked in bold letters.

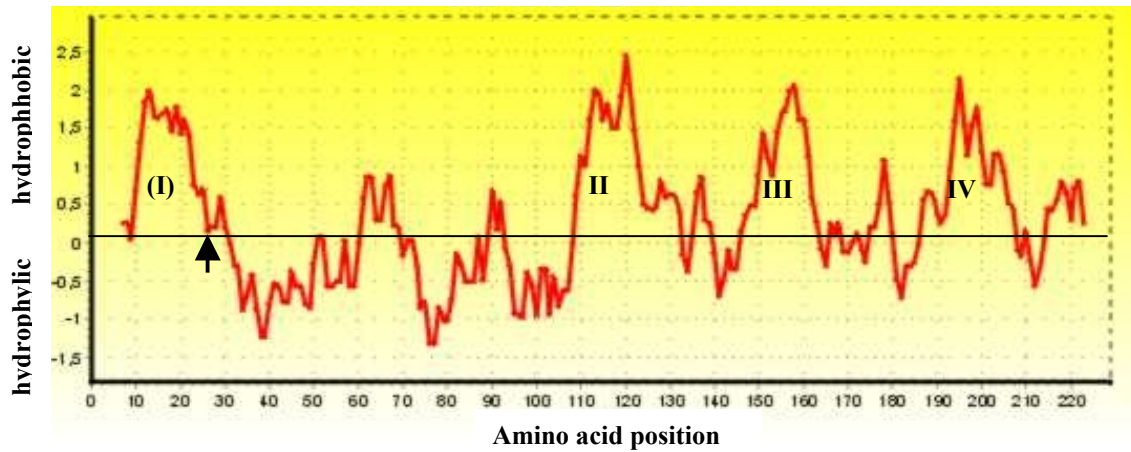


Fig. 36. Hydrophathy profile of Ycf10 (CemA; according to Kyte and Doolittle 1982). Amino acid positions are indicated at the bottom of the graph. The scan window size was 13 amino acid residues. Four hydrophobic, trans-membrane α -helices, designated (I), II, II and IV are indicated above the zero line. The putative cleavage site is marked by arrow.

3.2.2 Construction of a recombinant plasmid for *ycf10* inactivation

An inactivation vector for the *ycf10* gene was constructed by introducing the promoterless *aadA* cassette into the BbsI restriction site in the *ycf10* gene. The correct integration of the *aadA* gene onto the pGEM*ycf10* construct was monitored by PCR, restriction and nucleotide sequence analyses.

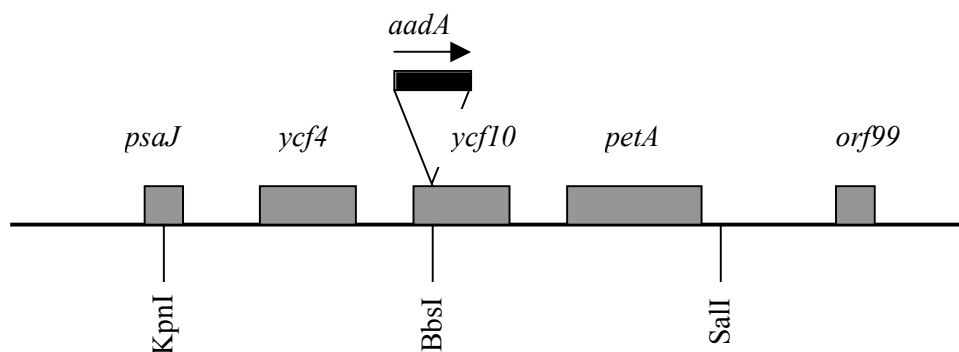


Fig. 37. Construction of the plastid transformation vector for disruption of the *ycf10* gene. The KpnI/SalI fragment of the plasmid pTB22 (Shinozaki et al. 1986), containing the *ycf10* gene and approximately 1 kb flanking regions was cloned into the pGEM vector. The inactivation of the *ycf10* gene was performed by insertion of the *aadA* cassette into a gene-internal BbsI site. A plasmid clone with the *aadA* cassette inserted in the same orientation as *ycf10* was used for plant transformation. The transcription direction of the *aadA* gene is indicated by an arrow.

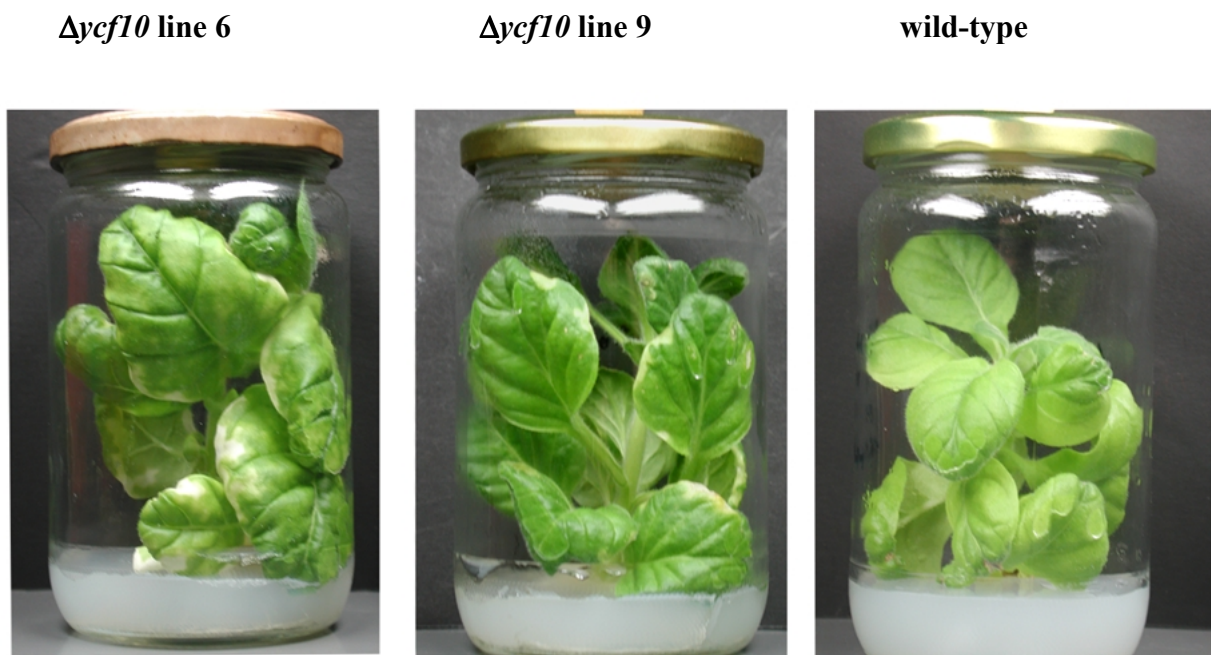
3.2.3 Plant transformation, selection and regeneration of mutants

Twenty leaves of *Nicotiana tabacum* were bombarded with gold particles carrying the recombinant plasmid pGEMycf10. After three days of cultivation on non-selective RMOP medium transformed leaves were cut and transferred to RMOP medium supplemented with spectinomycin. Resistant green colonies (calli) began to appear after approximately three weeks and were transferred onto fresh selective RMOP medium. The transformation yielded three independent mutant lines. Segregation of the mutant plastomes was enhanced by transferring shoot tops onto fresh selection medium in three-week intervals. For molecular analyses, the mutant lines underwent at least five cycles of shoot regeneration.

3.2.4 Growth phenotypes of the $\Delta ycf10$ plants

$\Delta ycf10$ plants were regenerated from the green calluses on antibiotic-supplied medium, and further cultivated parallel *in vitro* and in the greenhouse. All three mutant *ycf10* lines were able to survive on soil and produced fertile seeds. This confirmed that their phenotype was photoautotrophic. However, the material showed a clear non-wild-type phenotype. Under standard heterotrophic conditions ($100 \mu\text{E m}^{-2} \text{s}^{-1}$, 25°C , medium supplemented with sucrose) $\Delta ycf10$ plants developed dark green leaves with numerous pale green to white regions, generally present at the margins of the leaves (Figure 38). The leaves of the $\Delta ycf10$ plants have a prolonged shape and longer petioles compared to those of wild-type material. This effect was less dominant when plants were grown on soil in the greenhouse.

A



B

*Δycf10*

wild-type

C



wild-type

Δycf10

Fig. 38. Growth phenotypes of *Δycf10* plants. Panels A and C: *Δycf10* plants grown *in vitro* ($100 \mu\text{E m}^{-2} \text{s}^{-1}$, 25°C , growth medium supplemented with sucrose) are compared with wild-type tobacco. White regions of *Δycf10* leaves are indicated by arrows in panel C. Panel B: wild-type and *Δycf10* plants grown photoautotrophically under greenhouse conditions.

3.2.5 Ultrastructure of the $\Delta ycf10$ chloroplasts

Electron microscopy of wild-type and $\Delta ycf9$ plants was performed in the laboratory of Prof. G. Wanner (Botanisches Institut, München). As previously described, the $\Delta ycf10$ plants displayed a characteristic phenotype of dark green leaves with numerous pale regions. Both areas were examined by electron microscopy. The green parts of $\Delta ycf10$ leaves showed a chloroplast structure indistinguishable from wild-type, with numerous stroma and grana thylakoids and evenly distributed plastoglobules, whereas the bleached regions of the leaves displayed a substantially altered structure, without defined stroma and grana thylakoids (Figure 39). Further experiments (see Section 3.2.12) demonstrated that pale leaf regions lacked photosynthetic activity.

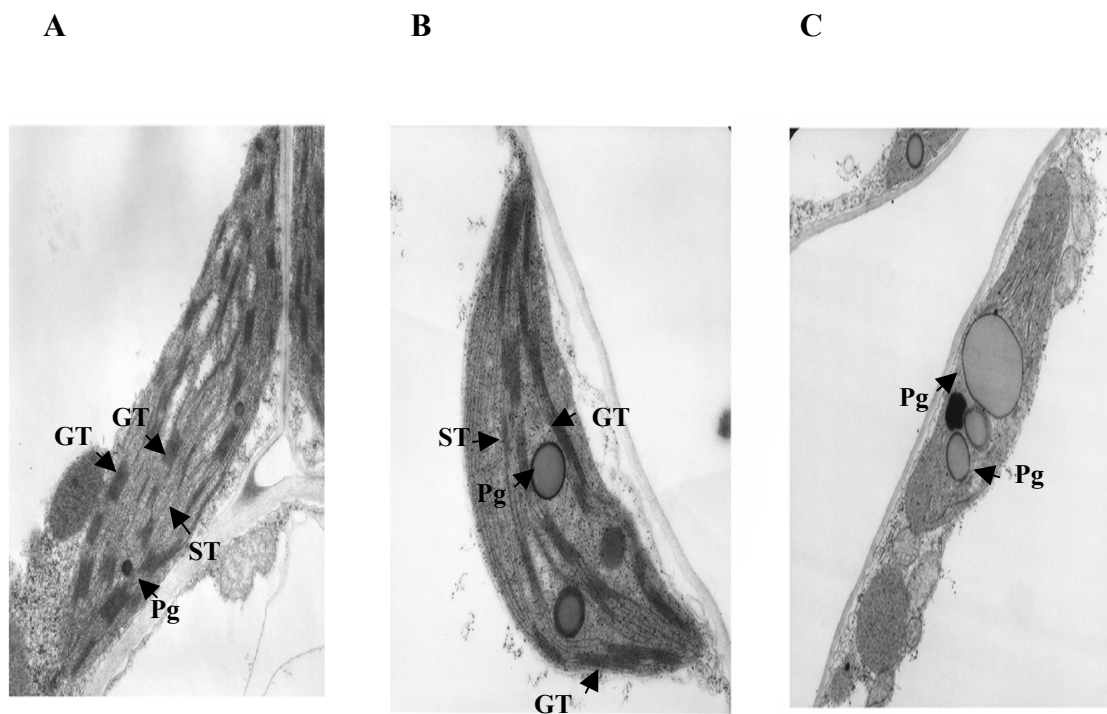


Fig. 39. Electron micrographs of plastids from wild-type and $\Delta ycf10$ plants of *Nicotiana tabacum*. (a) Typical lens-shaped wild-type chloroplast with numerous stroma (ST) and grana (GT) thylakoids, (b) chloroplast from green regions of the $\Delta ycf10$ mutant indistinguishable from wild-type, (c) plastid from a pale leaf region of the $\Delta ycf10$ mutant: no grana or stroma thylakoid structures were detected. Large plastoglobules (Pg) show a uniform distribution.

3.2.6 Investigation of the homoplasmic state of the $\Delta ycf10$ mutants

To confirm the homoplasmic state of $\Delta ycf10$ plants the strategy outlined in Section 3.1.6 was employed, including nucleotide sequence analysis, Southern analysis and PCR with total, plastid and PFGE - purified DNA.

3.2.6.1 Nucleotide sequence analysis

To confirm the correct integration into the tobacco plastid chromosome of the construct carrying the *aadA* gene, the segment of plastid DNA encoding *ycf10* was sequenced in transformants. For this purpose, an amplification product of *ycf10*for and *ycf10*rev primers was purified from an agarose gel that served as a template for nucleotide sequencing (Hupfer et al. 2000). This analysis established the successful disruption of *ycf10*. Moreover, insertion of the *aadA* causes a frame-shift in the gene, preventing a translational re-initiation of the transcript containing the C-terminal gene segment.

```

63347      TGTGTGTAAG AAATATTCGA TCGCATAGAG TGTACGAATG GGTTGATTAA
63397      CAATTCACAG ATGAAAAAAT GCAAAAAAG AAAGCATTCA CTCCTCTTTT
63447      CTATCTTGCA TCTATAGTAT TTTTGCCCTG GTGGATTTCT TTCTCAGTTA
63497      ATAAATGTCT GGAATCTTGG GTTACCAATT GGTGGAATAC TGGGCAATCC
63547      GAAATTTTTT TGAATAATAT TCAAGAAAAA ATTCGCCGTC GTTCAATGAG
AATGGATAAG AGGCTCGTGG GATTGACGTG AGGGGGCAGG GATGGCTATA
TTTCTGGGAG CGAACTCCGG GCGATATCAC TAGTTGTAGG GAGGGATCCA
TGGCTCGTGA AGCGGTTATC GCCGAAGTAT CAACTCAACT ATCAGAGGTA
GTTGGCGTCA TCGAGCGCCA TCTCGAACCG ACGTTGCTGG CCGTACATTT
GTACGGCTCC GCAGTGGATG GCGGCCTGAA GCCACACAGT GATATTGATT
TGCTGGTTAC GGTGACCGTA AGGCTTGATG AAACAACGCG GCGAGCTTTG
ATCAACGACC TTTTGGAAAC TTCGGCTTCC CCTGGAGAGA GCGAGATTCT
CCGCGCTGTA GAAGTCACCA TTGTTGTGCA CGACGACATC ATTCCGTGGC
GTTATCCAGC TAAGCGCGAA CTGCAATTTG GAGAATGGCA GCGCAATGAC
ATTCTTGCAG GTATCTTCGA GCCAGCCACG ATCGACATTG ATCTGGCTAT

```

CTTGCTGACA AAAGCAAGAG AACATAGCGT TGCCTTGGTA GGTCCAGCGG
CGGAGGAACT CTTTGATCCG GTTCCTGAAC AGGATCTATT TGAGGCGCTA
AATGAAACCT TAACGCTATG GAACTCGCCG CCCGACTGGG CTGGCGATGA
GCGAAATGTA GTGCTTACGT TGTCCCGCAT TTGGTACAGC GCAGTAACCG
GCAAAATCGC GCCGAAGGAT GTCGCTGCCG ACTGGGCAAT GGAGCGCCTG
CCGGCCCAGT ATCAGCCCGT CATACTTGAA GCTAGACAGG CTTATCTTGG
ACAAGAAGAA GATCGCTTGG CTTCCGCGCG AGATCAGTTG GAAGAATTTG
TCCACTACGT GAAAGGCGAG ATCACTAAGG TAGTTGGCAA ATAACTGCAG
63576 GCATGCAAGC TAAAAGAGTC TTCTAGAAAA ATTCATAGAA TTAGAGGAAC
63611 TCCTCTTCTT GGACGAAATG ATCAAGGAAT ACTCGGAAAC ACATCTCGAA
63661 GAGTTTGGGA TAGGAATCCA TAAAGAAACG ATCCAATTAA TCAAGATACA
63711 AAATGAGAAT CGTATCCATA CGATTTTGCA CTTCTCGACA AATATCATCT
63761 GTTTTATTAT TCTAAGCGGG TATTCAATTT TGGGTAATGA AAAACTTGTT
63811 ATTCTTAACT CTTGGGCTCA GGAATTCCTA TATAACTTAA GTGACACAGT
63861 AAAAGCTTTT TCTATTCTTT TATTAAGTGA TTTATGTATC GGATTCCATT
63911 CACCCACGG TTGGGAATTA ATGATTGGCT CTATCTATAA AGATTTTGGG
63961 TTTGTTTCATA ATGATCAAAT CATATCTGGT CTTGTTTCCA CCTTTCCAGT
64011 CATTCTCGAT ACAATTTTTA AATATTGGAT TTTCCGTTAT TTAAATCGTC
64061 TGTCTCCGTC ACTTGTAGTT ATTTATCATT CAAT**GA**ATGA CTGATAAAGG
64111 ATCCATTGAT ATTAATCTAA TCCAATTAGA ATGCTTGGTA CTTTGTAGTT
64161 GTACATAAGC AGAGTATTG

Fig. 40. Nucleotide sequence of the *ycf10* gene from a transformed tobacco lines. Start and stop codons of orf229 are indicated in bold letters. The *aadA* sequence is underlined.

3.2.6.2 Southern analysis

Plant material after 6 - 8 regeneration cycles on selective medium was chosen to test the proportion of transformed/wild-type plastome copies by Southern analysis. The isolated plastid DNA was used for RFLP analysis and subsequent hybridization with a radiolabeled *ycf10* probe. In all transgenic lines no hybridization signal for wild-type plastome copies was detected.

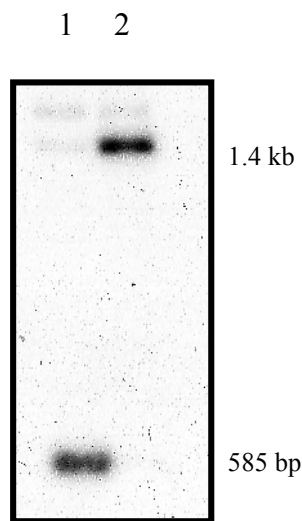


Fig. 41. RFLP analysis to test homoplastomy of the *ycf10* knock-out mutants. Plastid DNA of wild-type and transformed plants was digested with EcoRI and hybridized to a radiolabeled *ycf10* probe (PCR product). Restriction yields a 585 bp fragment for the WT plastome and a 1.4 kb fragment for the *ycf10* transformant. The lack of the wild-type band in the transformant DNA establishes the homoplastomy of the *ycf10* knock-out mutant; 1: wild-type plastid DNA, 2: Δ *ycf10* plastid DNA.

3.2.6.3 PCR analysis

To confirm the homoplastomic state of the Δ *ycf10* plants the more sensitive PCR method was applied. The reaction was performed using a primer pair designed for the regions flanking the *ycf10* gene (*ycf10forPF* and *ycf10revPF*). This primer combination allowed to distinguish between the signals originating from transformed and wild-type DNA sequences. The signal expected from the wild-type plastome was apparent when total DNA was used as a template. To reduce the possibility of contamination of the sample by nuclear and/or mitochondrial DNA sequences, Percoll-gradient purified plastid DNA was subsequently used as template for PCR. A strong reduction of the wild-type plastome product was detected, although the signal arising from the hybridization between the transformed and wild-type amplification products was still present. Subsequent analyses of plastid DNA purified by pulsed-field gel electrophoresis lacked the wild-type signal in Δ *ycf10* material, thus establishing its homoplastomy (Figure 42).

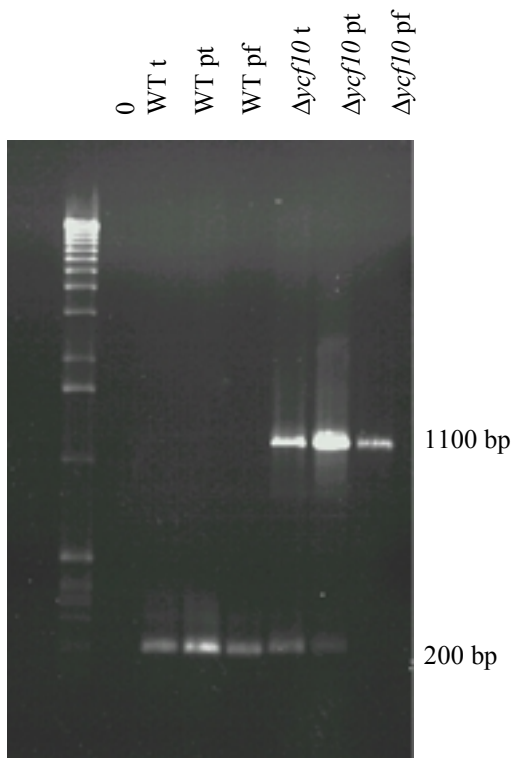


Fig. 42. An example of PCR analysis of $\Delta ycf10$ plants. The *ycf10* fragment was amplified from wild-type and transformed plants using the *ycf10*forPF and *ycf10*revPF primers. The wild-type signal should appear as a 200 bp band, and the transplastomic fragment should be 900 bp larger (1100 bp). Different preparations of plant DNA were used to investigate the homoplasmic state of the mutant, as indicated at the top of the picture. 0: zero control, t: total DNA, pt: plastid DNA, pf: pulsed-field gel isolated DNA.

3.2.6.3.1 Hybridization analysis of $\Delta ycf10$ PCR products

To confirm the $\Delta ycf10$ PCR analyses, reaction products were hybridized to a radiolabeled probe. The PCR products were electrophoretically separated in an agarose gel, visualized by ethidium bromide staining, as presented in Figure 42, subsequently blotted onto nylon membrane, and hybridized with a radiolabeled *ycf10* specific probe (Figure 43). In contrast to the total cellular DNA and DNA from gradient-purified plastids, no wild-type-specific signal was found in PFGE-purified plastid DNA sample (Figure 43). The detection level of this approach was estimated at one wild-type DNA copy detectable in one plant cell.

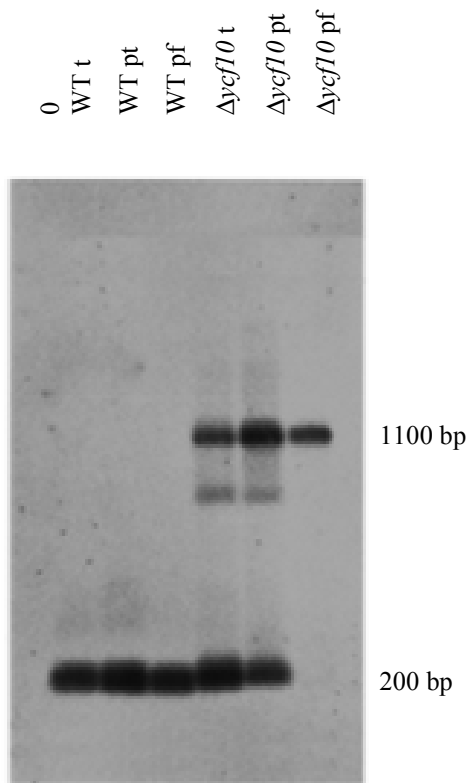


Fig. 43. PCR analysis of wild-type and $\Delta ycf10$ plants. *Ycf10* was amplified from transformed plants using *ycf10*forPF and *ycf10*revPF primers. PCR products were electrophoretically separated, blotted onto nylon membrane and hybridized with radiolabeled *ycf10*-specific probe. The wild-type signal appears as a 200 bp band, while the transplastomic fragment is 900 bp larger (1100 bp). Different preparations of plant DNA, as indicated at the top, were used to investigate the homoplasmic state of the mutant; t: total DNA, pt: DNA from Percoll-gradient-purified plastids, pf: PFGE-purified plastid DNA, 0: primer control.

3.2.7 Northern analysis

In tobacco, the *ycf10* gene was shown to be located upstream of the *petA* gene encoding cytochrome *f* (Shinozaki et al. 1986), and being cotranscribed with that gene in pea (Willey and Gray 1990; Nagano et al. 1991). The complex pattern of the transcripts suggests that in tobacco the *ycf10* gene is a part of a gene cluster including also *psaI*, encoding PsaI subunit of PSI, *ycf4* upstream and *petA* downstream of *ycf10*. The presence of at least two promoters can be deduced from the transcription map of the *psaI-ycf4-ycf10-petA* operon (Figure 44). RNA filter hybridizations performed with all relevant probes (*ycf10*, *ycf4*, *petA*, *aadA*) were consistent with the above described genome structure. Four different transcripts emanating from the *psaI-ycf4-ycf10-petA* cluster were identified, which were about 0.9 kb (*aadA* cassette) larger in the $\Delta ycf10$ plants. Two additional transcripts, arising from the *aadA* gene promoter, were localized in the $\Delta ycf10$ material.

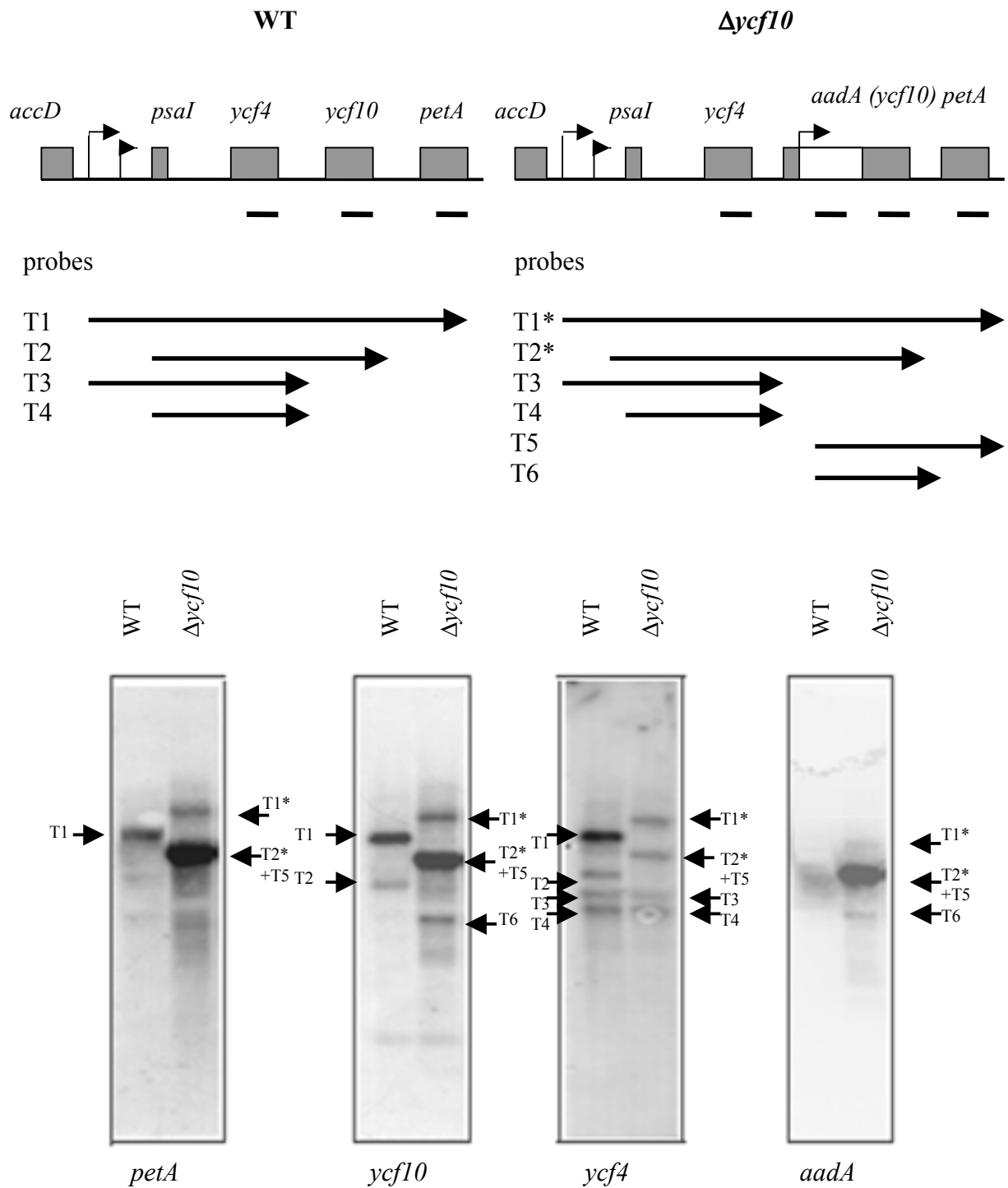


Fig. 44. Deduced maps of the *psal-ycf4-ycf10-petA* gene cluster in wild-type (left) and $\Delta ycf10$ (right) tobacco chloroplasts. Potential promoters are shown as bent arrows. Below each map, horizontal lines indicate the positions of the probes used for RNA filter hybridization. The deduced transcripts are shown below the maps. Transcript sizes in wild-type are: T1: 4.4 kb, T2: 1.9 kb, T3: 1.7 kb, T4: 1.4 kb. In the transformant the sizes of the transcripts modified by the *aadA* insertion (indicated by asterisks) are: T1*: 5.3 kb, T2*: 2.8 kb, *aadA*-specific transcripts in the mutant are T5: 2.6 kb and T6: 1.4 kb.

3.2.8 Localization of the *ycf10* product

To localize the Ycf10 protein polyclonal monospecific antibodies, generated against Ycf10 from pea (kindly provided by Dr. Sasaki), were tested on thylakoid membranes, stroma and inner chloroplast envelope fractions isolated from chloroplasts of wild-type and the $\Delta ycf10$ tobacco. The pea inner envelope preparation served as a positive control and showed cross-reaction of two proteins of approximately 30 and 26 kDa with the antiserum. A single band of 30 kDa was observed in tobacco wild-type, but not $\Delta ycf10$ inner envelope fraction. No cross-reaction was obtained with thylakoid and stroma subfractions of chloroplasts (Figure 45, Panel A). To estimate the purity of chloroplast subfractions, the samples from the wild-type and $\Delta ycf10$ tobacco were reacted with an antiserum directed against mixed envelope proteins (Figure 45, Panels B and C).

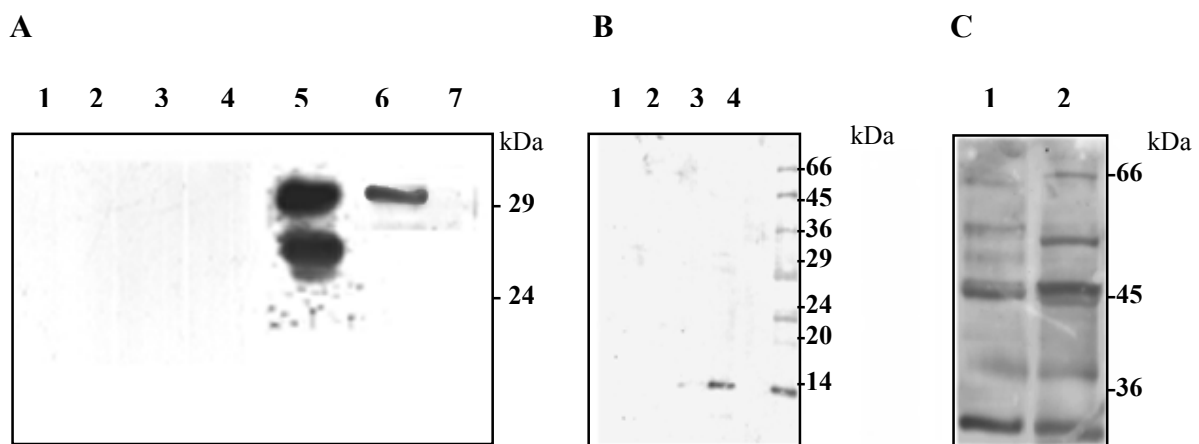


Fig. 45. Panel A: Localization of the Ycf10 protein in chloroplast subfractions; Lane 1: wild-type stroma proteins, lane 2: $\Delta ycf10$ stroma proteins, lane 3: wild-type thylakoid proteins, lane 4: $\Delta ycf10$ thylakoid proteins, lane 5: pea inner envelope proteins, lane 6: wild-type tobacco inner envelope proteins, lane 7: $\Delta ycf10$ inner envelope proteins. Panel B: Immunoblot analysis of chloroplast subfractions with antiserum directed against inner and outer chloroplast envelope proteins; lane 1: wild-type thylakoid membranes, lane 2: $\Delta ycf10$ thylakoid membranes, lane 3: wild-type stroma fraction, lane 4: $\Delta ycf10$ stroma fraction. Panel C: Immunoblot analysis of inner envelope preparations from wild-type (Lane 1) and $\Delta ycf10$ (Lane 2) tobacco with antiserum directed against inner and outer chloroplast envelope proteins. Molecular weights in kDa are indicated at the right of each panel.

3.2.9 Isolation of thylakoid protein complexes from $\Delta ycf10$ mutants by sucrose density gradient centrifugation

The isolation and characterization of thylakoid protein complexes from wild-type and $\Delta ycf10$ plants was performed as described in Section 3.1.10. As expected, no qualitative nor quantitative differences in thylakoid protein composition were detected in the $\Delta ycf10$ mutants compared to wild-type, as shown on Figure 46.

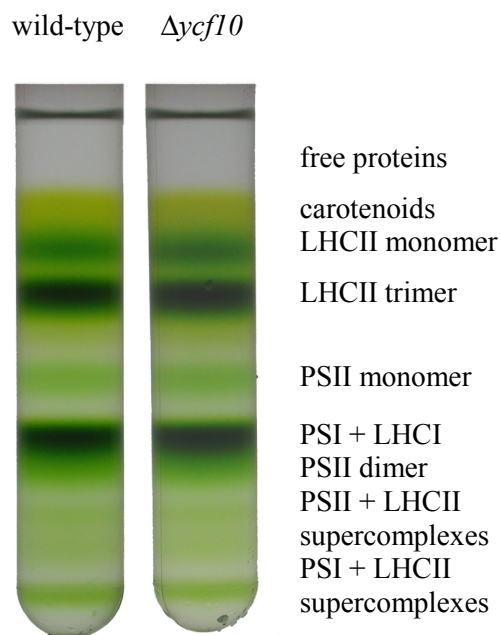


Fig. 46. Comparison of the sucrose gradients from β -dodecylmaltoside solubilized thylakoids from wild-type and $\Delta ycf10$ plants. The biochemical identification of each chlorophyll-containing band, indicated at the right, was assessed by collecting 0.3 ml fractions for silver staining and analysis using antisera against constituents of the major photosynthetic complexes (see Section 3.1.11.3.1).

3.2.10 Serological analysis of the $\Delta ycf10$ mutants

To examine the content and distribution of the major photosynthetic complexes in the $\Delta ycf10$ mutants in comparison to wild-type tobacco, several antisera were tested on membranes containing total thylakoid proteins of wild-type and $\Delta ycf10$ tobacco (Figure 47). The immunodetection was performed using the enhanced chemiluminescence system (ECL). The immunoblots were scanned and the intensities of signals were estimated using the TINA software package v2.08 beta (Raytest, Spröckhovel; Tabel 7). No quantitative differences of the proteins tested were detected in $\Delta ycf10$ tobacco as compared to the wild-type.

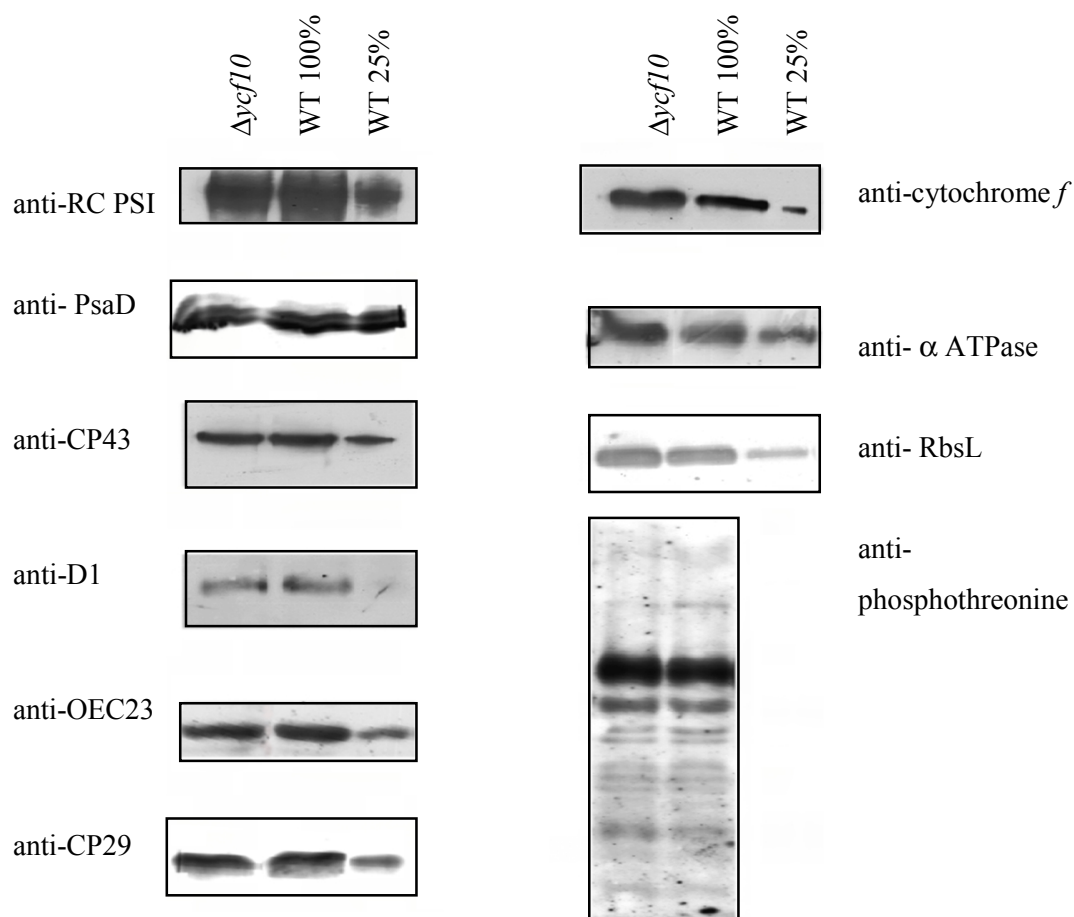


Fig. 47. Serological analyses of $\Delta ycf10$ mutants. Thylakoid proteins from the wild-type and $\Delta ycf10$ tobacco were separated by SDS-PAGE, electroblotted onto nitrocellulose and incubated with the specific antisera indicated at the right or left of the panels. Two concentrations of the wild-type (WT) were tested to quantify possible differences in protein amounts in $\Delta ycf10$ mutants.

Table 7. Immunological analyses of the $\Delta ycf10$ mutants and wild-type tobacco. Signals of intensity identical as in wild-type material are marked (+++). OEC: oxygen evolution complex.

Gene	Product	wild-type	$\Delta ycf10$ mutants
<i>psbP</i>	23 kDa protein of OEC	+++	+++
<i>psbA</i>	D1 protein of PSII core	+++	+++
<i>psbD</i>	CP43	+++	+++
<i>psaA</i>	P700 chl- <i>a</i> protein 1 of PSI core	+++	+++
<i>psaB</i>	P700 chl- <i>a</i> protein 2 of PSI core	+++	+++
<i>psaD</i>	ferredoxin-binding protein of PSI	+++	+++
<i>Lhcb4</i>	CP29	+++	+++
<i>petA</i>	cytochrome <i>f</i>	+++	+++
<i>atpA</i>	α -subunit of ATPase complex	+++	+++
<i>rbsL</i>	large subunit of RuBisCo	+++	+++
Phosphothreonine		+++	+++

3.2.11 Chlorophyll fluorescence analysis

Chlorophyll fluorescence measurements under continuous light (Kautsky effect in continuous light, measurement performed using a FluorCam device) provides a fast test for the photosynthetic performance of plants *in vivo*. Wild-type and $\Delta ycf10$ tobacco plants of two distinct phenotypes, namely young green leaves and older leaves, displaying bleached sections (see Section 3.2.7), were analyzed. The young green leaves of $\Delta ycf10$ plant showed a similar fluorescence induction as the wild-type, while the isolated white tissue regions showed a lack of photosynthetic activity (Figure 48).

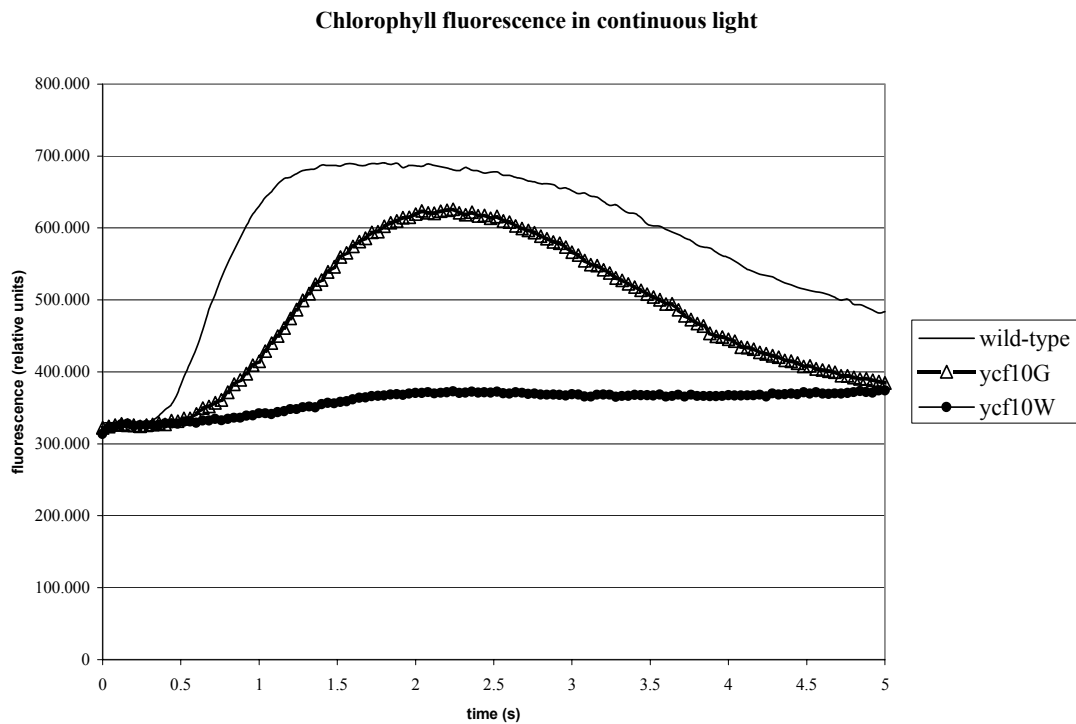


Fig. 48. Chlorophyll fluorescence under continuous light (Kautsky effect) of wild-type and $\Delta ycf10$ mutant. The graph presents data proven by at least 5 independent experiments. Legend: wild-type, $\Delta ycf10$ green leaf (G), $\Delta ycf10$ white leaf regions (W). All plants were grown *in vitro* at 25°C under 100 $\mu\text{E m}^{-2} \text{s}^{-1}$. Presented data are not normalized for chlorophyll amount.

For a more detailed spectroscopic analysis of the chlorophyll fluorescence using a PAM fluorometer (Walz, Germany), plants of wild-type and $\Delta ycf10$ tobacco were grown under 25°C and 100 $\mu\text{E m}^{-2} \text{s}^{-1}$. The maximum fluorescence (F_M) and the ratio $(F_M - F_0)/F_M = F_V/F_M$, as well as the fluorescence quenching parameters qP (photochemical quenching) = $(F_M' - F_S)/(F_M' - F_0')$, and qN (non-photochemical quenching) = $1 - (F_M' - F_0')/(F_M - F_0)$ (Schreiber 1986) were determined for all samples. The average results of at least three measurements are presented in Table 8.

Table 8. Spectroscopic analyses of wild-type and $\Delta ycf10$ mutant plants.

	WT 25°C, 100 $\mu\text{E m}^{-2} \text{s}^{-1}$	$\Delta ycf10$ 25°C, 100 $\mu\text{E m}^{-2} \text{s}^{-1}$
F_V/F_M	0.80	0.80
qP	0.90	0.95
qN	0.20	0.20

As presented above, the ratio F_V/F_M (reflecting the photosynthetic activity of a plant), and the fluorescence quenching parameters were identical for wild-type and $\Delta ycf10$ plants, indicating an unaltered photosynthetic activity of $\Delta ycf10$ tobacco.

3.2.12 C_i -dependent O_2 evolution

Figure 49 shows the estimated O_2 evolution as a function of the external C_i concentration in protoplasts and chloroplasts of wild-type and $ycf10$ -deficient tobacco. In each case, 1 ml of protoplast or chloroplast suspension with a chlorophyll concentration between 0.03 and 0.07 mg/ml was measured with an increase of the external HCO_3^- concentration from 0 to 5 mM. Since the isolated intact tobacco chloroplasts remained stable for approximately 20 minutes under the chosen experimental conditions, only two measurement points, for 0 and 5 mM HCO_3^- , were taken. The graphs represent an average of at least 5 independent experiments.

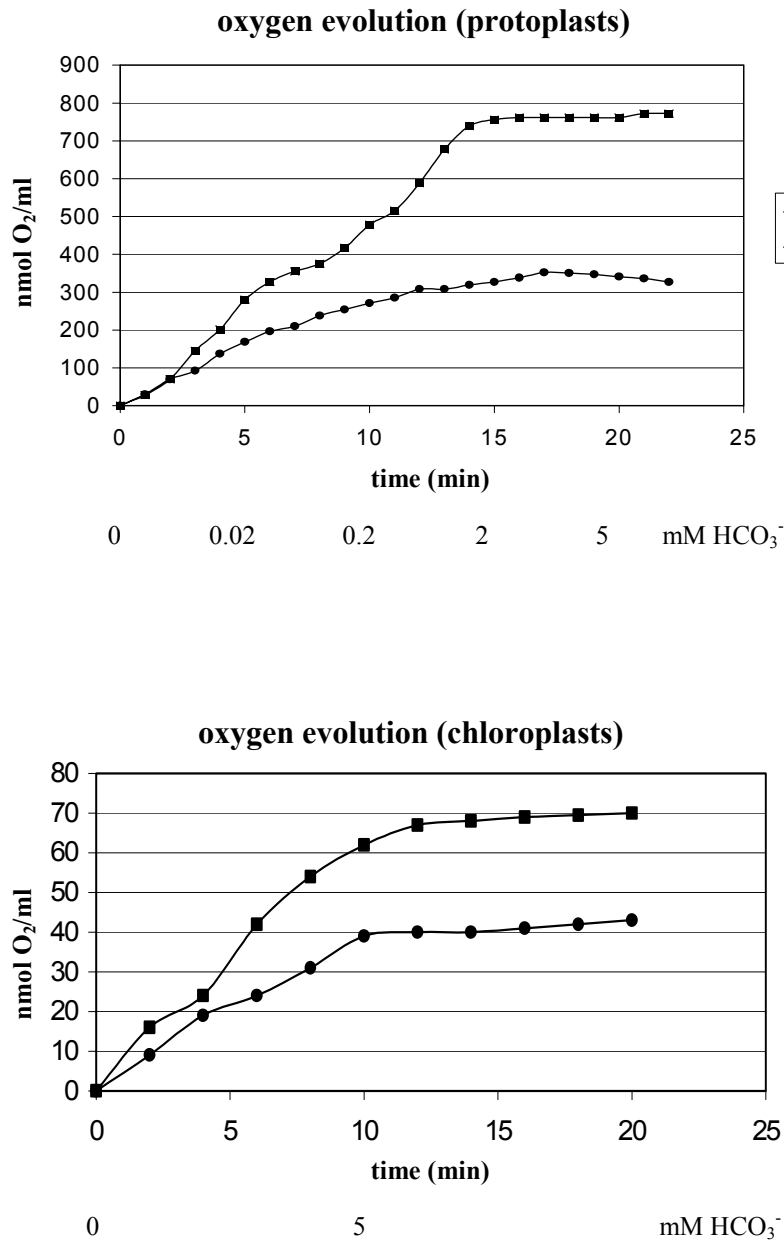


Fig. 49. Substrate dependence of O₂ evolution in wild-type and $\Delta ycf10$ plants. For the measurements, the isolated intact chloroplasts or protoplasts were resuspended in isolation medium or PCN medium, respectively (see Methods), with a chlorophyll concentration that ranged between 0.03 - 0.07 mg/ml.

An efficient C_i-dependent oxygen evolution was observed with both isolated protoplasts and chloroplasts from wild-type, and, to a lesser degree, from $\Delta ycf10$ plants. Both wild-type and $\Delta ycf10$ cells obtained a maximum O₂ evolution with an external C_i concentration of about 2 mM, although the maximum photosynthetic rate of the mutant was 40 - 50% lower than in the wild-type.

3.3 Pulsed-field electrophoresis as a new method for the determination of the homoplastomic status of transformed plants

3.3.1 DNA separation in pulsed-field agarose gel electrophoresis

Pulsed-field gel electrophoresis (described 1984 by Schwartz and Cantor) allows to separate DNA fragments with the lengths of up to 10 Mbp. Changes of the direction of an electrical field cause a continuous reorientation of DNA molecules, which results in their separation. A schematic picture of the pulsed-changed electrical field electrodes is presented in Figure 50. As presented below, the method of pulsed-field gel electrophoresis served as an efficient tool for the isolation of uncontaminated plastid DNA molecules, and was successfully applied for the investigation of the homoplastomic state of transformed plants.

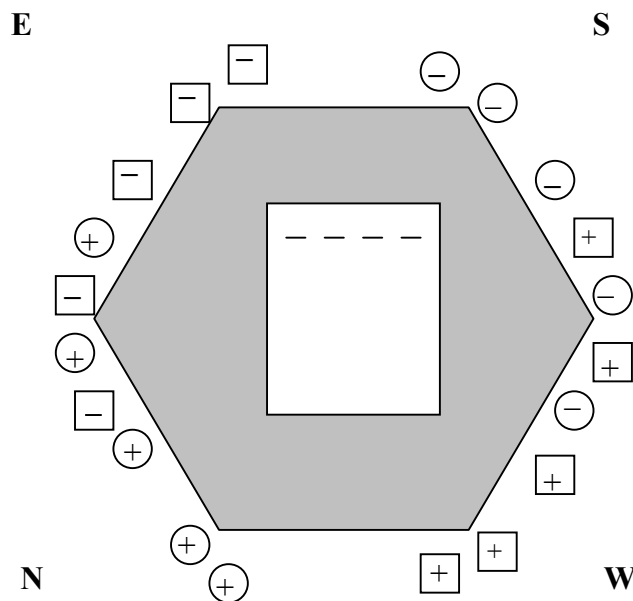


Fig. 50. A schematic drawing of the pulsed-field gel electrophoresis system used. The gel is represented by the white square, the main electrode as a grey hexagon, the electrodes of the pulsed-changed electrical field: squares represent (E/W) direction, circles (S/N) direction.

3.3.2 Isolation of monomeric plastid DNA from the agarose gel

Plastid samples from wild-type and $\Delta ycf10$ plants and pulsed-field gel electrophoresis were performed as described in Methods. After the electrophoresis, the agarose gels were stained with ethidium bromide and the results visualized under UV light. Several distinct DNA bands were detected, corresponding to the different oligomerization states of the plastid DNA. The monomeric DNA bands were excised from the gel and the DNA was eluted from agarose using the QIAEX kit. The extracted DNA was further used for PCR analysis.

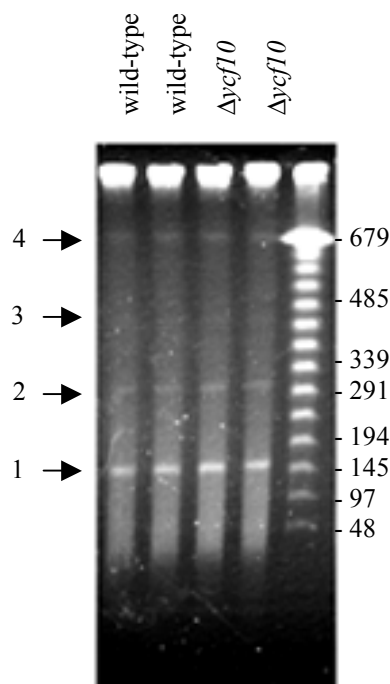


Fig. 51. Purified intact plastids were immobilized in low-melting agarose blocks and their DNA was separated in a pulsed electrical field. Different forms of plastid DNA are visible: (from the bottom to the top) monomer (1), dimer (2), trimer (3), tetramer (4). Molecular weights in kbp are indicated at the right.

3.3.3 Investigation of the purity of plastid DNA isolated by pulsed-field gel electrophoresis

3.3.3.1 Presence of contaminating nuclear DNA in different plant DNA preparations

The presence of nuclear DNA contamination was investigated with NEP (nuclear-encoded RNA polymerase)-specific primers in a PCR reaction with total plant DNA, DNA isolated from Percoll gradient-purified intact chloroplasts, and plastid DNA isolated by pulsed-field electrophoresis as templates. DNA preparations from wild-type and from $\Delta ycf10$ tobacco were used in these analyses. As shown by Figure 52A, PCR products derived from nuclear

DNA were detected in both total and DNA from Percoll-purified plastids, but no such signal was detected when the pulsed-field electrophoresis isolated plastid DNA was used as PCR template.

To reinforce and improve this result, the PCR products were blotted onto a nylon membrane and hybridized with a radiolabeled, nested oligonucleotide specific for the NEP primer-amplified DNA fragment. No amplification product was detected in the sample containing the pulsed-field isolated plastid DNA (Figure 52B).

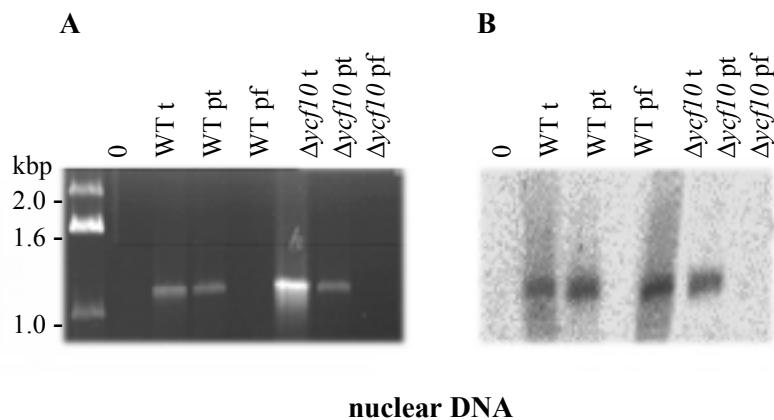


Fig. 52. Analysis of the purity of different DNA preparations from wild-type and $\Delta ycf10$ tobacco. The NEP-specific primer pair was used in a PCR reaction to amplify the DNA fragment originating from nuclear DNA contamination; (t): total DNA, (pt): DNA isolated from Percoll gradient purified plastids, (pf): plastid DNA purified by pulsed-field gel electrophoresis. Molecular weights of products in kbp are indicated at the left. The amplification products were separated electrophoretically and visualized by ethidium bromide staining (Panel A), and hybridization with a radiolabeled NEP-specific oligonucleotide (Panel B).

3.3.3.2 Presence of contaminating mitochondrial DNA in different plant DNA preparations

To investigate the presence of mitochondrial DNA contamination in different plant DNA preparations an analogous procedure as described in Section 3.3.3.1.1 was applied, with mitochondrial *coxII* gene-specific primers.

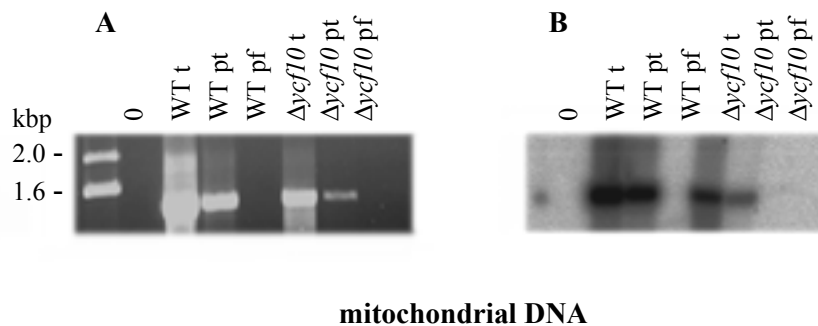


Fig. 53. Analysis of the purity of different DNA preparations from wild-type and $\Delta ycf10$ tobacco. The *cox*-specific primer pair was used in a PCR reaction to amplify a DNA fragment originating from a mitochondrial DNA contamination; (t): total DNA, (pt): DNA isolated from Percoll gradient-purified plastids, (pf): plastid DNA purified by pulsed-field gel electrophoresis. Molecular weights of the products in kbp are indicated at the left. The amplification products were separated electrophoretically, visualized by ethidium bromide staining (Panel A), and hybridization with a radiolabeled *cox*-specific oligonucleotide (Panel B).

Mitochondrial DNA-derived PCR products were detected in both the total and the Percoll gradient purified plastid DNA, but no such signal was detected when plastid DNA isolated by pulsed-field electrophoresis was used as PCR template.

To refine this result, the PCR products were blotted onto a nylon membrane and hybridized with a radiolabeled, nested oligonucleotide specific for the *cox*-primers amplified DNA fragment. No amplification product was detected in the sample containing the pulsed-field isolated plastid DNA.

3.3.4 Analysis of the $\Delta ycf10$ homoplastomic state by pulsed-field gel electrophoresis

The homoplastomic state of the $\Delta ycf10$ mutants was examined by a PCR reaction with *ycf10*-specific primers using total DNA, DNA isolated from the Percoll-purified intact plastids and plastid DNA isolated by pulsed-field gel electrophoresis as a template. Because the pulsed-field electrophoresis isolated plastid DNA is virtually free of promiscuous DNA, any wild-

type signal amplified from *ycf10* DNA will, with high probability, be derived from wild-type plastome copies still present in the transformed cells. The results of the PCR (Figure 54A) showed the presence of the wild-type size amplification product in samples where total DNA and DNA from Percoll gradient-purified plastids served as templates. No such amplification product was detected in the pulsed-field isolated DNA sample by staining of the gel with ethidium bromide.

To improve this result, radioactive probe hybridization was applied. The gel presented in Figure 54A was blotted and hybridized with a radiolabeled, *ycf10*-specific oligonucleotide (Figure 54B). No visible PCR products of the wild-type plastome were detected in the samples with $\Delta ycf10$ plastid DNA purified by pulsed-field electrophoresis.

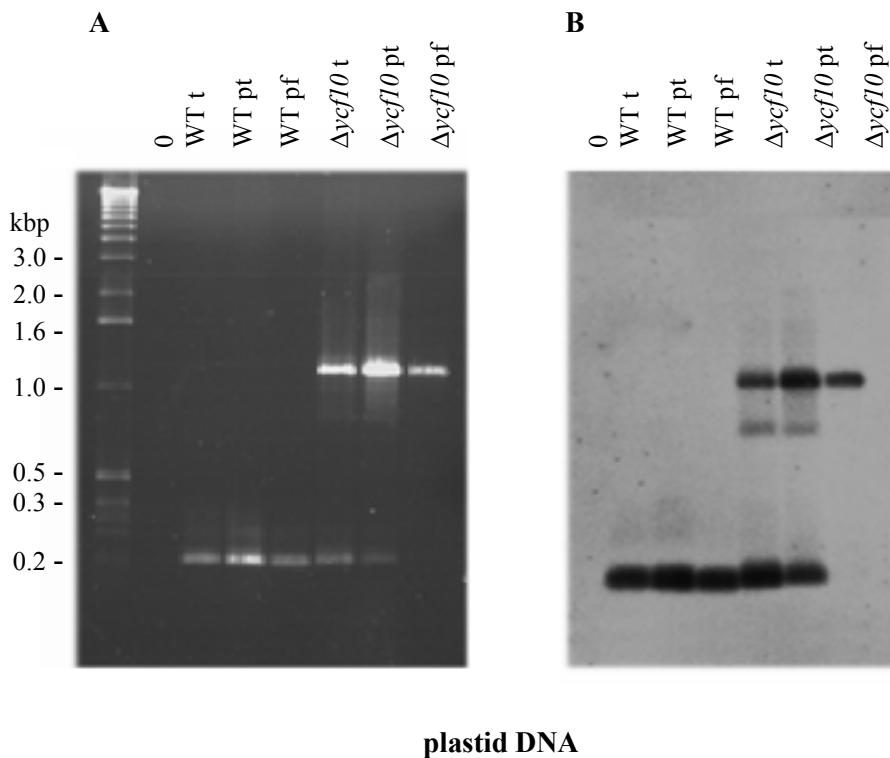


Fig. 54. PCR analysis of wild-type and $\Delta ycf10$ tobacco. The PCR reaction was performed using *ycf10*-specific primers and different DNA preparations as templates; (t): total DNA, (pt): DNA isolated from Percoll gradient-purified plastids, (pf): plastid DNA isolated by pulsed-field gel electrophoresis. The molecular weights of products in kbp are indicated at the left. Amplification products were separated electrophoretically and visualized by ethidium bromide staining (Panel A), and hybridization with a radiolabeled *ycf10*-specific oligonucleotide (Panel B).

3.3.5 Quantitative estimation of wild-type chromosome copies detected by PCR analysis

To analyze the number of wild-type chromosome copies detectable by PCR analysis of heteroplasmic material, PCR with plasmid DNA templates containing an insertion of *ycf10* (wild-type) or the *ycf10aadA* (mutant) gene was performed. Subsequently, a decreasing amount of wild-type template was mixed with the *ycf10aadA* plasmid DNA to estimate the ratio of wild-type/mutant DNA copies resulting in a detectable wild-type signal. For PCR analysis 5×10^9 wild-type and mutant plasmid DNA molecules served as templates (100%). The PCR products were separated electrophoretically and visualized by ethidium bromide staining, subsequently blotted onto a nylon membrane and hybridized with a radiolabeled, nested, *ycf10*-specific oligonucleotide (Figure 55, Panel A and B, respectively).

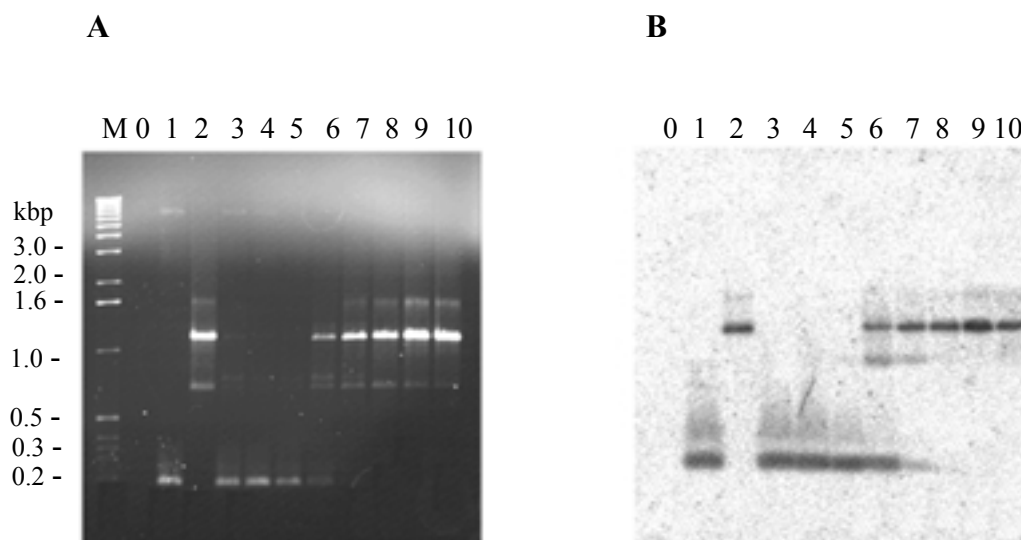


Fig. 55. PCR analysis of plasmid DNA containing *ycf10* (wt) or the *ycf10aadA* (mutant) gene insertion. Lanes: (0) zero control, (1) wt DNA template (100%; 5×10^9 plasmid DNA molecules), (2) mutant DNA template (100%; 5×10^9 plasmid DNA molecules), (3) mixed templates: mutant/wt = 1/1, (4) 1/0.1, (5) 1/10⁻², (6) 1/10⁻³, (7) 1/10⁻⁴, (8) 1/10⁻⁵, (9) 1/10⁻⁶, (10) 1/10⁻⁷. The molecular weights of the products are indicated at the left. The amplification products were separated electrophoretically, visualized by ethidium bromide staining (Panel A), and hybridized with a radiolabeled *ycf10*-specific oligonucleotide (Panel B).

3.3.6 Sensitivity level of the PCR

The detection level of the PCR analysis under the chosen conditions (described in Methods) was tested using a decreasing amount of plasmid DNA template. Both the ethidium bromide

staining and the hybridization with radioactive *ycf10* probe detected a PCR product when a template containing 50 plasmid DNA molecules was used.

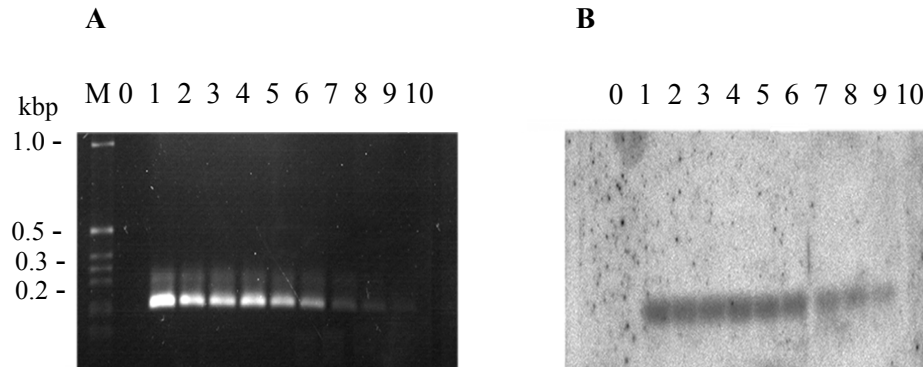


Fig. 56. PCR analysis of plasmid DNA containing the *ycf10* gene insertion. Lanes: (0) zero control, (1) 5×10^9 plasmid DNA molecules serving as a template, (2) 5×10^8 DNA molecules, (3) 5×10^7 DNA molecules, (4) 5×10^6 DNA molecules, (5) 5×10^5 DNA molecules, (6) 5×10^4 DNA molecules, (7) 5×10^3 DNA molecules, (8) 5×10^2 DNA molecules, (9) 50 DNA molecules, (10) 5 DNA molecules. Molecular weights of the products are indicated at the left. The amplification products were separated electrophoretically and visualized by ethidium bromide staining (Panel A), and hybridization with a radiolabeled *ycf10*-specific oligonucleotide (Panel B).

4. DISCUSSION

The existence of a unique genetic system of plastids has first been suggested at the beginning of the 20th century. From analyses of variegated plants Correns (1909) and Baur (1909) deduced independently the hypothesis of plastid inheritance that did not obey Mendelian rules. Erwin Baur concluded in 1909 that (i) the plastids are carriers of hereditary factors which are able to mutate, (ii) in variegated plants the random process of plastid sorting-out takes place, and (iii) genetic plastid factors are inherited biparentally. In contrast, Carl Correns (1909), using a different model, described maternal inheritance of factors localized in the cytoplasm (summarized in Hagemann 2000). Only fifty years later, the specific cytochemical staining of plastid-localized DNA in the green algae *Chlamydomonas moewussii* (Ris and Plaut 1962), as well as the isolation and description of a unique DNA species of *Chlamydomonas reinhardtii*, enriched in chloroplasts (Sager and Ishida 1963) proved Baur's hypothesis. The subsequent isolation and microscopic characterization of chloroplast DNA from higher plants (Wells and Birnstiel 1969, Herrmann et al. 1975, Kolonder and Tewari 1975) provided an insight into the structure, conformation and coding capacity of plastid DNA. The development of techniques for identification and isolation of genes as well as sequence analyses of entire plastid chromosomes (Ohyama et al. 1986, Shinozaki et al. 1986) allowed to assess the coding potential of plastid chromosomes. Recently, the development of chloroplast transformation methods first established in *Chlamydomonas reinhardtii* (Boynton et al. 1988) and then in tobacco (Svab et al. 1990, Golds et al. 1993) as well as the availability of additional techniques for analysis, such as protein sequencing or two-dimensional gel electrophoresis, allowed to identify and characterize most of the plastid-encoded genes and their products. Nevertheless, higher plant plastomes still comprise several open reading frames (ORFs) of unknown function. Conserved ORFs, which are found in almost all known plastid chromosomes are designated *ycfs*, and at present are subject of intense molecular, biochemical and biophysical analyses. The work presented in this thesis has concentrated on the functional characterization of two *ycfs* of unknown function, namely *ycf9* (*psbZ*, ORF62), and *ycf10* (*cemA*, ORF229). With respect to chloroplast transformation, a PFGE-based plastid DNA isolation protocol was established which allowed to verify the status of homoplastomy of transformed plants.

4.1 Functional analysis of the *ycf9* gene product

A reverse genetic approach was applied to analyze the function of the conserved *ycf9* gene in *Nicotiana tabacum* and, in cooperation with the group of Prof. F.-A. Wollman (Université Paris, France), in *Chlamydomonas reinhardtii*.

Inactivation of the *ycf9* gene in *Nicotiana tabacum*, assessment of the homoplastomic status. The *ycf9* gene was an interesting case for the reverse genetic approach not only because of its enigmatic function, but also because parallel attempts to inactivate the gene had yielded controversial results. Disruption of *ycf9* in *Chlamydomonas* generated a mutant line displaying a wild-type phenotype (Higgs et al. 1998). A more recently described *ycf9* knock-out mutant in tobacco did not reach the homoplastomic state and the gene product was assigned to the PSI complex (Mäenpää et al. 2000). Studies of Ruf et al. (2000), in turn, had demonstrated homoplastomic $\Delta ycf9$ mutants, and the gene product was proposed to be a member of a small antenna protein family. The biolistic transformation performed in our laboratory yielded four independent mutant lines, which, after six cycles of regeneration, reached homoplastomy. The homoplastomic state of all transformed lines was established by sequence analysis, PCR, Southern and Northern analyses, as well as by a combination of pulsed-field analysis and PCR of relevant regions of the DNA band containing intact plastid chromosomes. Northern and Southern analyses demonstrated the absence of wild-type transcripts and DNA copies, respectively, in $\Delta ycf9$ plants, although wild-type signals were detected in PCR analyses. The pulsed field electrophoresis approach followed by PCR of relevant chromosomal regions and hybridization with radiolabeled probes, developed in this study, demonstrated that those wild-type signals arose, in all likelihood, from promiscuous DNA, i.e. copies of plastid DNA residing in nucleus or chondriome, and proved homoplastomy at a level lower than 0.00001%.

The estimation of the homoplastomic state is a crucial, but also a controversial issue in the analysis of plants with transformed plastids. Due to about 100 chloroplasts per cell and approximately 100 chromosome copies per chloroplast (Herrmann and Possingham 1980), the primary transformant is heteroplastomic, containing both wild-type and mutant plastid chromosomes. The homoplastomic state, in which all wild-type copies are replaced by mutant ones, is generally achieved after several rounds of regeneration, but plants can be “fixed” in the heteroplastomic state, if the transformed gene is essential for vital functions (Drescher et

al. 2000). Multiple copies of chloroplast DNA per cell, as well as the existence of promiscuous plastid DNA fragments in both the nuclear genome and the chondriome (Ellis 1982, Stern and Lonsdale 1982, Ayliffe and Timmis 1992, Brennicke et al. 1993) complicate the analysis of the homoplastomic state of transformed plants.

Generally, two strategies are applied to verify the presence of residual wild-type plastid DNA in transplastomic plants: (i) Southern and Northern analysis of plastid DNA and RNA, respectively, and (ii) PCR using sequence specific oligonucleotides flanking the insertion. Southern and Northern analyses give general information about the presence of the wild-type DNA copies (RFLP) or wild-type transcripts, respectively, but both methods lack sensitivity to unambiguously determine the homoplastomic status of transformed plants. On the other hand, the PCR approach is more sensitive and allows the detection of minute quantities of wild-type DNA copies undetectable by Southern analysis, but it bears the risk of (co)amplifying promiscuous plastid DNA sequences residing in the nucleus or mitochondrial genome. This risk can be reduced, but not eliminated, by using DNA extracted from intact plastids purified by isopycnic, isotonic gradient centrifugation (Schmitt and Herrmann 1977, Herrmann 1982) as a template for amplification. However, as a consequence of the mechanical disruption of plant material prior to gradient centrifugation, and/or insufficient phase separation, traces of nuclear and/or mitochondrial DNA generally copurify with intact chloroplasts, thus mimicking genuine plastid chromosomes in the subsequent PCR reaction.

To ensure the absence of wild-type plastid chromosome copies left in a transplastomic plant, an additional, more reliable method is required. One alternative to judge the homoplastomic state of fertile mutant plants is to screen the progeny for the presence of a marker gene by germinating them on selective medium (Maliga and Nixon 1998). In this thesis, pulsed-field gel electrophoresis (PFGE) was applied to obtain seemingly contamination-free plastid DNA from transplastomic mutants. Without the PFGE purification step the Percoll-gradient purified plastid DNA yielded a 200 bp amplification product characteristic for wild-type chloroplast chromosomes in the subsequent PCR. Its wild-type origin was unambiguously proven by the use of plastid-, mitochondria- and nucleus-specific oligonucleotides, and DNA templates derived from different extraction methods, including PFGE. In wild-type plants, the 200 bp amplification product was obtained with total DNA isolated from leaves as well as with plastid DNA extracted from intact, Percoll-purified chloroplasts before and after PFGE. The insertion of the marker cassette into the mutant plants, in turn, was detected in three

subfractions of DNA from transplastomic plants. Wild-type-derived amplification products were obtained, whenever DNA extracted from leaves and Percoll-purified chloroplasts served as a template. In striking contrast, no such signal was detected, if a PFGE step was included into the DNA extraction procedure. The finding that neither mitochondrial nor nuclear sequences were amplified with gene-specific oligonucleotides using PFGE-purified plastid DNA as a template demonstrates the high purity of the extracted DNA, free of any cross-contamination with mitochondrial and/or nuclear DNA. In contrast, both mitochondrial and nuclear DNA fragments were amplified from DNA extracted from leaves or even Percoll gradient-purified plastids. The sensitivity of the PCR was estimated with a plasmid DNA containing either the wild-type gene (*ycf10*) or the gene with insertion of the *aadA* cassette. With a ratio of one wild-type gene copy to 10.000 transformed gene copies ($1/10^4$) the wild-type derived 200 bp amplification product was clearly detectable in ethidium bromide-stained agarose gels. The sensitivity of detection was increased by transfer of amplified products onto nylon membrane and hybridization with a radiolabeled probe. Taking into consideration that in a fully developed tobacco leaf cell, the ratio of nuclear DNA copies (4 haploid copies in the allotetraploid nucleus) to plastid DNA copies (100 per chloroplast and 50 - 100 chloroplasts per cell) is less than $1/10^3$, and much stronger signals are generated for the wild-type fragment with the non-pulsed field gel purified fractions than with the $1/10^3$ molar WT/mutant mixture, the promiscuous DNA copies most probably do not only originate in the nucleus, but also in mitochondria (several hundreds per cell). To sum up, the absence of a wild-type-derived signal in PFGE-purified plastid DNA isolated from transplastomic plants can either be due to (i) their complete segregation (homoplastomy), or (ii) to few wild-type plastid chromosome copies (less as one wild-type gene per 10.000 transformed chromosomes), which corresponds to less than one wild-type plastid chromosome per plant cell containing 100 chloroplasts with approximately 100 plastid chromosome copies per chloroplast.

Phenotypes of the $\Delta ycf9$ plants. $\Delta ycf9$ plants grown under different light and temperature regimes differed in their phenotypes. These variations did not arise from the heterotrophic *in vitro* conditions but were as well visible under photoautotrophic growth conditions using the same light and temperature regimes. As recently reported, similar phenotypes were observed in $\Delta ycf9$ plants grown in the greenhouse under regulated light conditions (Baena-González et al. 2001). To understand how growth conditions and $\Delta ycf9$ phenotypes are interconnected, detailed biochemical analyses of transformed plants were required.

Localization of the *ycf9* gene product. The co-transcription of *ycf9* together with the *psbD* and *psbC* genes, encoding subunits of the PSII core, suggested its localization in PSII complexes as well. However, the first attempt to localize the *ycf9* gene product serologically revealed co-migration with PSI (Mäenpää et al. 2000). Subsequent analyses of Ruf et al. (2000) demonstrated co-purification of the Ycf9 protein with the LHCII complexes. Analyses of tobacco and *Chlamydomonas reinhardtii* demonstrated compellingly that the Ycf9 protein is a new subunit of the PSII core complex (Swiatek et al. 2001). By eliciting specific antibodies against the *Chlamydomonas* and tobacco proteins it was shown that in both organisms the accumulation of Ycf9 is strictly correlated with the other PSII core subunits (Swiatek et al. 2001). Furthermore, recent analyses of plants lacking the PSII core proteins PsbE and PsbF, but with an unaltered level of minor antennae or LHCII (Swiatek et al. manuscript in preparation), demonstrated that those plants also failed to accumulate the Ycf9 protein, implying its close relationship and dependence on other PSII compounds. In *Chlamydomonas*, the protein co-purified with PSII after sucrose gradient centrifugation of detergent-solubilized thylakoid membranes. Interestingly, in tobacco silver staining of solubilized thylakoid membranes revealed two protein components of 4 and 6 kDa detectable in wild-type, but lacking in mutant fractions. The 4 kDa component co-migrated clearly with PSII complexes, while the second protein of approximately 6 kDa, which was also missing in $\Delta ycf9$, resided in the upper region of the sucrose gradient containing carotenoids and free protein fraction, and its distribution profile did not match that of LHCII complexes, as suggested by Ruf et al. (2000). Isolation of thylakoid protein complexes by native Deriphat-PAGE, followed by denaturing SDS-PAGE revealed the existence of the minor antenna protein complex (CP24, CP26 and CP29) localized above the trimeric LHCII band. The sucrose-gradient centrifugation of β -dodecylmaltoside-solubilized thylakoid membranes demonstrated comigration of the minor antennae complex with the monomeric LHCII complex, which was not resolved using the Deriphat-PAGE technique. The 6 kDa protein comigrated with those complexes, although its maximal amount was detected above, in fractions enriched in carotenoids. It has been described that, on denaturing polyacrylamide gels, strongly hydrophobic proteins can migrate faster than expected from their molecular weight. On the basis of SDS-PAGE with total thylakoid proteins, the deficiency of only one protein of approximately 4 kDa was observed in $\Delta ycf9$ plants. The size of this component is identical to the protein immunodetected by Ycf9 antibodies. These results strongly suggest that the lack of the 4 kDa protein in PSII complexes of transformed plants is due to the disruption of the *ycf9* gene. Since the Ycf9 is localized in PSII cores, it was designated PsbZ

(Swiatek et al. 2001). The 6 kDa component, missing in $\Delta ycf9$ tobacco, could represent the PsbZ precursor form unassociated with PSII, or an unrelated protein which is unstable in the absence of PsbZ. It remains unclear, why only one protein deficiency was detected on basis of total thylakoid protein SDS-PAGE. To answer this question an improved gel system for resolution of small proteins in overloaded gels has to be developed. Recent analyses of several transformed plants lacking small proteins of PSII (Swiatek et al., manuscript in preparation) demonstrated the presence of numerous proteins in the range of 6 - 8 kDa, which might not be individually separated even using the Schagger/von Jagow gel system, optimized specifically for the resolution of small proteins.

Sequence analyses of PsbZ from various species favour a putative cleavage site for a peptidase directly following the first of the two transmembrane helices. Although Ruf et al. (2000) have shown a virtual co-purification of this protein with LHCII complexes, the refinement of the separation techniques of thylakoid protein complexes in sucrose density gradients as well as in 2D gels clearly demonstrated its localization in the carotenoid/free protein fraction and thus argues against its co-migration with LHCII.

In recent years, the application of advanced electron microscopy and single-particle image techniques solved the PSII structure and, based on biochemical work, allowed to divide PSII into various subcomplexes, including PSII reaction centers (RCII), PSII core complexes (CCII), which contain the core antenna proteins CP47 and CP43 together with the reaction center and other subunits, and several antenna complexes whose association strengthens the functional PSII unit (Green and Durnford 1996, Barber et al. 1997, Wollman et al. 1999, Barber and Kühlbrandt 1999, Nield et al. 2000, Zouni et al. 2001). Although RCII and CCII have been purified and characterized, the function of most of the subunits in the formation of a functional PSII unit remains poorly understood. During the past decade, several small PSII subunits have been identified, generally by reverse genetic approaches. Although these subunits have been tentatively attributed to functions, their physiological importance is still elusive (Wollman et al. 1999). Recent studies of the supramolecular organization of PSII, based on mild detergent solubilization procedures and refined electron microscopic analysis, including single particle averaging (Boekema et al. 1999a), cryoelectron microscopy (Nield et al. 2000), and two-dimensional crystal electron diffraction (Barber and Kühlbrandt 1999, Hankamer et al. 1999, Rhee et al. 1998), have shown various PSII forms ranging from a large protein complex retaining its peripheral antenna complement to subcore particles.

Furthermore, the three-dimensional structure of a cyanobacterial PSII core preparation yielded molecular insight into the positions of the major PSII transmembrane helices (Zouni et al. 2001). Studies of the supramolecular organization of PSII revealed existence of minimum 36 transmembrane helices (Barber and Kühlbrandt 1999, Hankamer et al. 1999, Zouni et al. 2001) from which 24 have been attributed to D1, D2, CP43, CP47, PsbE, and PsbF. Several small subunits, including PsbI, PsbL, PsbH, PsbK and PsbX have been tentatively assigned in PSII core, and seven helices could not be correlated with known subunits. Of particular interest is the structural domain within a PSII monomer where D1 stands in close contact to CP43, which, in turn, is suggested to associate with CP26. Adjacent to D1 and CP43 are several transmembrane helices of unknown origin (Nield et al. 2000, Zouni et al. 2001). PsbZ is regarded as a potential candidate for providing one or two of these transmembrane helices, which are in close contact to D1, CP43 and CP26. As will be discussed below, the interaction of PsbZ with the PSII core and peripheral antennae strongly supports this localization.

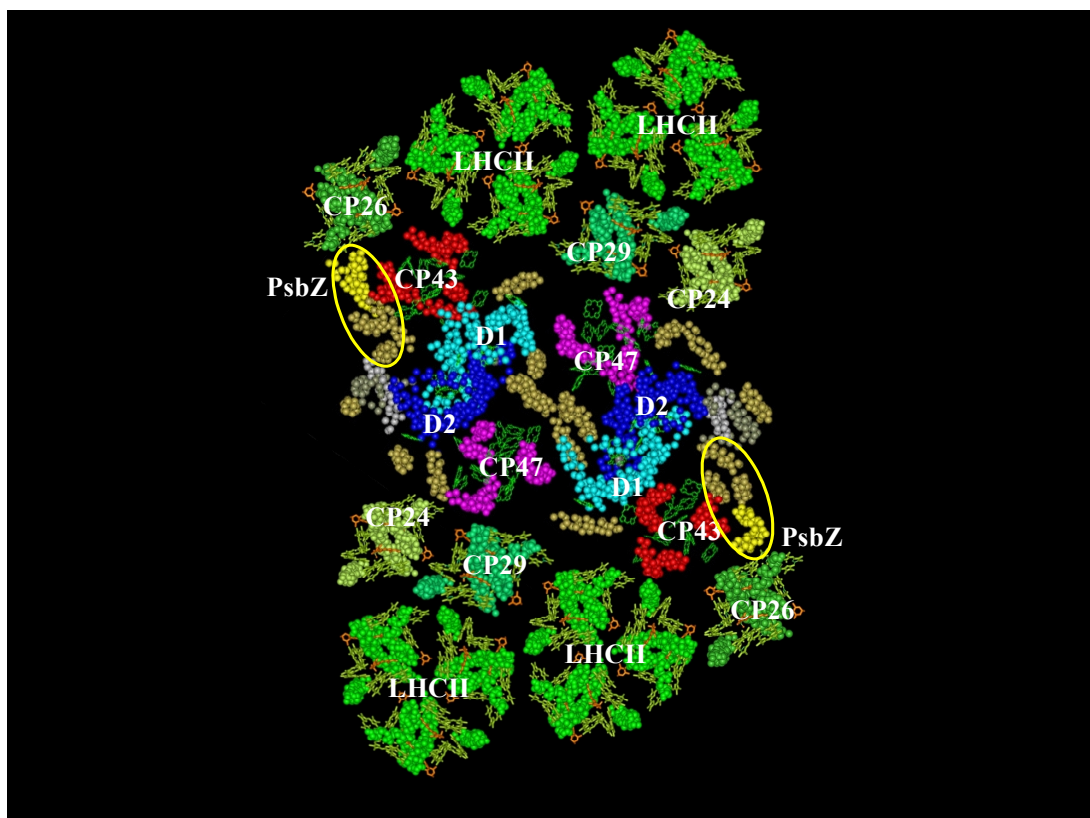


Fig. 57. Molecular reconstruction of the PSII-LHCII supercomplex showing the putative localization of PsbZ. The presentation of PSII and LHCII proteins are based on data published by Zouni et al. (2001) and Kühlbrandt et al. (1994), respectively. The location and orientation of the peripheral antenna complexes with respect to the PSII core are based on Harrer et al. (1998), Boekema et al. (1999b), and Nield et al. (2000). Protein moieties are shown by space-filling models of the C- α carbon atoms, and chlorophylls are shown as dark green frame models. The helices belonging to the PSII core that have no attribution by Zouni et al. (2001) are shown in dark yellow. The putative localization of PsbZ is among five helices circled in yellow. Model kindly provided by R. Kuras and R. Bassi.

The effect of PsbZ deletion on minor antenna protein complexes. The analyses of the protein pattern of wild-type and $\Delta ycf9$ plants demonstrated the absence of a protein of approximately 25 kDa in mutant material. Subsequent Western analyses indicated that, in fact, the amount of two proteins of similar masses, namely the CP26 and CP29 minor antennae proteins, was reduced in transformed plants. The application of different growth conditions allowed further analyses of minor antennae accumulation in $\Delta ycf9$ plants. In agreement with data from Ruf et al. (2000), mutant plants displayed a reduced amount of CP26 under most growth conditions. The deficiency in CP26 was most pronounced at 20°C in dim light, conditions at which plants exhibited a dwarf phenotype. Under the same conditions the amount of CP29 protein, otherwise comparable to wild-type levels, was decreased by approximately 50%. The amount of the third minor antenna apoprotein, CP24, remained unchanged under all conditions applied. Thus, the absence of PsbZ enhanced the light- and temperature-dependent loss of two minor antenna proteins. CP29, CP26 and CP24, together with LHCII, form the light-harvesting complex of PSII. Detailed electron transfer studies, as well as single-particle image techniques, localized CP26 in close proximity with the CP43 protein of PSII core center (Zouni et al. 2001). As illustrated by Figure 57, PsbZ possibly represents one or two unidentified transmembrane helices identified in this region. This indicates a role of PsbZ in attachment of LHCII complexes *via* CP26 to the PSII core center, and, consequently, in the energy transfer from the LHCII to PSII. This also explains, as will be discussed below, the role of PsbZ in the assembly of PSII supercomplexes and alteration of xanthophyll cycle observed in $\Delta ycf9$ plants. In contrast to CP26, the observed instability of CP29 can not be explained by its direct interaction with PsbZ. CP29 has been shown to reside near the PSII dimer groove, and on the opposite side of PSII monomer as CP26. The impaired stability of CP29 in absence of PsbZ is likely a secondary effect, possibly caused by altered protein phosphorylation observed in $\Delta ycf9$ plants.

Functional role of PsbZ in the assembly of PSII-LHCII supercomplexes. As mentioned above, PsbZ is dispensable for photoautotrophic growth and CCII assembly. However, it appears to play a key role in the interaction between CCII and the peripheral antenna complement. When growth conditions were chosen in such a way that limited biochemical defects were detectable in thylakoid membranes of the mutant (heterotrophic and autotrophic growth at 25°C), the stability of PSII supercomplexes, which results from a tight interaction between CCII and peripheral antenna complexes, was severely decreased: these supercomplexes no longer resisted freeze-fracturing (Swiatek et al. 2001) or detergent

solubilization of thylakoid membranes. These observations confirm the idea that PsbZ is a key CCII subunit mediating its interaction with the peripheral antenna complexes.

Alteration of the protein phosphorylation pattern in tobacco $\Delta ycf9$ plants. The interaction between peripheral antennae components and PSII cores is controlled by the phosphorylation of several antennae subunits in an acclimation process known as the state transition (reviewed by Allen 1992). Analyses of thylakoid protein phosphorylation in tobacco and *Chlamydomonas* provided some intriguing insights into the mechanism enabling PsbZ to act as a linker between CCII and peripheral antenna complexes. In $\Delta ycf9$ mutants the steady state level of CCII phosphorylation relative to LHCII was markedly decreased, as demonstrated by anti-phosphothreonine antibodies and radiolabeling with ^{32}P . Since an increased phosphorylation of LHCII vs. CCII under state II conditions is accompanied by detachment of peripheral antennae components from PSII (Allen 1992), the reduced stability of PSII-LHCII supercomplexes is not surprising, and very likely induced by the relative increase of LHCII vs. CCII phosphorylation observed in the absence of PsbZ. These results further imply that the content of CP26 may be controlled by the distribution of phosphate groups among the polypeptides that interact in the PSII units. Biochemical analyses of PSII-LHCII subcomplexes indicated an interaction of CP26 with CP43 and LHCII (Harrer et al. 1998), both of which are subject to reversible phosphorylation. Thus, the accumulation of CP26 in PSII units may rely on the presence of its interacting partners in a phosphorylated state, which itself is dramatically reduced at 20°C under dim light in the absence of CP26 in mutant membranes. A putative physiological function of the PSII core subunit phosphorylation as a prerequisite for stable assembly of PSII unit (CCII + chlorophyll *a/b* binding proteins) has been proposed (de Vitry et al. 1989), and is supported by the observation that BF4, a *Chlamydomonas* mutant devoid of chlorophyll *a/b* binding antenna proteins as well as of CP26, CP29 and CP24, does not display any PSII core phosphorylation (de Vitry and Wollman 1988). Reversible phosphorylation of D1 and D2 proteins is also part of the PSII repair cycle process. Under stress conditions, dephosphorylation of photodamaged D1 is prerequisite for its degradation (Koivuniemi et al. 1995, Rintamäki et al. 1996, Kruse et al. 1997). It remains unknown if PsbZ could take part in repair cycle processes. The presence of phosphorylatable amino acids residues in PsbZ sequence suggests the possibility of its reversible phosphorylation. The possibility of phosphorylation of PsbZ and its role in regulation of protein turn-over will be an interesting subject for future studies. The work of Baena-González et al. (2001) confirmed an altered thylakoid protein phosphorylation pattern

in $\Delta ycf9$ plants. These authors observed a similar decrease in the steady state level of CCII phosphorylation, whereas LHCII phosphorylation level contradicted the results presented in this thesis. These differences might be due to a different treatment of the plants prior to the experiment. The studies performed in my thesis relied on plants grown under strictly controlled light and temperature regimes. The transfer of plants to different light conditions induces changes in the phosphorylation state of thylakoid proteins and could therefore result in phosphorylation patterns different from those presented in this thesis.

Analysis of non-photochemical quenching and xanthophyll cycle in $\Delta ycf9$ plants. The PsbZ-dependent interaction of PSII cores with peripheral antenna proteins significantly influences the ability of PSII to regulate the flux of light excitation. Inactivation of the *ycf9* gene encoding PsbZ not only reduced the stability of minor antenna proteins, especially CP26, but also impaired adaptation mechanisms in PSII, namely NPQ and the xanthophyll cycle. NPQ protects PSII against photoinhibition by dissipating excess excitation energy as heat (Demmig-Adams 1990, Horton 1996, Ramelli et al. 1999, Croce et al. 1999, Bassi et al. 1999, Verhoeven et al. 1999, Havaux and Niyogi 1999, Ruban et al. 1999, Ruban et al. 2000). The molecular mechanism of NPQ is not yet fully understood. However, its full expression involves de-epoxidation of violaxanthin to zeaxanthin as shown by the marked decrease in NPQ in *Arabidopsis* mutants inhibited in the violaxanthin de-epoxidation process (Niyogi et al. 1998). Furthermore, NPQ seems to require the interaction of xanthophylls with LHCII proteins as indicated by a reduced NPQ in the barley *chlorina f2* mutant, lacking Chlorophyll *b* and functional LHCII complexes (Tardy and Havaux 1997). As mentioned above, the major violaxanthin binding proteins, CP26 and CP29, are located at the interface between the PSII core and the trimeric LHCII at the periphery of the PSII complexes (Harrer et al. 1998, Boekema et al. 1999a and 1999b). Minor antenna proteins contain protonatable amino acid residues which might sense a low lumenal pH, thus triggering NPQ (Walters et al. 1994, Walters et al. 1996, Pesaresi et al. 1997, Ruban et al. 1998). The depletion of CP26 can explain the paradoxical behavior of $\Delta ycf9$ mutants: although CP29 and CP26 are both able to exchange violaxanthin for zeaxanthin, this process is much more rapid with CP26 than with CP29 (Ruban et al. 1994, Croce et al. 1996). At sub-optimal temperatures (17°C and 20°C), the de-epoxidation of violaxanthin to zeaxanthin could be inhibited by the loss of CP26 and a reduced amount of CP29 in $\Delta ycf9$ mutants, whereas at higher temperatures remaining CP29 and CP26 might be sufficient to maintain this process, thus leading to the recovery of NPQ at 25°C. However, antisense inhibition of the CP26 and CP29 proteins in *Arabidopsis* excluded their direct role in the formation of NPQ (Andersson et al. 2001), even though CP26 and

CP29 antisense plants exhibited variations in quenching, namely a reduction of NPQ at intermediate light levels, especially in CP29 antisense plants (Andersson et al. 2001). Thus, it was proposed that CP26 and CP29 are not directly involved in NPQ, but rather in LHCII antenna coordination. Another possibility is, that either CP29 or CP26 alone is sufficient for NPQ formation. Up to date, no successful generation of CP26/CP29 double mutants was performed to resolve this question. Nevertheless, unaltered levels of other LHCII proteins, as well as a wild-type level of PsbS in $\Delta ycf9$ plants imply a role of CP26 or/and CP29 in NPQ formation. In addition, the increased amplitude of the quenching process could be due to a much higher content of xanthophyll cycle pigments observed in the mutant as well as an increased zeaxanthin to violaxanthin ratio induced under strong illumination. The dramatic increase of the carotenoid content in mutant plants could, in turn, express their low capacity for excitation energy dissipation under high-light conditions. A similar effect has been observed in *Chlorella* in response to high-light treatment, which increases the excitation energy pressure on PSII (Maxwell et al. 1995).

The results discussed above are consistent with the dwarf phenotype of $\Delta ycf9$ plants grown at low temperature, which corresponds to the effect of PSII overexcitation induced by moderate illumination at low temperature in barley (Huner et al. 1998). To sum up, it can be concluded that the inactivation of *ycf9* disrupts the PSII-LHCII supercomplex architecture, exerting its effect mainly on the regulation of Chl *a*-excited states by mainly destabilizing the CP26 subunit, and to a lesser extent CP29, under certain growth conditions. The decreased capacity for energy dissipation leads to a “bleached” phenotype and an over-stimulation of xanthophyll synthesis, required for both the recovery of NPQ and for scavenging of reactive oxygen species in the photosynthetic membrane (Havaux and Niyogi 1999).

An additional influence of PsbZ on carotenoid biosynthesis was reported recently (Baena-González et al. 2001). In this work, a reduced amount of the plastid terminal oxidase (PTOX), a key enzyme for carotenoid biosynthesis, has been demonstrated in $\Delta ycf9$ tobacco plants. PTOX desaturates phytoene, a C₄₀ acyclic precursor, which subsequently leads to the formation of lycopene. Carotenoid biosynthesis itself is redox-regulated and requires quinones as redox mediators. The reduction of plastoquinone is led through the NDH complex at the expense of oxygen in a process known as chlororespiration (Bennoun 1982, Carol et al. 1999, Carol and Kuntz 2001). Thus, in $\Delta ycf9$ plants, de-regulation of the carotenoid

biosynthesis might be a consequence of the altered ability of PSII to regulate the flux of light excitation.

The functional analyses of $\Delta ycf9$ tobacco plants presented in this thesis indicate a critical role of PsbZ in NPQ, which previously has been attributed mainly to PsbS and CP29 (Crofts and Yerkes 1994, Pesaresi et al. 1997, Li et al. 2000). Although the content of CP29 varied as well in mutant plants under certain growth conditions, these variations did not correlate convincingly with the amplitude of the major NPQ changes. A direct role of CP29 in the regulation of NPQ-related processes could be as well excluded from the analyses of CP29 antisense *Arabidopsis* plants (Andersson et al. 2001). Furthermore, the accumulation of PsbS in $\Delta ycf9$ plants was unaltered. Interestingly, PsbZ is present in phycobilisome-containing organisms which contain neither PsbS, CP29 nor the xanthophyll cycle. Nonetheless, these organisms display NPQ upon exposure to high light distinct from state transitions or photoinhibition (Campbell et al. 1998, El Bissati et al. 2000). It is therefore tempting to speculate that PsbZ is the key player in the formation of NPQ which remained in phycobilisome-containing photosynthetic organisms, although the altered, but still functioning NPQ observed in a *Synechocystis* PCC6803 *ycf9* knock-out strain (S. V. Shestakov and R. Bassi, personal communication) suggested an involvement of additional factors, unknown so far, in the regulation of this process. The PsbZ-CP43 interaction, which was based on its influence on CP26 stability and CP43 phosphorylation, places PsbZ at a position where it could interact with the PSII cores to elicit an adaptation response that dissipates excess light excitation *via* a molecular mechanism that remains to be investigated. In higher plants, the xanthophyll cycle and NPQ, together with other mechanisms, namely alternate electron-donation pathways, are involved in the regulation of excitation energy in PSII. PSII contains two accessory chlorophylls (Chl_Z ligated to D1-His118, and Chl_D ligated to D2-His117), carotenoid and cytochrome *b*₅₅₉ cofactors that function as alternative electron donors under physiological conditions when the primary electron-donation pathway from the O₂-evolving complex to P680⁺ is inhibited. Oxidized Chl_Z is known as a potent quencher of chlorophyll fluorescence that may act together with Cyt *b*₅₅₉ in the dissipation of excess excitation energy under high light conditions (Tracewell et al. 2001). Chl_Z and Chl_D are supposed to be bound near small PSII subunits associated with the D1 and D2 proteins. The proposed localization of the PsbZ protein in the proximity of D1 and CP43 implies its regulative role in an adaptation response that can lead to the dissipation of excess light energy in more than one way.

The role of PsbZ in the photosynthetic electron transport. The localization of PsbZ in PSII complexes as well as the discovery of PsbZ-dependent PSII-LHCII interactions reflected its possible influence on the photosynthetic electron transport. It has been published that inactivation of *ycf9* in tobacco leads to an accelerated electron flux to PSI without a simultaneous change in the maximum electron transfer capacity of PSII (Baena-González et al. 2001). These alterations did not influence carbon fixation in the Calvin-Benson cycle, neither the recycling of electrons from ferredoxin back to PQ (ferredoxin-dependent cyclic electron transport) nor back to plastoquinon *via* the NDH complex. The NDH complex reduces PQ using stromal NAD(P)H as a substrate, and it has been supposed that it contributes to both the electron flow around PSI in the light and in a putative respiratory chain within the chloroplast (Bennoun 1982, Carol et al. 1999, Cournac et al. 2000, Carol and Kuntz 2001). Baena-González et al. (2001) demonstrated an increased ascorbate peroxidase activity in $\Delta ycf9$ plants, which suggests an increased Mehler reaction, in which superoxide is reduced by superoxide dismutase and ascorbate peroxidase (Asada 1999). The increased amount of superoxide could be the effect of an electron leak resulting from impaired electron transfer from PSII to PSI. In this context, the role of PsbZ in the fine-tuning of the photosynthetic reaction, optimization of the distribution of excitation energy between PSII and PSI, and the protection of the two photosystems against photodamage is of particular interest. As discussed above, the results of non-photochemical quenching (NPQ) and the xanthophyll cycle in $\Delta ycf9$ mutants presented in this thesis correspond to these suggestions.

4.2 Functional analysis of the *ycf10* gene product

Similarly to *ycf9* described above, the *ycf10* open reading frame belongs to the few plastid encoded genes, whose function is still a matter of debate. The putative gene product, first designated HBP (heme-binding-protein; Willey and Gray 1990), was renamed CemaA (chloroplast envelope membrane protein A) due to its immunolocalization in the inner envelope membrane of pea chloroplasts (Sasaki et al. 1993). The topology of the protein localization remains unclear because of the uncertainty about the number of membrane-spanning regions in the polypeptide. In their work, Willey and Gray (1990) indicated a putative cleavage site between residues Ser-24 and Phe-25. Cleavage at this side would result in a 24-amino acid signal sequence, corresponding to the first hydrophobic region of Ycf10. However, further analyses of Ycf10 in pea (Sasaki et al. 1993) did not support this hypothesis.

The cyanobacterial *cotA* gene product, which displays high sequence homology to the *ycf10*-encoded polypeptide of higher plants has been shown to be involved in the light-induced proton extrusion (Kato et al. 1996ab), whereas the inactivation of *ycf10* in *Chlamydomonas* suggested its role in inorganic carbon uptake into chloroplasts (Rolland et al. 1997).

Inactivation of the *ycf10* gene in *Nicotiana tabacum*. The reverse genetic approach was applied to analyze the function of the conserved gene in *Nicotiana tabacum*. To this day, no successful inactivation of the *ycf10* reading frame in higher plants was reported, despite several attempts (P. Maliga and J.-D. Rochaix, personal communication). In our case, the biolistic chloroplast transformation yielded three independent mutant lines, which reached homoplastomy after seven cycles of regeneration. The homoplastomic state of the transformed plants, indicated by the absence of wild-type derived DNA copies, was ultimately confirmed by PFGE, PCR and Southern analyses. Results, similar to those obtained for $\Delta ycf9$ plants, demonstrated that a wild-type specific amplification product, detectable when total or Percoll-gradient-purified DNA served as a template, arose from promiscuous DNA copies residing in the nucleus or/and in the chondriome, and proved homoplastomy at a level lower as 0.00001%. Northern analysis further supported the homoplastomy of mutants. In addition, co-transcription of *ycf10* with the upstream located *psaI* and *ycf4* genes and the downstream *petA* gene, as well as the existence of at least two promoters were deduced from the transcription map of the *psaI-ycf4-ycf10-petA* operon, displaying similarities to the transcription pattern observed in pea (Willey and Gray 1990; Nagano et al. 1991). The segregation of homoplastomic $\Delta ycf10$ plants strongly indicates that the $\Delta ycf10$ open reading frame is not required for cell viability, supporting the results observed in the *Chlamydomonas ycf10* inactivation mutant (Rolland et al. 1997).

Phenotypes of the $\Delta ycf10$ plants. Transplastomic $\Delta ycf10$ plants were able to grow photoautotrophically in the greenhouse, and did not show any phenotypic alterations upon the *in vivo* cultivation. White tissue regions, characteristic for $\Delta ycf10$ plants cultivated *in vitro*, were observed as well in $\Delta ycf10$ seedlings grown on medium without antibiotic, thus excluding a spectinomycin effect on the $\Delta ycf10$ phenotype. The analysis of the $\Delta ycf10$ *Chlamydomonas* mutants indicated an increased light sensitivity of the transformed cells, resulting in bleached mutant cultures (Rolland et al. 1997). The bleaching of certain tissue regions in tobacco mutants could be a light-dependent effect as well, however, no such

phenotype was observed when plants were grown in dim light ($10 \mu\text{E m}^{-2} \text{s}^{-1}$, 25°C , data not shown).

Photosynthetic activity of the $\Delta ycf10$ plants. In all analyzed plant species so far, the *ycf10* reading frame is part of a gene cluster encoding essential photosynthetic genes, for example *psaI* and *petA*, suggesting a possible physiological function of the product in the photosynthetic processes. However, the chlorophyll fluorescence spectra of three $\Delta ycf10$ mutants generated independently were undistinguishable from wild-type plants, thus indicating that photosystems I and II, as well as the cytochrome *b₆f* complex were not significantly affected. This supports the data of Rolland et al. (1997) reported for the $\Delta ycf10$ mutant of *C. reinhardtii*. Chlorophyll fluorescence measurements of the $\Delta ycf10$ mutant plants using the FluorCam device revealed a small decrease in the maximal fluorescence under continuous illumination (F_p) relative to the wild-type, indicating slightly impaired reduction of PSII. However, these observations were not supported by more detailed and standardized analyses of PSII activity using the PAM device. Nevertheless, all fluorescence analyses have shown an absence of photosynthetic activity in bleached tissue regions. This result was supported by electron micrographs of $\Delta ycf10$ mutant cells, showing structured plastids in the green tissue regions indistinguishable from wild-type cells, whereas plastid structure in bleached regions was dramatically altered, with stroma and grana thylakoids generally lacking. Analyses of protein complexes isolated from photosynthetic membranes of $\Delta ycf10$ plants, did not uncover any differences between wild-type and transformed tobacco plants, further supporting an unaltered membrane structure and photosynthetic activity of $\Delta ycf10$ plants.

CO₂-dependent photosynthesis in $\Delta ycf10$ plants. The loss of *ycf10* obviously affects the response to the external C_i concentration of mutant plants and causes a reduction of their photosynthetic activity of approximately 50% relative to wild-type plants. The same effect was observed in *ycf10*-deficient *Chlamydomonas* cells (Rolland et al. 1997). Nevertheless, nature and detailed mechanism of the CO₂ uptake are still unknown so that secondary effects of the gene loss on inorganic carbon uptake can not be ruled out. As mentioned above, the cyanobacterial homologue of *ycf10* (*cemA*), *cotA*, is supposed to be involved in light-induced proton extrusion rather than CO₂ uptake and/or transport (Kato et al. 1996ab). The extrusion of protons, observed in *Synechocystis*, causes the acidification of wild-type cell suspension in light and generates a transmembrane pH gradient across the cytoplasmic membrane, which

drives the transport of other ions, including C_i ions. Interestingly, the *ycf10* reading frame is conserved among all photosynthetically active plant species, except *Euglena* (Hallic et al. 1993), an organism without a CO_2 concentrating mechanism that can raise the CO_2 concentration, e.g. in mesophyll cells (in higher plants), in order to favour the carboxylase activity of RuBisCo, the key CO_2 -fixation enzyme (Badger and Price 1994). The marker enzyme of a CO_2 concentrating mechanism, carbonic anhydrase, converts HCO_3^- into CO_2 (Badger and Price 1994). Both, carbonic anhydrase and C_i transport systems are present in several organisms, including cyanobacteria, algae, C3 and C4 plant species. The interrelation between *ycf10* and the presence of a CO_2 concentrating mechanism in different organisms is shown in Table 9.

Table 9. Conservation of the *ycf10* open reading frame in different plant species and its relation to the CO_2 concentrating mechanism (CCM).

species	<i>ycf10</i>	CCM		references
<i>Synechocystis</i> PCC6803	+	+	Cyanobacteria	Katoh et al. 1996a and 1996b
<i>Euglena gracilis</i>	-	-	Euglenophyta	Hallic et al. 1993 Yakota et al. 1989
<i>Chlamydomonas</i> <i>reinhardtii</i>	+	+	Chlorophyta	Rolland et al. 1997
<i>Chlorella vulgaris</i>	+	+	Chlorophyta	Wakasugi et al. 1997 Polloc and Colman 2001
<i>Porphyra purpurea</i>	+	+	Rhodophyta	Reith and Munholland 1995 Uemura et al. 1997
<i>Plasmodium</i> <i>falciparum</i>	-	-	apicomplexan parasite	Wilson et al. 1996
<i>Epifagus virginiana</i>	-	-	nonphotosynthetic root parasite	Wolfe et al. 1992
<i>Cyanophora</i> <i>paradoxa</i>	-	?	Glaucocystophyta	Stirewalt et al. 1995
<i>Marchantia</i> <i>polymorpha</i>	+	+	Bryophyta	Ohyama et al. 1986
<i>Pinus thurinbergii</i>	+	+	Gymnospermae (C3)	Wakasugi et al. 1994
<i>Nicotiana tabacum</i>	+	+	Angiospermae (C3)	Shinozaki et al. 1986
<i>Spinacia oleracea</i>	+	+	Angiospermae (C3)	Schmitz-Linneweber et al. 2001
<i>Oryza sativa</i>	+	+	Angiospermae (C3)	Hiratsuka et al. 1989
<i>Oenothera elata</i>	+	+	Angiospermae (C3)	Hupfer et al. 2000
<i>Zea mays</i>	+	+	Angiospermae (C4)	Maier et al. 1995

Regarding the Glaucocystophyte *Cyanophora paradoxa* the absence of *ycf10* in the cyanoplast genome was not surprising, because it encodes less than 10% of the genetic information encoded by the cyanobacterial genome. As most of the organelle-specific proteins are nucleus-encoded, it is likely that the *ycf10* reading frame, similarly to the *ndh* gene cluster,

was transferred to the nuclear genome (Löffelhardt and Bohnert 1994). Unfortunately, detailed analyses of C_i uptake into *Cyanophora* cells are not available. Therefore, it remains under debate whether the Ycf10 (CemA) protein exerts its effect on inorganic carbon uptake directly or indirectly, although the data of Katoh et al. (1996a and 1996b) suggested a role of cyanobacterial CotA protein as an ion transporter rather than a component of the C_i uptake system. To clarify the functional role of *ycf10* in the envelope membrane, detailed analyses of proton movements from the chloroplast into the cytosol are required for both *Chlamydomonas* and tobacco. As *cotA* was the first gene found to be involved in light-induced proton extrusion in *Synechocystis* (Katoh et al. 1996a and 1996b), it is tempting to assume a similar involvement of the *cemA* gene product in the energization and/or regulation of an ion transport system in the chloroplasts.

5. SUMMARY

Plastid chromosomes from the variety of plant species contain several conserved open reading frames of unknown function, which most probably represent functional genes. The primary aim of this thesis was the analysis of the role of two such ORFs, designated *ycfs* or hypothetical chloroplast reading frames, namely *ycf9* (ORF62) and *ycf10* (ORF229, *cemA*). Both were analyzed in *Nicotiana tabacum* (tobacco) via their inactivation using biolistic plastid transformation. A new experimental protocol, based on pulsed-field gel electrophoresis (PFGE), was established to reliably assess the homoplasmic state of transformed plants.

1. *Functional analysis of the ycf9 gene product:* The inactivation of *ycf9* in *N. tabacum* as well as in *Chlamydomonas reinhardtii* yielded a homoplasmic mutant phenotype after several rounds of regeneration under selective pressure. The mutant plants grew photoautotrophically, but displayed two clear phenotypes, a light-sensitive one, increasing with the light intensity, and a dwarf phenotype under low-light combined with temperatures below 20°C. The *ycf9* gene product was exclusively located in PSII core complexes. This localization was based on the isolation of protein complexes released from thylakoids by controlled, partial lysis, followed by sucrose density gradient centrifugation or 2D gel electrophoresis. This finding revised data of the literature. Biochemical analysis indicated an involvement of the protein in the interaction of the light harvesting antenna II complex (LHCII) with PSII cores. In particular, PSII-LHCII supercomplexes could no longer be isolated from transplastomic tobacco plants. Furthermore, the minor chlorophyll *a/b*-binding proteins CP26, and to a lesser extent CP29, were substantially reduced under most growth conditions analyzed, in both, tobacco and photoautotrophically grown *Chlamydomonas* mutants (Swiatek et al. 2001). The gene was therefore renamed *psbZ*. The $\Delta psbZ$ -related alterations in the supramolecular organization of PSII complexes were accompanied by considerable modification in (i) the phosphorylation pattern of PSII subunits, (ii) the rate of de-epoxydation of xanthophylls, and (iii) the kinetics and amplitude of non-photochemical quenching. The proposed position of *PsbZ* in close proximity to CP43 enables the protein to interact with PSII cores to elicit an adaptation process in response to excess light excitation. The molecular mechanism underlying this energy dissipation process remains to be investigated.

2. *Functional analysis of the ycf10 gene product:* Biolistic plastid transformation was also used to inactivate the *ycf10* reading frame in tobacco. After several rounds of regeneration under selective pressure, homoplastomic plants were obtained. Northern analysis uncovered co-transcription of *ycf10* within the *psaI-ycf4-ycf10-petA* gene cluster, with at least two promoter regions upstream of the *psaI* gene. The mutant plants grew photoautotrophically and developed dark green leaves with numerous pale green to white regions, the latter devoid of photosynthetic activity. The loss of *ycf10* did not affect photosynthetic activity, as indicated by unaltered chlorophyll fluorescence. The tobacco *ycf10* gene product was localized in the chloroplast inner envelope membrane. Neither protein composition of stroma or thylakoid fractions, nor the stability of the photosynthetic protein complexes were affected in the mutant plants. In contrast, CO₂-dependent oxygen evolution was strongly reduced, with a maximum rate of C₁-dependent photosynthesis being approximately 50% lower than in wild-type plants. Two explanations can account for the observed phenomenon: (i) de-regulation of carbon-concentrating mechanisms in transformed cells, or (ii) an indirect effect on CO₂-uptake in $\Delta ycf10$ plants.
3. *Pulsed-field gel electrophoresis is an ideal tool to verify the homoplastomic state of transformed plants:* To enhance the sensitivity of detection of heteroplastomic states, and to distinguish between plastome-located wild-type segments in transplastomic material and promiscuous DNA, a new approach was developed. Customary Southern and PCR techniques are not sensitive enough or not discriminating the latter alternatives, respectively. Pulsed-field gel electrophoresis allows to isolate virtually contamination-free plastid DNA. Plastid DNA isolated this way lacked traces of nuclear and mitochondrial DNA at a detection level of 50 DNA molecules. This excludes that gene-specific PCR amplification products originate from promiscuous nuclear or mitochondrial gene copies. Therefore, PFGE appears to be an ideal tool to investigate the homoplastomic state of transformed plants, especially when combined with radiolabeled probes and Southern techniques.

6. REFERENCES

- Abrahams, J. P., Leslie, A. G. W., Lutter, R., and Walker, J. E.** (1994). Structure at 2.8 Å resolution of F₁-ATPase from bovine heart mitochondria. *Nature* **370**, 621-628.
- Adamska, I.** (1997). ELIPs-Light-induced stress proteins. *Physiol. Plant.* **100**, 794-805.
- Allen, J. F., Bennett, J., Steinback, K. E., and Arntzen, C. J.** (1981). Chloroplast protein phosphorylation couples plastochinone redox state to distribution of excitation energy between photosystems. *Nature* **291**, 25-29.
- Allen, J. F.** (1992). Protein phosphorylation in regulation of photosynthesis. *Biochim. Biophys. Acta* **1098**, 275-335.
- Allen, J. F., and Nillson, A.** (1997). Redox signalling and the structural basis of regulation of photosynthesis by protein phosphorylation. *Phys. Plant.* **100**, 863-868.
- Allison, L. A., Simon, L. D., and Maliga, P.** (1996). Deletion of *rpoB* reveals a second distinct transcription system in plastid of higher plants. *EMBO J.* **15**, 2802-2809.
- Altschul, S. F., Madden, T. L., Schaffer, A. A., Zhang, J., Zhang, Z., Miller, W., and Lipman, D. J.** (1997). Gapped BLAST and PSI-BLAST: a new generation of protein database search programs. *Nucleic Acids Res.* **25**, 3389-3402.
- Andersson, J., Walters, R. G., Horton, P., and Jansson, S.** (2001). Antisense Inhibition of the Photosynthetic Antenna Proteins CP29 and CP26: Implications for the Mechanism of Protective Energy Dissipation. *Plant Cell* **13**, 1193-1204.
- Armond, P. A., Staehelin, L. A., and Arntzen, C. J.** (1977). Spatial relationship of PSI, PSII and LHC in chloroplast membranes. *J. Cell. Biol.* **73**, 400-418.
- Arnon, D. I.** (1949). Copper enzymes in isolated chloroplasts. Polyphenol oxidase in *Beta vulgaris*. *Plant Physiol.* **24**, 1-14.
- Asada, K.** (1999). The Water-Water Cycle in Chloroplasts: Scavenging of Active Oxygens and Dissipation of Excess Photons. *Annu. Rev. Plant Physiol. Plant. Mol. Biol.* **50**, 601-639.
- Ausubel, F. M., Brent, R., Kingston, R. E., Moore, D. D., Seidnan, J. G., Smith, J. A., and Struhl, K.W.** (1987). *Current protocols in molecular biology*. Current Protocols New York.
- Ayliffe, M. A., and Timmis, J. N.** (1992). Tobacco nuclear DNA contain long tracts of homology to chloroplast DNA. *Theor. Appl. Genet.* **85**, 229-238.
- Badger, M. R., and Price, G. D.** (1994). The role of carbonic anhydrase in photosynthesis. *Annu. Rev. Plant Physiol. Plant Mol. Biol.* **45**, 369-392.

- Baena-González, E., Gray, J. C., Tyystjarvi, E., Aro, E. M., and Mäenpää, P.** (2001). Abnormal Regulation of Photosynthetic Electron Transport in a Chloroplast *ycf9* Inactivation Mutant. *J. Biol. Chem.* **276**, 20795-20802.
- Barbato, R., Frisco, G., Rigoni, F., Frizzo, A., and Giacometti, G. M.** (1992). Characterization of a 41 kDa photoinhibition adduct in isolated photosystem II reaction centres. *FEBS Lett.* **309**, 165-169.
- Barber, J., Nield, J., Morris, E. P., Zheleva, D., and Hankamer, B.** (1997). The structure, function and dynamics of photosystem II. *Physiol. Plant.* **100**, 817-827.
- Barber, J., and Kühlbrandt, W.** (1999). Photosystem II. *Curr. Opin. Struct. Biol.* **9**, 469-475.
- Bassi, R., Croce, R., Cugini, D., and Sandona, D.** (1999). Mutational analysis of a higher plant antenna protein provides identification of chromophores bound into multiple sites. *Proc. Natl. Acad. Sci. USA* **96**, 10056-10061.
- Baur, E.** (1909). Das Wesen und die Erblchkeitsverhältnisse der "Variatates albomarginate hort" von *Pelargonium zonale*. *Z. indukt. Abstammungs. Vererbungsl.* **1**, 330-351.
- Bendall, D. S., and Manasse, R. S.** (1995). Cyclic phosphorylation and electron transport. *Biochim. Biophys. Acta* **1229**, 23-38.
- Bennett, J., Shaw, E. K., and Michel, H.** (1988). Cytochrome *b₆f* complex is required for phosphorylation of light-harvesting chlorophyll *a/b* complex in chloroplast photosynthetic membranes. *Eur. J. Biochem.* **171**, 95-100.
- Bennoun, P.** (1982). Evidence for a respiratory chain in the chloroplast. *Proc. Natl. Acad. Sci. USA* **79**, 4352-4356.
- Bhattacharya, D., and Medlin, L.** (1998). Algal Phylogeny and the Origin of Land Plants. *Plant Physiol.* **116**, 9-15.
- Birnboim, H. C., and Doley, J.** (1979). A rapid alkaline extraction procedure for screening recombinant plasmid DNA. *Nucleic Acids Res.* **7**, 1513-1524.
- Boekema, E. J., van Roon, H., van Breemen, J. F., and Dekker, J. P.** (1999a). Supramolecular organization of photosystem II and its light-harvesting antenna in partially solubilized photosystem II membranes. *Eur. J. Biochem.* **266**, 444-452.
- Boekema, E. J., van Roon, H., Calkoen, F., Bassi, R., and Dekker, J. P.** (1999b). Multiple types of association of photosystem II and its light-harvesting antenna in partially solubilized photosystem II membranes. *Biochemistry* **38**, 2233-2239.

- Boekema, E. J., van Breemen, J. F., van Roon, H., and Dekker, J. P.** (2000). Conformational Changes in Photosystem II Supercomplexes upon Removal of Extrinsic Subunits. *Biochemistry* **39**, 12907-12915.
- Bookjans, G. B., Stummann, B. M., Rasmussen, O. F., and Henningsen, K. W.** (1986). Structure of a 3.2 kb region of pea chloroplast DNA containing the gene for the 44 kD photosystem II polypeptide. *Plant Mol. Biol.* **6**, 359-366.
- Boyer, P. D.** (1993). The binding change mechanism for ATP synthase-some probabilities and possibilities. *Biochim. Biophys. Acta* **1140**, 215-250.
- Boynton, J. E., Gillham, N. W., Harris, E. H., Hosler, J. P., Johnson, A. M., Jones, A. R., Randolph-Anderson, B. L., Robertson, D., Klein, T. M., Shark, K. B., and Sandford, J. C.** (1988). Chloroplast transformation in *Chlamydomonas* with high velocity microprojectiles. *Science* **240**, 1534-1538.
- Bradford, M. M.** (1976). A rapid and sensitive method for the quantification of microgram quantities of protein utilizing the principle of protein-dye binding. *Anal. Biochem.* **7**, 248-254.
- Brennicke, A., Grohmann, L., Hiesel, R., Knoop, V., and Schuster, W.** (1993). The mitochondrial genome on its way to the nucleus: different stages of gene transfer in higher plants. *FEBS Lett.* **325**, 140-145.
- Breyton, C., Tribet, C., Olive, J., Dubacq, J.-P., and Popot J.-L.** (1997). Dimer to monomer Conversion of Cytochrome *b₆f* Complex. *J. Biol. Chem.* **272**, 21892-21900.
- Bron, P., Lacapère, J.-J., Breyton, C., and Mosser, G.** (1999). The 9 Å Projection Structure of Cytochrome *b₆f* Complex Determined by Electron Crystallography. *J. Mol. Biol.* **287**, 117-126.
- Brunner, C.** (1997). Plasmidtransformation bei *Nicotiana tabacum* L.: Expression des Reportergens *gusA* nach mRNA-Edierung. Diplomarbeit an der Fakultät für Biologie der Ludwig-Maximilian-Universität München.
- Burrows, P. A., Sazanow, L. A., Svab, Z., Maliga, P., and Nixon, P. J.** (1998). Identification of a functional respiratory complex in chloroplasts through analysis of tobacco mutants containing disrupted plastid *ndh* genes. *EMBO J.* **17**, 868-876.
- Campbell, D., Hurry, V., Clarke, A. K., Gustafsson, P., and Oquist, G.** (1998). Chlorophyll fluorescence analysis of cyanobacterial photosynthesis and acclimation. *Microbiol. Mol. Biol. Rev.* **62**, 667-683.
- Carlberg, I., Rintamäki, E., Aro, E.-M., and Andersson, B.** (1999). Thylakoid protein phosphorylation and the thiol redox state. *Biochemistry.* **38**, 3197-3204.

- Carol, P., Stevenson, D., Bisanz, C., Breitenbach, J., Sandmann, G., Mache, R., Coupland, G., and Kuntz, M.** (1999). Mutations in the Arabidopsis gene IMMUTANS cause a variegated phenotype by inactivating a chloroplast terminal oxidase associated with phytoene desaturation. *Plant Cell* **11**, 57-68.
- Carol, P., and Kuntz, M.** (2001). A plastid terminal oxidase comes to light: implications for carotenoid biosynthesis and chlororespiration. *Trends Plant Sci.* **6**, 31-36.
- Casano, L. M., Zapata, J. M., Martín, M., and Sabater, B.** (2000). Chlororespiration and Poisoning of Cyclic Electron Transport. *J. Biol. Chem.* **275**, 942-948.
- Chitnis, P. R.** (1996). Photosystem I. *Plant Physiol.* **111**, 661-669.
- Cline, K., and Henry, R.** (1996). Import and routing of nucleus-encoded chloroplast proteins. *Annu. Rev. Cell Dev. Biol.* **12**, 1-26.
- Correns, C.** (1909). Vererbungsversuche mit blass(gelb)grünen und buntblättrigen Sippen bei *Mirabilis jalapa*, *Urtica pilulifera* und *Lunaria annua*. *Z. indukt. Abstammungs. Vererbungsl.* **1**, 291-329.
- Cournac, L., Redding, K., Ravenel, J., Rumeau, D., Josse E.-M., Kuntz, M., and Peltier, G.** (2000). Electron Flow between Photosystem II and Oxygen in Chloroplasts of Photosystem I-deficient Algae Is Mediated by a Quinol Oxidase Involved in Chlororespiration. *J. Biol. Chem.* **275**, 17256-17262.
- Croce, R., Breton, J., and Bassi, R.** (1996). Conformational changes induced by phosphorylation in the CP29 subunit of photosystem II. *Biochemistry* **35**, 11142-11148.
- Croce, R., Weiss, S., and Bassi, R.** (1999). Carotenoid-binding Sites of the Major Light-harvesting Complex II of Higher Plants. *J. Biol. Chem.* **274**, 29613-29623.
- Crofts, A. R., Meinhardt, S. W., Jones, K. R., and Snozzi, M.** (1983). The role of the quinone pool in the cyclic-electron transfer chain of *Rhodospseudomonas sphaeroides*: a modified Q-cycle mechanism. *Biochim. Biophys. Acta* **723**, 202-218.
- Crofts, A. R., and Yerkes, C. T.** (1994). A molecular mechanism for q(E)-quenching. *FEBS Letters* **352**, 265-270.
- Demmig-Adams, B.** (1990). Carotenoids and Photoprotection in Plants: a role for the xanthophyll zeaxanthin. *Biochim. Biophys. Acta* **1020**, 1-24.
- Demmig-Adams, B., and Adams, W. W. I.** (1992). Carotenoid composition in sun and shade leaves of plants with different life forms. *Plant Cell Environ.* **15**, 411-419.
- de Vitry, C., and Wollman, F.-A.** (1988). Changes in phosphorylation of thylakoid membrane proteins in light-harvesting complex mutants from *Chlamydomonas reinhardtii*. *Biochim. Biophys. Acta* **933**, 444-449.

- de Vitry, C., Olive, J., Drapier, D., Recouvreur, M., and Wollman, F.-A.** (1989). Posttranslational events leading to the assembly of photosystem II protein complex: a study using photosynthesis mutants from *Chlamydomonas reinhardtii*. *J. Cell Biol.* **109**, 991-1006.
- Dolganov, N. A. M., Bhaya, D., and Grossman, A. R.** (1995). Cyanobacterial protein with similarity to the chlorophyll a/b binding proteins of higher plants: Evolution and regulation. *Proc. Natl. Acad. Sci. USA* **92**, 636-640.
- Dovzhenko, A., Bergen, U., and Koop, H.-U.** (1998). Thin-alginate-layer technique for protoplast culture of tobacco leaf protoplasts: shoot formation in less than two weeks. *Protoplasma* **204**, 114-118.
- Doyle, J. J., and Doyle, J. L.** (1990). Isolation of plant DNA from fresh tissue. *Focus* **12**, 13-15.
- Drescher, A., Ruf, S., Calsa Jr., T., Carrer, H., and Bock, R.** (2000). The two largest chloroplast genome-encoded reading frames of higher plants are essential genes. *Plant J.* **22**, 97-104.
- El Bissati, K., Delphin, E., Murata, N., Etienne, A., and Kirilovsky, D.** (2000). Photosystem II fluorescence quenching in the cyanobacterium *Synechocystis PCC 6803*: involvement of two different mechanisms. *Biochim. Biophys. Acta* **1457**, 229-242.
- Ellis, J.** (1982). Promiscuous DNA-chloroplast genes inside plant mitochondria. *Nature* **299**, 678-679.
- Engelbrecht, S., and Junge, W.** (1997). ATP synthase: a tentative structural model. *FEBS Lett.* **414**, 485-491.
- Funk, C., Schroder, W. P., Napiwotzki, A., Tjus, S. E., Renger, G., and Andersson, B.** (1995). The PSII-S protein of higher plants: a new type of pigment-binding protein. *Biochemistry* **34**, 11133-11141
- Gal, A., Zer, H., and Ohad, I.** (1987). Specific loss of LHCII phosphorylation in *Lemna* mutant 1073 lacking the cytochrome *b₆f* complex. *FEBS Lett.* **221**, 205-210.
- Gal, A., Zer, H., and Ohad, I.** (1997). Redox-controlled thylakoid protein phosphorylation, news and views. *Phys. Plant.* **100**, 869-885.
- Galili, G.** (1995). Regulation of lysine and threonine biosynthesis. *Plant Cell* **7**, 899-906.
- Gamborg, O. L., Miller, R. A., and Ojima, K.** (1968). Nutrient requirements of suspension cultures of soybean root cells. *Exp. Cell Res.* **50**, 151-158.
- Gilmore, A. M., and Yamamoto, H. Y.** (1991). Resolution of lutein and zeaxanthin using a nonendcapped, lightly carbon-loaded C-18 high-performance liquid chromatographic column. *J. Chromatogr.* **543**, 137-145.

- Golds, T. J., Maliga, P., Koop, H.-U.** (1993). Stable plastid transformation in PEG-treated protoplast of *Nicotiana tabacum*. *Bio/Technology* **11**, 95-97.
- Goldschmidt-Clermont, M.** (1991). Transgenic expression of aminoglycoside adenyl transferase in the chloroplast: a selectable marker for site-directed transformation of *Chlamydomonas*. *Nucleic Acid Res.* **19**, 4083-4089.
- Gray, M. W.** (1992). The endosymbiont hypothesis revisited. *Int. Rev. Cytol.* **141**, 233-357.
- Green, B. R., and Kühlbrandt, W.** (1995). Sequence conservation of light-harvesting and stress-response proteins in relation to the three-dimensional molecular structure of LHCII. *Photosynth. Res.* **44**, 139-148.
- Green, B. R., and Durnford, D. G.** (1996). The chlorophyll-carotenoid proteins of oxygenic photosynthesis. *Annu. Rev. Plant Physiol. Plant. Mol. Biol.* **47**, 685-714.
- Hagemann, R.** (2000). Erwin Baur or Carl Correns: Who Really Created the Theory of Plastid Inheritance? *Journal of Heredity* **91**, 435-440.
- Hallic, R. B., Hong, L., Drager, R. G., Faureau, M. R., Montfort, A., Orset, B., Spielmann, A., and Stutz, E.** (1993). Complete sequence of *Euglena gracilis* chloroplast DNA. *Nucleic Acids Res.* **25**, 3537-3544.
- Hamel, P., Olive, J., Pierre, Y., Wollman, F.-A., and de Vitry, C.** (2000). A New Subunit of Cytochrome *b₆f* Complex Undergoes Reversible Phosphorylation upon State Transition. *J. Biol. Chem.* **275**, 17072-17079.
- Hanahan, D.** (1983). Studies on transformation of *Escherichia coli* with plasmids. *J. Mol. Biol.* **166**, 557-580.
- Hankamer, B., Morris, E. P., and Barber, J.** (1999). Revealing the structure of the oxygen-evolving core dimer of photosystem II by cryoelectron crystallography. *Nat. Struct. Biol.* **6**, 560-564.
- Harlow, E., and Lane, D.** (1988). *Antibodies. A laboratory manual.* Cold Spring Harbor Laboratories, 55-116.
- Harrer, R., Bassi, R., Testi, M. G., and Schafer, C.** (1998). Nearest-neighbor analysis of a photosystem II complex from *Marchantia polymorpha* L. (liverwort), which contains reaction center and antenna proteins. *Eur. J. Biochem.* **255**, 196-205.
- Havaux, M., and Niyogi, K. K.** (1999). The violaxanthin cycle protects plants from photooxidative damage by more than one mechanism. *Proc. Natl. Acad. Sci. USA* **96**, 8762-8767.

- Herrmann, R. G., Bohner, H.-J., Kowallik, K. V., and Schmitt, J. M.** (1975). Size, conformation and purity of chloroplast DNA of some higher plants. *Biochim. Biophys. Acta.* **378**, 305-317.
- Herrmann, R. G., and Possingham, J. V.** (1980). Plastid DNA - The Plastome. In: *Results and Problems in Cell Differentiation Vol. 10*, 45-96. eds. Reinert, J. Springer-Verlag Berlin, Heidelberg.
- Herrmann, R. G.** (1982). The preparation of circular DNA from plastids. In: *Methods in Chloroplast Molecular Biology*. eds. Edelman, M., Hallick, R. B., Chua, N.-H. Elsevier Biomedical Press, Amsterdam-New York, Oxford, 259-280.
- Herrmann, R. G., Oelmüller, R., Bichler, J., Schneiderbauer, A., Steppuhn, J., Wedel, N., Tyagi, A., and Westhoff, P.** (1991). The thylakoid membrane of higher plants: Genes, their expression and interaction. In: *Herrmann R. G. and Larkin B. : Plant Molecular Biology* **2**, 411-427. Plenum Publ. Corp., New York.
- Herrmann, R. G.** (1997). Eukaryotism, towards a new interpretation. In: *Eukaryotism and Symbiosis*, eds. Schenk H. E. A., Herrmann R. G., Jeon K. W., Müller N. E., Schwemmler W., Springer Heidelberg, Berlin, New York, 73-118.
- Higgs, D. C., Kuras, R., Kindle, K. L., Wollman, F.-A., and Stern, D. B.** (1998). Inversions in the *Chlamydomonas* chloroplast genome suppress a *petD* 5' untranslated region deletion by creating functional chimeric mRNAs. *Plant J.* **14**, 663-671.
- Hiratsuka, J., Shimada, H., Whittier, R., Ishibashi, T., Sakamoto, M., Mori, M., Kondo, C., Honji, Y., Sun, C. R., and Meng, B. Y.** (1989). The complete sequence of the rice (*Oryza sativa*) chloroplast genome: intermolecular recombination between distinct tRNA genes accounts for a major plastid DNA inversion during the evolution of the cereals. *Mol. Gen. Genet.* **217**, 185-194.
- Horton, P.** (1996). Non-photochemical quenching of chlorophyll fluorescence. In *Light as energy source and information carrier in plant physiology*. Jennings et al., eds. (London: Plenum Press), pp. 99-112.
- Huner, N. P., Oquist, G., and Sarhan, F.** (1998). Energy balance at acclimation to light and cold. *Trends Plant Sci.* **3**, 224-230.
- Hupfer, H., Swiatek, M., Hornung, S., Herrmann, R. G., Maier, R. M., Chiu, W. L., and Sears, B.** (2000). Complete nucleotide sequence of the *Oenothera elata* plastid chromosome, representing plastome I of the five distinguishable euoenothera plastomes. *Mol. Gen. Genet.* **263**, 581-585.

- Jansson, S.** (1999). A guide to the *Lhc* genes and their relatives in *Arabidopsis*. *Trends Plant Sci.* **4**, 236-240.
- Jeanmougin, F., Thompson, J. D., Gouy, M., Higgins, D. G., and Gibson, T. J.** (1998). Multiple sequence alignment with Clustal X. *Trends Biochem. Sci.* **23**, 403-405.
- Jensen, P. E., Gilpin, M., Knoetzel, J., and Scheller, H. V.** (2000). *J. Biol. Chem.* **275**, 24701-24708.
- Joët, T., Cournac, L., Horvath, E. M., Medgyesy, P., and Peltier, G.** (2001). Increased Sensitivity of Photosynthesis to Antimycin A Induced by Inactivation of the Chloroplast *ndhB* Gene. Evidence for a Participation of the NADH-Dehydrogenase Complex to Cyclic Electron Flow around Photosystem I. *Plant Physiol.* **125**, 1919-1929.
- Jordan, P., Fromme, P., Witt, H. T., Klukas, O., Saenger, W., and Krauß, N.** (2001). Three-dimensional structure of cyanobacterial photosystem I at 2.5 Å resolution. *Nature* **411**, 909-917.
- Katoh, A., Lee, K. S., Fukuzawa, H., Ohyama, K., and Ogawa, T.** (1996a). *cema* homologue essential to CO₂ transport in the cyanobacterium *Synechocystis* PCC6803. *Proc. Natl. Acad. Sci. USA.* **93**, 4006-4010.
- Katoh, A., Sonoda, M., Katoh, H., and Ogawa, T.** (1996b). Absence of light-induced proton extrusion in a *cotA*-less mutant of *Synechocystis* sp. strain PCC6803. *J. Bacteriol.* **178**, 5452-5455.
- Kofer, W., Koop, H.-U., Wanner, G., Steinmüller, K.** (1998). Mutagenesis of the genes encoding subunits A, C, H, I, J and K of the plastid NAD(P)H-plastoquinone-oxidoreductase in tobacco by polyethylene glycol-mediated plastome transformation. *Mol. Gen. Genet.* **258**, 166-173.
- Koivuniemi, A., Aro, E.-M., and Andersson, B.** (1995). Degradation of the D1- and D2-Proteins of Photosystem II in Higher Plants Is Regulated by Reversible Phosphorylation. *Biochemistry* **34**, 16022-16029.
- Kolonder, R., and Tewari, K. K.** (1975). Molecular size and conformation of chloroplast DNA from higher plants. *Biochim. Biophys. Acta* **402**, 372-390.
- Koop, H.-U., and Kofer, W.** (1995). Plastid transformation by polyethylene glycol treatment of protoplasts and regeneration of transplastomic tobacco plants. *Gene transfer to plants, Springer Lab Manual. Heidelberg: Springer Verlag, D.,* 75-82.
- Koop, H.-U., Steinmüller, K., Wagner, H., Rossler, C., Eibl, C., and Sacher, L.** (1996). Integration of foreign sequences into the tobacco plastome via polyethylene glycol-mediated protoplast transformation. *Planta* **199**, 193-201.

- Koop, H.-U., Kofer, E., and Steinmüller, K.** (1998). Judging the homoplastomic state of plastid transformants-reply. *Trends Plant Sci.* **3**, 377-378.
- Kruse, O., Zheleva, D., and Barber, J.** (1997). Stabilization of photosystem two dimers by phosphorylation: Implication for the regulation of the turnover of D1 protein. *FEBS Lett.* **408**, 276-280.
- Kühlbrandt, W., Wang, D. N., and Fujiyoshi, Y.** (1994). Atomic model of plant light-harvesting complex by electron crystallography. *Nature* **367**, 614-621.
- Kyte, J., and Doolittle, R. F.** (1982). A simple method for displaying the hydrophobic character of a protein. *J. Mol. Biol.* **157**, 105-32.
- Laemmli, U. K.** (1970). Cleavage of structural proteins during the assembly of the head of bacteriophage T4. *Nature* **227**, 680-685.
- Li, X. P., Bjorkman, O., Shih, C., Grossman, A. R., Rosenquist, M., Jansson, S., and Niyogi, K. K.** (2000). A pigment-binding protein essential for regulation of photosynthetic light harvesting. *Nature* **403**, 391-395.
- Löffelhardt, W., and Bohnert, H. J.** (1994). In: *The Molecular Biology of Cyanobacteria*. Bryant, D. A., eds. (Dordrecht/Boston/London: Kluwer academic publishers).
- Lunde, C., Jensen, P. E., Haldrup, A., Knoetzel, J., and Scheller, H. V.** (2000). The PSI-H subunit of photosystem I is essential for state transitions in plant photosynthesis. *Nature* **408**, 613-615.
- Mäenpää, P., Gonzalez, E. B., Chen, L., Khan, M. S., Gray, J. C., and Aro, E.-M.** (2000). The *ycf 9 (orf 62)* gene in the plant chloroplast genome encodes a hydrophobic protein of stromal thylakoid membranes. *J. Exp. Bot.* **51**, 375-382.
- Maier, R. M., Neckermann, K., Igloi, G. L., and Kossel, H.** (1995). Complete sequence of the maize chloroplast genome: gene content, hotspots of divergence and fine tuning of genetic information by transcript editing. *J. Mol. Biol.* **251**, 614-628.
- Maliga, P., and Nixon, P. J.** (1998). Judging the homoplastomic state of plastid transformants. *Trends Plant Sci.* **3**, 376-377.
- Margulis, L.** (1970). Recombination of non-chromosomal genes in *Chlamydomonas*: assertion of mitochondria and chloroplast? *J. Theor. Biol.* **26**, 337-342.
- Martin, W., and Müller, M.** (1998). The hydrogen hypothesis for the first eukaryote. *Nature* **392**, 37-41.
- Martin, W., Stoebe, B., Goremykin, V., Hansmann, S., Hasegawa, M., and Kowallik, K. V.** (1998). Gene transfer to the nucleus and the evolution of chloroplasts. *Nature* **393**, 162-165.

- Martin, W., and Herrmann, R. G.** (1998). Gene Transfer from Organelles to the Nucleus: How Much, What Happens, and Why? *Plant Physiol.* **118**, 9-17.
- Martinez, S. E., Huang, D., Ponomarev, M., Cramer, W. A., and Smith, J. L.** (1996). The heme redox center of cytochrome f is linked to a buried five-water chain. *Protein Sci.* **5**, 1081-1092.
- Maxwell, D. P., Falk, S., and Huner, N. P. A.** (1995). Photosystem II excitation pressure and development of resistance to photoinhibition. Light-harvesting complex II abundance and zeaxanthin content in *Chlorella vulgaris*. *Plant Physiol.* **107**, 687-694.
- Menz, R. I., Walker, J. E., and Leslie, A. G. W.** (2001). Structure of Bovine Mitochondrial F1-ATPase with Nucleotide Bound to All Three Catalytic Sites: Implications for the Mechanism of Rotary Catalysis. *Cell* **106**, 331-341.
- Messinger, J.** (2000). Towards understanding the chemistry of photosynthetic oxygen evolution: dynamic structural changes, redox states and substrate water binding of the Mn cluster in photosystem II. *Biochim. Biophys. Acta* **1459**, 481-488.
- Meurer, J., Meierhoff, K., and Westhoff, P.** (1996). Isolation of high-chlorophyll-fluorescence mutants of *Arabidopsis thaliana* and their characterization by spectroscopy, immunoblotting and Northern hybridisation. *Planta* **198**, 385-396.
- Mitchell, P.** (1975). Protonmotive redox mechanisms of the cytochrome *bc*₁ complex in the respiratory chain: protonmotive ubiquinone cycle. *FEBS Lett.* **56**, 1-6.
- Mullet, J. E., Burke, J. J., and Arntzen, C. J.** (1980a). Chlorophyll Proteins of Photosystem I. *Plant Physiol.* **65**, 814-822.
- Mullet, J. E., Burke, J. J., and Arntzen, C. J.** (1980b). A Developmental Study of Photosystem I Peripheral Chlorophyll Proteins. *Plant Physiol.* **65**, 823-827.
- Müller, B., and Eichacker, L. A.** (1999). Assembly of the D1 precursor in monomeric photosystem II reaction center precomplexes precedes chlorophyll a-triggered accumulation of reaction center II in barley etioplasts. *Plant Cell* **11**, 2365-2378.
- Nagano, Y., Ishikawa, H., Matsuno, R., and Sasaki, Y.** (1991). Nucleotide sequence and expression of the ribosomal protein L2 gene in pea chloroplasts. *Plant Mol. Biol.* **17**, 541-545.
- Nelson, N.** (1992). Evolution of organellar proton-ATPases. *Biochim. Biophys. Acta.* **1100**, 109-124.
- Nield, J., Orlova, E. V., Morris, E. P., Gowen, B., van Heel, M., and Barber, J.** (2000). 3D map of the plant photosystem II supercomplex obtained by cryoelectron microscopy and single particle analysis. *Nat. Struct. Biol.* **7**, 44-47.

- Niyogi, K. K., Grossman, A. R., and Bjorkman, O.** (1998). Arabidopsis mutants define a central role for the xanthophyll cycle in the regulation of photosynthetic energy conversion. *Plant Cell* **10**, 1121-1134.
- Ohlrogge, J., and Browse, J.** (1995). Lipid biosynthesis. *Plant Cell* **7**, 957-970.
- Ohyama, K., Fukuzawa, H., Kohchi, T., Shirai, H., Sano, T., Sano, S., Umesono, K., Shiki, Y., Takeuchi, M., Chang, Z., Aota, S., Inokuchi, H., and Ozeki, H.** (1986). Chloroplast gene organization deduced from complete sequence of liverwort *Marchantia polymorpha* chloroplast DNA. *Nature* **322**, 572-574.
- O'Neil, D., Horvath, G. V., Horvath, E., Dix, P. J., and Medgyesy, P.** (1993). Chloroplast transformation in plants: Polyethylene glycol (PEG) treatment of protoplast is an alternative to biolistic delivery systems. *Plant J.* **3**, 729-738.
- Pesaresi, P., Sandona, D., Giuffra, E., and Bassi, R.** (1997). A single point mutation (E166Q) prevents dicyclohexylcarbodiimide binding to the photosystem II subunit CP29. *FEBS Lett.* **402**, 151-156.
- Peter, G. F., Thornber, J. P.** (1991). Biochemical Composition and Organization of Higher Plant Photosystem II Light-harvesting Pigment-Proteins. *J. Biol. Chem.* **266**, 16745-16754.
- Polloc, S. V., and Colman, B.** (2001). The inhibition of the carbon concentrating mechanism of the green alga *Chlorella saccharophila* by acetazolamide. *Physiol. Plant.* **111**, 527-532.
- Race, H. L., Herrmann, R. G., and Martin, W.** (1999). Why have organelles retained genomes? *TIG* **15**, 364-370.
- Ramelli, R., Varotto, C., Sandona, D., Croce, R., and Bassi, R.** (1999). Chlorophyll Binding to Monomeric Light-harvesting Complex. *J. Biol. Chem.* **274**, 33510-33521.
- Reith, M., and Munholland, J.** (1995). Complete nucleotide sequence of the *Porphyra purpurea* chloroplast genome. *Plant Mol. Biol. Repr.* **13**, 333-335.
- Rhee, K. H., Morris, E. P., Barber, J., and Kühlbrandt, W.** (1998). Three-dimensional structure of the plant photosystem II reaction centre at 8 Å resolution. *Nature* **396**, 283-286.
- Rintamäki, E., Kettunen, R., and Aro, E.-M.** (1996). Differential D1 Dephosphorylation in Functional and Photodamaged Photosystem II Centers. *J. Biol. Chem.* **271**, 14870-14875.
- Rintamäki, E., Salonen, M., Suoranta, U.-M., Carlberg, I., Andersson, B., and Aro, E.-M.** (1997). Phosphorylation of Light-Harvesting Complex II and Photosystem II Core Proteins Shows Different Irradiance-dependent Regulation *in Vivo*. *J. Biol. Chem.* **272**, 30476-30481.

- Rintamäki, E., Martinsuo, P., Pursiheimo, S., Aro E.-M.** (2000). Cooperative regulation of light-harvesting complex II phosphorylation via the plastoquinol and ferredoxin-thioredoxin system in chloroplasts. *Proc. Natl. Acad. Sci. USA* **97**, 11644-11649.
- Ris, H., and Plaut, W.** (1962). The ultrastructure of DNA-containing areas in the chloroplasts of *Chlamydomonas*. *J. Cell. Biol.* **13**, 383-391.
- Rochaix, J.-D.** (1995). *Chlamydomonas reinhardtii* as the photosynthetic yeast. *Annu. Rev. Genet.* **29**, 209-230.
- Rochaix, J.-D.** (1997). Chloroplast reverse genetics: new insights into the function of plastid genes. *Trends Plant Sci.* **2**, 419-425.
- Rolland, N., Dorne, A.-J., Amoroso, G., Sültemeyer, D. F., Joyard, J., and Rochaix, J.-D.** (1997). Disruption of the plastid *ycf10* open reading frame affects uptake of inorganic carbon in the chloroplast of *Chlamydomonas*. *EMBO J.* **16**, 6713-6726.
- Rousseau, F., Sétif, P., and Lagoutte, B.** (1993). Evidence for the involvement of PSI-E subunit in the reduction of ferredoxin by photosystem I. *EMBO J.* **12**, 1755-1765.
- Ruban, A. V., Young, A. J., Pascal, A. A., and Horton, P.** (1994). The effects of illumination on the xanthophyll composition of the photosystem II light-harvesting complexes of spinach thylakoid membranes. *Plant Physiol.* **104**, 227-234.
- Ruban, A. V., Pesaresi, P., Wacker, U., Irrgang, K. D., Bassi, R., and Horton, P.** (1998). The relationship between the binding of dicyclohexylcarbodiimide and quenching of chlorophyll fluorescence in the light-harvesting proteins of photosystem II. *Biochemistry* **37**, 11586-11591.
- Ruban, A. V., Lee, P. J., Wentworth, M., Young, A. J., and Horton, P.** (1999). Determination of the Stoichiometry and Strength of Binding of Xanthophylls to the Photosystem II Light Harvesting Complexes. *J. Biol. Chem.* **274**, 10458-10465.
- Ruban, A. V., Pascal, A. A., and Robert, B.** (2000). Xanthophylls of the major photosynthetic light-harvesting complex of plants: identification, conformation and dynamics. *FEBS Lett.* **477**, 181-185.
- Ruf, S., Biehler, K., and Bock, R.** (2000). A small chloroplast-encoded protein as a novel architectural component of the light-harvesting antenna. *J. Cell. Biol.* **149**, 369-378.
- Ruf, S., Hermann, M., Berger, I. J., Carrer, H., and Bock, R.** (2001). Stable genetic transformation of tomato plastids and expression of foreign protein in fruit. *Nat. Biotechnol.* **19**, 870-875.
- Sager, R., and Ishida, M. R.** (1963). Chloroplast DNA in *Chlamydomonas*. *Proc. Natl. Acad. Sci. USA* **50**, 725-730.

- Sambrook, J., Fritsch, E. F., and Maniatis, T.** (1989). *Molecular Cloning*, Second Edition, Cold Spring Harbor Laboratory Press, ed.
- Sanger, F., Nicklen, S., and Coulson, A. R.** (1977). DNA sequencing with chain-terminating inhibitors. *Proc. Natl. Acad. Sci. USA* **74**, 5463-5467.
- Sasaki, Y., Sekiguchi, K., Nagano, Y., and Matsuno, R.** (1993). Chloroplast envelope protein encoded by chloroplast genome. *FEBS Lett.* **316**, 93-98.
- Sato, S., Nakamura, Y., Kaneko, T., Asamizu, E., and Tabata, S.** (1999). Complete structure of the chloroplast genome of *Arabidopsis thaliana*. *DNA Res.* **6**, 283-290.
- Schägger, H., and von Jagow, G.** (1987). Tricine-sodium dodecyl sulfate-polyacrylamide gel electrophoresis for the separation of proteins in the range from 1 to 100 kDa. *Anal. Biochem.* **166**, 368-379.
- Schägger, H., and von Jagow, G.** (1991). Blue native electrophoresis for isolation of membrane protein complexes in enzymatically active form. *Anal. Biochem.* **199**, 223-231.
- Schmitt, J. M., and Herrmann, R. G.** (1977). Fractionation of cell organelles in silica sol gradients. In: *Methods in Cell Biology* **15**, 177-200. eds. Prescott, M. Academic Press, London-New York.
- Schmitz-Linneweber, C., Maier, R., Alcaraz, J. P., Cottet, A., Hermann, R. G., and Mache, R.** (2001). The plastid chromosome of spinach (*Spinacia oleracea*): complete nucleotide sequence and gene organization. *Plant Mol. Biol.* **45**, 307-315.
- Schreiber, U.** (1986). Detection of rapid induction kinetics with a new type of high-frequency modulated chlorophyll fluorometer. *Photosynth. Res.* **9**, 261-272.
- Schwartz, D. C., and Cantor, L. R.** (1984). Separation of yeast chromosome sized DNAs by pulsed field gradient gel electrophoresis. *Cell* **37**, 67-75.
- Seidell and Linke.** (1965). *Am. Chem. Soc. Div. Grad. Res.* **2**, p. 1228.
- Shikanai, T., Endo, T., Hashimoto, T., Yamada, Y., Asada, K., and Yokota, A.** (1998). Directed disruption of the tobacco *ndhB* gene impairs cyclic electron flow around photosystem I. *Proc. Natl. Acad. Sci. USA* **95**, 9705-9709.
- Shinozaki, K., Ohme, M., Tanaka, M., Wakasugi, T., Hayashida, N., Matsubayashi, T., Chunwongse, J., Obokata, J., Yamaguchi-Shinozaki, K., Ohto, C., Torazawa, K., Meng, B. Y., Sugita, M., Deno, H., Kamohgashira, T., Yamada, K., Kusuda, J., Takaiwa, F., Kato, A., Tohdoh, N., Shimada, H., and Sugiura, M.** (1986). The complete nucleotide sequence of the tobacco chloroplast genome: its gene organization and expression. *EMBO J.* **5**, 2043-2049.

- Sidorov, V. A., Kasten, D., Pang, S. Z., Hajdukiewicz, P. T., Staub, J. M., and Nehra, N. S.** (1999). Technical Advance: Stable chloroplast transformation in potato: use of green fluorescent protein as a plastid marker. *Plant J.* **19**, 209-216.
- Singh, A. K., and Singhal, G. S.** (1999). Specific degradation of D1 protein during exposure of thylakoid membranes to high temperature in the dark. *Photosynthetica* **36**, 433-440.
- Snyders, S., and Kohorn, B. D.** (1999). TAKs, thylakoid membrane protein kinases associated with energy transduction. *J. Biol. Chem.* **274**, 9137-9140.
- Spurr, A. R.** (1969). A low-viscosity epoxy resin embedding medium for electron microscopy. *J. Ultrastruct. Res.* **26**, 31-43.
- Stachelin, L. A., and Arntzen, C. J.** (1983). Regulation of Chloroplast Membrane Function: Protein Phosphorylation Changes the Spatial Organization of Membrane Components. *J. Cell Biol.* **97**, 1327-1337.
- Stern, D. B., and Lonsdale, D. M.** (1982). Mitochondrial and chloroplast genomes of maize have a 12-kilobase DNA sequence in common. *Nature* **299**, 698-702.
- Stirewalt, V. L., Michalowski, C. B., Löffelhardt, W., Bohnert, H. J., and Bryant, D. B.** (1995). Nucleotide sequence of the cyanelle genome from *Cyanophora paradoxa*. *Plant Mol. Biol. Repr.* **13**, 327-332.
- Stock, D., Leslie, A. G. W., and Walker, J. E.** (1999). Molecular Architecture of the Rotary Motor in ATP Synthase. *Science* **286**, 1700-1705.
- Svab, Z., Hajdukiewicz, P., and Maliga, P.** (1990). Stable transformation of plastids of higher plants. *Proc. Natl. Acad. Sci. USA* **90**, 913-917.
- Svab, Z., and Maliga, P.** (1993). High-frequency plastid transformation in tobacco by selection for a chimeric *aadA* gene. *Mol. Gen. Genet.* **228**, 316-319.
- Swiatek, M., Kuras, R., Sokolenko, A., Higgs, D., Olive, J., Cinque, G., Müller, B., Eichacker, L. A., Stern, D. B., Bassi, R., Herrmann, R. G., and Wollman, F.-A.** (2001). The Chloroplast Gene *ycf9* Encodes a Photosystem II (PSII) Core Subunit, *PsbZ*, That Participates in PSII Supramolecular Architecture. *Plant Cell* **13**, 1347-1368.
- Tardy, F., and Havaux, M.** (1997). Thermostability and photostability of photosystem II in leaves of the Chlorina-F2 barley mutant deficient in light-harvesting chlorophyll *a/b* protein. *Plant Physiol.* **113**, 913-923.
- Tracewell, C. A., Cua, A., Stewart, D. H., Bocian, D. F., and Brudvig, G. W.** (2001). Characterization of Carotenoid and Chlorophyll Photooxidation in Photosystem II. *Biochemistry* **40**, 193-203.

- Uemura, K., Anwaruzzaman, S., Miyachi, S., and Yokota, A.** (1997). Ribulose-1,5-Biphosphate Carboxylase/Oxygenase from Thermophilic Red Algae with a Strong Specificity for CO₂ Fixation. *Biochem. Biophys. Res. Comm.* **233**, 568-571.
- Vasil'ev, S., Orth, P., Zouni, A., Owens, T. G., and Doug, B.** (2001). Excited-state dynamics in photosystem II: insights from the x-ray crystal structure. *Proc. Natl. Acad. Sci. USA* **98**, 8602-8607.
- Vener, A. V., van Kan, P. J. M., Rich, P. R., Ohad, I., and Andersson, B.** (1997). Plastoquinol at the quinol oxidation site of reduced cytochrome *bf* mediates signal transduction between light and protein phosphorylation: Thylakoid protein kinase deactivation by a single-turnover flash. *Proc. Natl. Acad. Sci. USA* **94**, 1585-1590.
- Vener, A. V., Harms, A., Sussman, M. R., and Vierstra, R. D.** (2001). Spectrometric resolution of reversible protein phosphorylation in photosynthetic membranes of *Arabidopsis thaliana*. *J. Biol. Chem.* **276**, 6959-6966.
- Verhoeven, A. S., Adams III, W. W., Demmig-Adams, B., Croce, R., and Bassi, R.** (1999). Xanthophyll Cycle Pigment Localization and Dynamics during Exposure to Low Temperatures and Light Stress in *Vinca major*. *Plant Physiol.* **120**, 727-737.
- Wakasugi, T., Tsudzuki, J., Ito, S., Nakashima, K., Tsudzuki, T., and Sugiura, M.** (1994). Loss of all *ndh* genes as determined by sequencing the entire chloroplast genome of the black pine *Pinus thunbergii*. *Proc. Natl. Acad. Sci. USA* **91**, 9794-9798.
- Wakasugi, T., Nagai, T., Kapoor, M., Sugita, M., Ito, S., Tsudzuki, J., Nakashima, K., Tsudzuki, T., Suzuki, Y., Hamada, A., Ohta, T., Inamura, A., Yoshinaga, K., and Sugiura, M.** (1997). Complete nucleotide sequence of the chloroplast genome from the green alga *Chlorella vulgaris*: the existence of genes possibly involved in chloroplast division. *Proc. Natl. Acad. Sci. USA* **94**, 5967-5972.
- Walters, R. G., Ruban, A. V., and Horton, P.** (1994). Higher plant light-harvesting complexes LHCIa and LHCIc are bound by dicyclohexylcarbodiimide during inhibition of energy dissipation. *Eur. J. Biochem.* **226**, 1063-1069.
- Walters, R. G., Ruban, A. V., and Horton, P.** (1996). Identification of proton-active residues in a higher plant light-harvesting complex. *Proc. Natl. Acad. Sci. USA* **93**, 14204-14209.
- Wells, R., and Birnstiel, M.** (1969). Kinetic complexity of chloroplast deoxyribonucleic acid and mitochondrial deoxyribonucleic acid from higher plants. *Biochem. J.* **112**, 777-786.
- White, T. J., Arnheim, N., and Erlich, H. A.** (1989) The polymerase chain reaction. *Trends Genet.* **5**, 185-189.

- Willey, D. L., and Gray, J. C.** (1990). An open reading frame encoding a putative haem-binding polypeptide is cotranscribed with the pea chloroplast gene for apocytochrome *f*. *Plant Mol. Biol.* **15**, 347-356.
- Wilson, R. J. M., Denny, P. W., Preiser, P. R., Rangachari, K., Roberts, K., Roy, A., Whyte, A., Strath, M., Moore, D. J., Moore, P. W., and Williamson, D. H.** (1996). Complete gene map of the plastid-like DNA of the malaria parasite *Plasmodium falciparum*. *J. Mol. Biol.* **261**, 155-172.
- Wolfe, K. H., Morden, C. W., and Palmer, J. D.** (1992). Function and evolution of a minimal plastid genome from nonphotosynthetic parasite plant. *Proc. Natl. Acad. Sci. USA* **89**, 10648-10652.
- Wollman, F.-A., Minai, L., and Nechushtai, R.** (1999). The biogenesis and assembly of photosynthetic proteins in thylakoid membranes. *Biochim. Biophys. Acta* **1411**, 21-85.
- Wollman, F.-A.** (2001). State transitions reveal the dynamics and flexibility of the photosynthetic apparatus. *EMBO J.* **20**, 3623-3630.
- Xiao-Ping, L., Björkman, O., Shih, C., Grossman, A. R., Rosenquist, M., Jansson, S., and Niyogi, K. K.** (2000). A pigment-binding protein essential for regulation of photosynthetic light harvesting. *Nature* **403**, 391-395.
- Xu, Q., Armbrust, T. S., Guikema, J. A., and Chitnis, P. R.** (1994). Organization of Photosystem I Polypeptides. *Plant Physiol.* **106**, 1057-1063.
- Yakota, A., Harada, A., and Kitaoka, S.** (1989). Characterization of ribulose 1,5-biphosphate carboxylase/oxygenase from *Euglena gracilis* Z. *J. Biochem. (Tokyo)* **105**, 400-405.
- Yao, W. B., Meng, B. Y., Tanaka, M., and Sugiura, M.** (1989). An additional promoter within the protein-coding region of the *psbD-psbC* gene cluster in tobacco chloroplast DNA. *Nucleic Acids Res.* **17**, 9583-9591.
- Yu, L., Zhao, J., Mühlenhoff, U., Bryant, D. A., and Golbeck, J. H.** (1993). PsaE Is Required for in In Vivo Cyclic Electron Flow around Photosystem I in the Cyanobacterium *Synechococcus* sp. PC 7002. *Plant Physiol.* **103**, 171-180.
- Zhang, Z., Huang, L., Schulmeister, V.-M., Chi, Y.-I., Kim, K. K., Hung, L.-W., Crofts, A. R., Berry, E. A., and Kim, S.-H.** (1998). Electron transfer by domain movement in cytochrome *bc₁*. *Nature* **392**, 677-684.
- Zito, F., Finazzi, G., Delosme, R., Nitschke, P., Picot, D., and Wollman, F.-A.** (1999). The Qo site of cytochrome *b₆f* complexes controls the activation of the LHCII kinase. *EMBO J.* **18**, 2961-2969.

Zouni, A., Witt, H. T., Kern, J., Fromme, P., Krauss, N., Saenger, W., and Orth, P. (2001). Crystal structure of photosystem II from *Synechococcus elongatus* at 3.8 Å resolution. *Nature* **409**, 739-743.

ACKNOWLEDGMENTS

This work was performed at the Botanisches Institut of the Ludwig-Maximilians-Universität in Munich, in the laboratory of Prof. Dr. R. G. Herrmann. I am specially thankful to Prof. Dr. R. G. Herrmann for accepting me in his laboratory and for providing the excellent working conditions. I also want to thank him for his consistent support and advices during the whole study.

I am grateful to Prof. Dr. H.-U. Koop for reviewing this work.

I would like to thank Dr. A. Sokolenko and Dr. R. M. Maier for their constant support and valuable discussions during my Ph.D. time. Dr. B. Mueller I thank for his help in all aspects and for introducing me to the protein biochemistry and sequencing methods.

A big thank-you to my friends and colleagues, especially to Dr. Petra Weber, Martin Lensch, Anja Drescher, and Julia Legen, for their friendship, sense of humor, great working atmosphere and all the time we have spent together. A lot of thanks to Ms. Claudia Nickel for her patience, professional assistance and the good time we had “after hours”.

I am very grateful to my parents for their personal and material support during difficult times.

Last but not least, a special thanks to Robert for being always here when I needed him, for his optimism and encourage. Thank you.

The work was supported by the Deutsche Forschungsgemeinschaft, SFB 184.

PUBLICATIONS

Hupfer, H., **Swiatek, M.**, Hornung, S., Herrmann, R. G., Maier, R. M., Chiu, W.-L., and Sears, B. (2000). Complete nucleotide sequence of the *Oenothera elata* plastid chromosome, representing plastome I of the five distinguishable *Euoenothera* plastomes. *Mol. Gen. Genet.* **263**, 581-585.

Swiatek, M., Kuras, R., Sokolenko, A., Higgs, D., Olive, J., Cinque, G., Müller, B., Eichacker, L. A., Stern, D. B., Bassi, R., Herrmann, R. G., and Wollman, F. A. (2001). The Chloroplast Gene *ycf9* Encodes a Photosystem II Core Subunit, PsbZ, That Participates in Photosystem II Supramolecular Architecture. *The Plant Cell* **13**, 1347-1367.

Swiatek, M., Greiner, S., Drescher, A., Koop, H.-U., Herrmann, R. G., and Maier, R. M. (2002). Pulsed-Field electrophoresis of plastid chromosomes: a sensitive tool to judge the homoplastomic state of plastid transformants. *Plant Biotechnology*, manuscript in revision.

Swiatek, M., Regel, R., Meurer, J., Wanner, G., Pakrasi, H. B., Ohad, I., and Herrmann, R. G. (2002). The *psbEFLJ* operon: disruption of the individual genes by chloroplast transformation in *Nicotiana tabacum*. Manuscript in revision.

CURRICULUM VITAE**Personal data**

Family name: Swiatek
First name: Magdalena
Date of birth: 23.03.1973
Place of birth: Wroclaw, Poland
Marrial status: single

Education

1988 – 1990 Secondary school in Wroclaw, Poland

Academic education

1992 – 1997 Study of biology at the Faculty of Natural Sciences of the University of Wroclaw, Poland with specialisation biotechnology
Supervisor:
Prof. Dr. J. Szopa

13.06.1997 Diplom of Biotechnology at Faculty of Natural Sciences of the University of Wroclaw, Poland

1997- 01.10.2001 Ph.D. study at the Botanisches Institut of the Ludwig-Maximilians-Universität, Munich
Head of the Department and supervisor:
Prof. Dr. R. G. Herrmann

01.10.2001 -
31.05.2002 Researcher at the Botanisches Institut of the Ludwig-Maximilians-Universität, Munich
Group of Dr. hab. L. A. Eichacker

01.06.2002 Researcher at Molecular Ophthalmology Clinical Cooperation Group, Klinikum Innenstadt, Ludwig-Maximilians-Universität, Munich
Group of Dr. M. Ueffing